ELECTROCHEMICAL PHENOMENA IN CHARGED MEMBRANES

A doctoral thesis submitted

by
Naoki Kamo

to
the Department of Polymer Science
the Faculty of Science
Hokkaido University, Sapporo.

CONTENTS

Chapter 1. Introduction

When two electrolyte solutions having different free energies are separated by a membrane, each movable species penetrates across the membrane, and various transport phenomena are simultaneously induced in the system. Due to the difference in dielectric constants of the membrane matrix and the external fluid, and/or due to the dissociable groups attached to the polymer skeletons constituting the membrane, a membrane in an aqueous solution has almost always electrical charges. The facts that the membrane is in charged state, and that the system considered is composed of three phases with two surfaces separating the membrane phase from the solutions, are two important characteristics of the system under consideration. The gradient of the chemical potential across the membrane arises from the differences in temperature, ΔT, pressure, ΔP, electrical potential, $\Delta\varphi$, and the concentration of component k, ΔC_k. The gravitational field (or the centrifugal force) g, may be considered, but, for membrane system, g is not important and hence is omitted here. The flows conjugate to the forces described above, are the heat flow, J_q, volume flow, J_v, the electric current, I, and the diffusion flux, J_k, respectively. According to the thermodynamics of

irreversible processes[1-3], these fluxes may be caused not only by the corresponding conjugate force but by non-congugate force. Fig. 1-1 shows typical phenomena which may appear in the membrane system considered[4]. Each cross phenomena had a specific name as indicated. These membrane phenomena have been the subject of extensive studies in the fields of physical chemistry, colloid science, biological science, and in technology, and have been successfully correlated with each other by the thermodynamics of irreversible processes[3]. However, these correlations do not provide insight into the actual mechamism of the ionic or molecular processes which occur in the membrane phase. On the other hand, the fixed charge concept of Teorell[5] and of Meyer and Sievers[6] (the TMS thory in abbreviation) for the charged membrane is a pertinent starting point for the investigation of the membrane phenomena. However, careful experiments did not give a quantitative account of the experimental results[7-10].

One of the reasons for this failure is the lack of precise information about the non-ideal behaviors of small ions within the charged membranes. This non-ideality will be explored in Chapters 2 - 5 of this thesis in the light of recent progress in the field of polyelectrolyte solution studies. Chapters 6-8 will be devoted to other characteristics of the membrane systems in question, i.e.

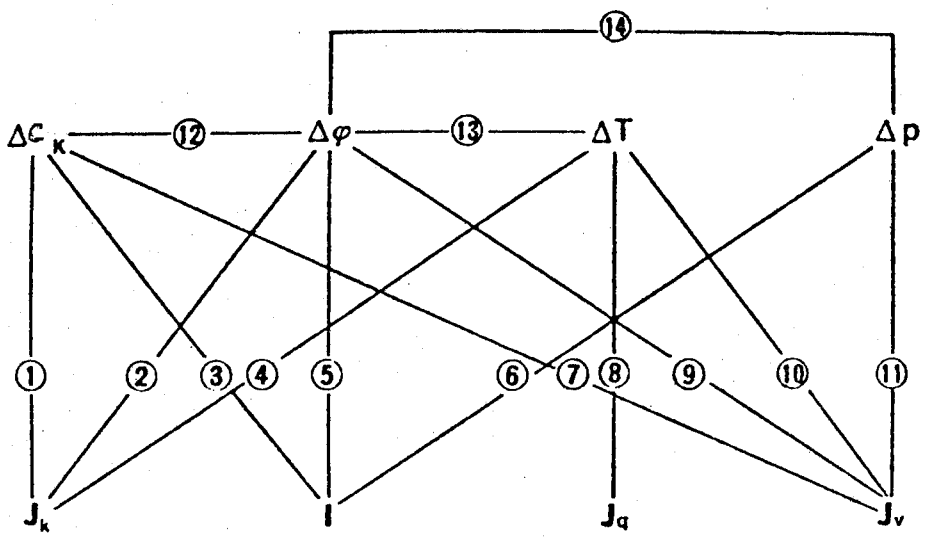

Fig. 1-1. Scheme of different transport phenomena across membranes. 1) Diffusion, 2) electrophoresis, 3) diffusion current, 4) thermal diffusion, 5) electric conductance, 6) streaming current, 7) osmosis, 8) heat conduction, 9) electroosmosis, 10) thermal osmosis, 11) hydraulic permeability, 12) membrane potential, 13) thermo-membrane potential, 14) streaming potential.

the volume flow in the membrane and its effect on the membrane phenomena. Chapters 9 and 10 deal with the membrane potential arisen between two electrolyte solutions separated by oil membranes containing ion-exchanging sites or compact membranes which are scarcely permeable to ions.

References

1) D. D. Fitts, "Non-equlibrium Thermodynamics", Mac-Graw Hill, New York, (1962).

2) S. R. de Groot, and P. Mazur, "Non-equilibrium Thermodynamics", North Holland, Amsterdam, (1962).

3) A. Katchalsky and P. F. Curran, "Non-equilibrium Thermodynamics In Biophysics", Harvard Univ. Press, Cambridge, Mass., (1965).

4) Y. Kobatake, Prog. Theor. Phys. Suppl. 10, 226 (1959).

5) T. Teorell, Proc. Soc. Exptl. Biol., 33, 282 (1935); Prog. Biophys. Biophys. Chem., 3, 305 (1953).

6) K. H. Meyer and J. F. Sievers, Helv. Chim. Acta, 19, 649, 665, 987 (1936).

7) G. J. Hills, P. W. M. Jacobs and N. Lakshminarayanaiah, Proc. Roy. Soc. (London), A262, 257(1961).

8) R. Schlögl, Z. Elektrochem. Soc., 57, 195 (1953).

9) K. S. Spiegler, Electrochem. Soc., 100, 303C (1953).

10) N. Laksminarayanaiah and V. Subrahmanyan, J. Polymer Sci., A-2, 4491 (1964).

Chapter 2. Basic Equations

Throughout the following considerations the discussion is confined to a system of charged membrane separating two aqueous solutions of a 1:1 type electrolyte of different electrochemical potentials with a constant temperature. The membrane is bounded by two planes normal to the x-axis at x = 0 and x = L. The fluxs of all mobile species under consideration are assumed to occur only in the direction of the x-axis. The bulk solutions on two sides of the membrane are stirred vigorously so as to maintain spatial uniformity of the concentration of every species in the solution phases. The density of the fixed charges in the membrane is assumed to be constant and independent of the concentrations of the external electrolyte solutions with which the membrane is in contact.

The thermodynamic force acting on each species is the negative gradient of its electrochemical potential, $\tilde{\mu}_k$, in the direction of the x-axis. The quantity $d\tilde{\mu}_k/dx$ at constant temperature may be written as

$$(d\tilde{\mu}_k/dx)_T = e_k(d\varphi/dx) + RT(d\ln a_k/dx) + v_k dP/dx \quad (2\text{-}1)$$

where φ, R, P and T are the electric potential, the gas constant, the pressure, and the absolute temperature, respectively; e_k, v_k and a_k are the molar electric charge, the partial molar volume and the single

ion activity of species k (= o, +, -), respectively. Here subscript o denotes the solvent species. The last term in Eq.(2-1) is legitimately neglected for the membrane systems considered here, since this term becomes important only in circumstances where the pressure gradient is extremely high as is encountered in an ultracentrifuge. Following to the thermodynamics of irreversible processes, one may write the following experssion for the flux $\mathbf{j}_k$ of ionic species k (k=+,-) relative to the membrane[1,2],

$$\begin{aligned} \mathbf{j}_+ &= -\ell_{++}\nabla\tilde{\mu}_+ - \ell_{+-}\nabla\tilde{\mu}_- + \tilde{c}_+ u_m \\ \mathbf{j}_- &= -\ell_{+-}\nabla\tilde{\mu}_+ - \ell_{--}\nabla\tilde{\mu}_- + \tilde{c}_- u_m \end{aligned} \qquad (2\text{-}2)$$

provided that the system is in mechanical equilibrium[1]. Here, ∇ stands for the gradient, $\tilde{c}_k$ is the local concentration of species k, and u_m is the velocity of the local center of mass. In the equation, ℓ'_{ki}s are the phenomenological coefficients referred to the local center of mass and obey the Onsager reciprocal relations, i.e. $\ell_{ki} = \ell_{ik}$ $(i \neq k)$. One should note that the Onsager reciprocal relations hold strictly only for the mass-fixed phenomenological coefficients ℓ_{ki}[1]. The velocity of the local center of mass u_m may be described in terms of the Navier-Stokes equation in continuum hydrodynamics.

As noted above, we have assumed that the flux of all components

occur only in the direction of the membrane thickness. Hence the electrochemical potential of each component is considered to be constant in the direction of the membrane surface, i.e. in the y- and z-directions. Therefore, if flux of species k averaged over the cross section of the membrane is defined by

$$J_k = \iint_A j_k \, dy\,dz \Big/ \iint_A dy\,dz \tag{2-3}$$

where the integrals extend over the membrane area, A, we have from Eq.(2-2)

$$J_+ = -L_{++}(d\hat{\mu}_+/dx) - L_{-+}(d\hat{\mu}_-/dx) + C_+^* U_m$$

$$J_- = -L_{+-}(d\hat{\mu}_+/dx) - L_{--}(d\hat{\mu}_-/dx) + C_-^* U_m \tag{2-4}$$

where L_{ki}'s are the averaged mass fixed phenomenological coefficients defined by

$$L_{ki} = \iint_A l_{ki} \, dy\,dz \Big/ \iint_A dy\,dz \tag{2-5}$$

Note that J_k is a measurable qunatity in the membrane system under consideration. It is easily shown that the Onsager reciprocal relation still holds for L_{ki}. In Eq.(2-4), U_m and C_k^* are defined by

$$U_m = \iint_A u_m \, dy dz \Big/ \iint_A dy dz \tag{2-6}$$

and

$$C_k^* = \iint \tilde{c}_k u_m \, dy dz \Big/ \iint_A dy dz \tag{2-7}$$

C_k^* is regarded as the concentration of ion species k which is conveyed by the averaged mass movement U_m defined by Eq.(2-6). Due to strong electrostatic and hydrodynamic interactions between ions and the charges fixed on the membrane matrix, the effective concentration C_k^* is not necessary equal to the averaged concentration of ion species k given by

$$C_k = \iint \tilde{c}_k \, dy dz \Big/ \iint dy dz \tag{2-8}$$

At this stage, it may be worthwhile to point out the relation between the flux equations of the Nernst-Planck equation and of the irreversible thermodynamics, since the Nernst-Planck equation is used as a pertinent starting point of the subsequent arguments. Since the Nernst-Planck equation governs the flow relative to the local center of mass, the flux of k-ion (k = +,-) relative to the membrane is written as

$$\begin{aligned} FJ_+ &= -u_+ c_+ (d\tilde{\mu}_+ / dx) + F c_+^* U_m \\ FJ_- &= -u_- c_- (d\tilde{\mu}_- / dx) + F c_-^* U_m \end{aligned} \tag{2-9}$$

where u_k is the mass fixed mobility of ion species k (k = +, -), and F is the Faraday constant. Since all the membrane phenomena given in Fig. 1-1 can be represented by appropriate combination of Eq.(2-9), it is indispensable to evaluate C_k and C_k^* in the membrane as a function of the concentration of external solutions for quantitative description of membrane phenomena. Comparison of Eq.(2-4) and Eq.(2-9) leads to

$$\begin{aligned} u_+ C_+ &= L_{++} F [1 + (L_{+-}/L_{++})(d\tilde{\mu}_-/d\tilde{\mu}_+)] \\ u_- C_- &= L_{--} F [1 + (L_{-+}/L_{--})(d\tilde{\mu}_+/d\tilde{\mu}_-)] \end{aligned} \qquad (2\text{-}10)$$

These equations together with Eq.(2-1) imply that the mobilities of movable ions are not independent of the activities or activity coefficients of small ions in the membrane. This may be reasonable, because a strong electrostatic interaction between the movable ions and the charges fixed on the membrane matrix exerts its effects on the static aspects as well as on transport processes of small ions. This is also true for the mass movement in the membrane. Thus the electrostatic interaction between fixed charges and small ions in the membrane phase deserves special attention.

References

1) D. D. Fitts, "Non-equilibrium Thermodynamics", McGraw-Hill, New York, (1962).

2) S. R. de Groot and P. Mazur, "Non-equilibrium Thermodynamics" North Holland, Amsterdam (1962).

Chapter 3. Activity Coefficients and Mobilities of Small Ions in Charged Membranes

Modern quantitative theories of membrane potentials can be said to have started in 1935 with the pioneering works of Teorell[1], and of Meyer and Sievers[2]. They have proposed that the membrane potential, $\Delta\varphi$, is composed of a diffusion potential within a membrane phase ($\Delta\varphi_{diff}$) and two phase boundary potentials at x =0 and x = L ($\Delta\varphi'$, $\Delta\varphi''$). In Fig. 3-1, a schematic potential profile is drawn. They have derived an equation for membrane potential, $\Delta\varphi$ under the following three assumptions; (1) all ion species both in the membrane phase and in the external solution behave ideally, (2) the ratio of the mobilities of positive ions to that of negative ions is constant throughout the membrane, and (3) the effect of mass movement, i.e. the last term of Eq.(2-9) is negligible. The equation is represented in terms of the fixed charge density, the ratio of the mobilities of cation and anion in the membrane, and the concentrations in the external solutions. Thus, the TMS theory provides an insight for the ionic process which actually occur in the membrane and contrasts to the treatment of irreversible thermodynamics[3] or pseudo-thermodynamics[4]. Previous investigators[5,6] however, drew the conclusion that experimental results do not agree evidently with the theory.(see Chapter 5) Various attempts have

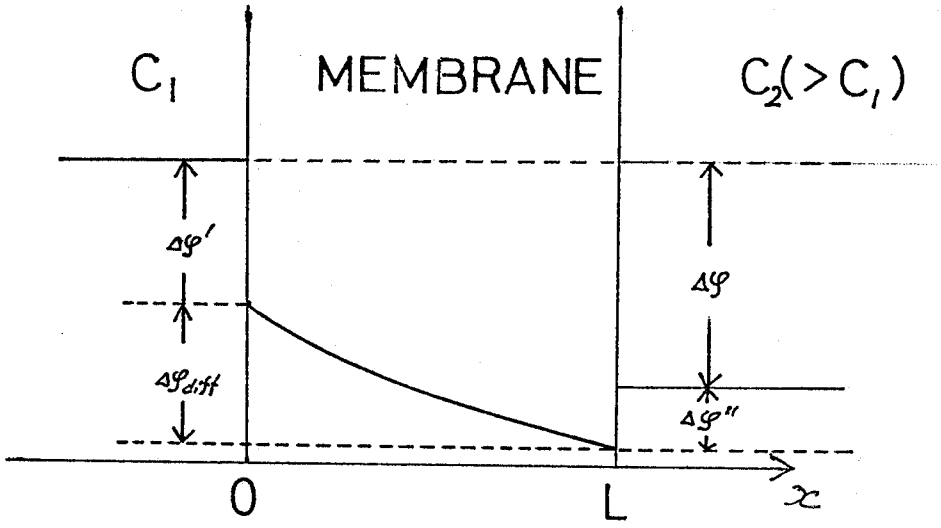

Fig. 3-1. Schematic diagram of potential profile in membrans.

been made to eliminate this defect of the theory[7,8], but no satisfactory results have been obtained. This defect of the TMS theory and its refinements must be attributed to the three assumptions described above. As will be shown in later chapters, the effects of mass movement on the observed potential and ion permeability are less than a few percent in a wide range of salt concentrations. Thus, assumptions (1) and (2) mentioned above, must be examined. For this purpose, it is desirable to examine a membrane whose stoichiometric charge density, X, fixed in the membrane is known.

Experimental

Materials Three kinds of collodion-based polystyrene sulfonic acid (PSSA) membranes were prepared by the method of Neihof[9], and were designated as PS-1, PS-2, and PS-3. The charges fixed on the membrane matrix are mainly coming from groups of sulfonate attached to the polyelectrolyte. Then, the density of charges fixed in the membrane, X, is considered to be constant provided that the water content of the membrane is not varied irrespective of external salt concentration, which is the case as shown later. Polystyrenesulfonic acid was prepared from a purified polystyrene by the method proposed by Kato et al.[10], and the degree of sulfonation was 0.80.

The electrolytes used were purified by repeated recrystallizations and the water used as solvent was distilled water treated with both

cation and anion exchangers.

Prior to measurements, the membrane was immersed in concentrated solution at least three days in order to convert the counterions into the species to be examined, and stored in deionized water. The charge density of the sample membrane remained constant for two years or more.

The water contents of a membrane equilibrated with a solution of given concentration were determined by weighing. The surface of a piece of the membrane was wiped with filter paper and weighed in a weighing bottle. Then the membrane was dried in vacuum over P_2O_5 until it weight became constant. The water content of each membrane was found to be independent of the external salt concentration ranging in concentration from pure water to 0.5 N KCl. This fact implied that the membrane does not swell.

Determination of X Two methods were used to determine the charge density X of PS-1 membrane. In method 1, the membrane was immersed in HCl solution in order to convert the polyelectrolyte impregnated in the membrane into the acidic form , and then the membrane was rinsed with deionized water repeatedly until no Cl ion was detected. A known weight of the wet membrane in acidic form was immersed in 2.0 N KCl solution under stirring for 2 hrs. The 2.0 N KCl solution was replaced by new one repeatedly until no extra H^+_{Λ} ion was detected

in the solution. Five times of replacement were sufficient for complete extraction of H^+ ion from the membrane in the present case. All solutions which were used in rinsing the membrane were collected carefully and total amount of H^+ ion was determined by titration against carbonate free NaOH. In method 2, the surface dried membrane in the acidic form of a given weight was chopped in fine pieces and soaked in ion exchanged water and the amount of H^+ ions in the membrane were titrated directly against NaOH in an atomosphere of N_2 in order to remove an influence of CO_2 in the air. The value of X for membrane PS-1 determined by the two methods described above agreed with each other within 0.2 %. In view of this agreement, the values of X for PS-2 and PS-3 membranes were determined by method 1 only. The values of X for three membranes examined are listed in table 3-1 together with the water contents of the membranes.

Determination of the mean activity coefficient of small ions in membranes

The system considered is a negatively ionized membrane of uniform thickness immersed in an aqueous solution of 1:1 type electrolyte of concentration C. The counterions of the polyelectrolyte skeletones constituting the membrane are assumed to be the same cation species as the external salt, and their density stays constant irrespective of the salt concentration in the external solution. When the equilibrium is established between the membrane phase and the external solution, the

Table 3-1. Some characteristics of membranes used

membrane	X equiv./l	water content wt %	f
PS-1	0.224	0.78	0.30 ± 0.01
PS-2	0.116	0.86	0.31 ± 0.01
PS-3	0.043_8	0.85	0.34 ± 0.01

activity of the electrolyte component must be the same in membrane and in solution phases provided that the difference of the osmotic pressure in both phases can be neglected. As discussed later, the osmotic pressure difference is negligibly small for the present system. Then, we have

$$a^2 = (\gamma_\pm^\circ)^2 c^2 = a_+ a_- \qquad (3\text{-}1)$$

In Eq.(3-1) a_+ and a_- are the activities of positive and negative ions in the membrane and may be represented by $\gamma_+ C_+$ and $\gamma_- C_-$ respectively, and $\gamma_\pm^\circ$ is the mean activity coefficient of the electrolyte component in the external solution at concentration C. Eq.(3-1) together with the condition of the electroneutrality ($C_+ = C_- + X$) leads to

$$\gamma_+ \gamma_- / (\gamma_\pm^\circ)^2 = c^2 / C_- (C_- + X) \qquad (3\text{-}2)$$

Eq.(3-2) indicates that the mean activity coefficent of small ions in the membrane $\gamma_+ \gamma_-$ can be evaluated as a function of C when C_- and X in the membrane are determined analytically.

The value of C_- was evaluated as follows; Known weight (about 15 g) of a surface dried membrane was immersed in an aqueous solution of KCl or NaCl (about 500 ml) at a given concentration C, and was allowed to stand about 3 hrs under stirring at 30°C, and then the solution was replaced with a new solution of the same concentration. This procedure was

repeated four times. The equilibrium for small ions between the membrane and the external solution phases might be established by this procedure. The membrane treated with solutions was wiped with a filter paper and immersed in 100 ml of deionized water for 2 hrs under agitation. This procedure was repeated several times until no Cl^- ions are detected in the external pure water. The Cl^- ions contained in the whole washings were analyzed by titration against $AgNO_3$ by the usual way or by the potentiometric titration. The value of C_- (equiv./l) in the membrane was evaluated as the total amounts of Cl ions(moles) determined above devided by the volume of the water contained within the membrane.

The surface dried membrane of PS-1 equilibrated with a given concentration of KCl solution was rinsed with 1 N HCl solution. The quantity of K^+ ions in the washings was determined by a flame photometer (Hitachi Manf. Co. Type EPU-2). The rinsing was continued until no trace of K^+ ion was detected. The total amount of K^+ ion is obtained by summing up the amount of K^+ ion in the washings.

As shown in table 3-2, the value of C_+ thus obtained at a given external salt concentration agreed quite well with the value calculated from the condition of the electroneutrality given by $C_+ = C_- + X$ using the experimental data of C_-. Therefore, C_+ for the other combination of membrane and electrolyte was evaluated from the

Table 3-2. Comparison between the values of C_+ determined directly with a flame photometer and those calculated from the relation, $C_+ = C_- + X$. The membrane is PS-1 and the electrolyte is KCl.

C (N)	$C_+ = C_- + X$	C_+ determined by a flame photometer
0.0039	0.225	0.215
0.0078	0.227	0.227
0.0156	0.229	0.252
0.0313	0.239	0.238
0.0625	0.269	0.278
0.125	0.328	0.325
0.250	0.444	0.444
0.500	0.690	0.723

neutrality condition. From these experimental values of C_- and X, we are able to estimate the acitivity coefficent $\gamma_+\gamma_-$ in the membrane with use of Eq.(3-2).

Determination of Mobilities of Small Ions in Membranes

The mobilities of Na^+ and Cl^- in membranes can be determined by measuring the isotope flux under the condition that two identical solutions, are separated by the membrane. The fluX of the isotope, J_k^*, is represented by the following equation[11],

$$J_k^* = \frac{RT u_k C_k \Delta C_k^*}{FLC} \qquad (3\text{-}3)$$

where C_k is the concentration of a cold ion species k in the membrane, L the effective thickness of the membrane, C the concentration of the external salt solution, and ΔC_k^* the difference between the tracer concentrations in the two compartments. In the derivation of Eq.(3-3), the effect of the stagnant liquid layer adjacent to the membrane surface is neglected. This is not unreasonable as long as the external solution is agitated vigorously and C is not extremely low.

The geometrical area of the membrane was 1.04 cm^2. Each compartment contained 40.0 ml of the salt solution. The solutions were stirred vigorously, and were replaced by a new solution several times every two or three hours before introducing the radio-isotope. This

procedure permits the memebrane and the bulk solution to equilibrate. An appropriate amount of radioactive isotope was added to one compartment. At a predetermined time interval, 0.20 ml of the solution was withdrawn from each compartment with micropipette. The radioactivity of the test solution containing Na^{22} or Cl^{36} was determined with a scintillation spectrometer (Aloka, model LSC 501). During one experiment, the radioactivity of the hot compartment, $(CPM)_2$, remained constant within the accuracy of the measurements, and that of the cold compartment, $(CPM)_1$ increased linearly with time after a short time lag at the outset. When the slope of this linear portion is denoted by S, i.e. $S = d(CPM)_1/dt$, the mobility u_k can be evaluated by the equation,

$$u_k = \left(\frac{FL}{RT}\right) J_k^* \frac{C}{C_k} \frac{1}{\Delta C_k^*} = fV\left(\frac{F}{RT}\right)\left(\frac{L_o}{A_o}\right)\left(\frac{C}{C_k}\right)\frac{S}{(CPM)_2} \qquad (3\text{-}4)$$

where V is the volume of electrolyte solution in each compartment, A_o and L_o are the geometrical area and thickness of the membrane, respectively, and f is the tortousity factor. In general, the effective area, A, is smaller than A_o, and the effective thickness of the membrane, L, is larger than L_o. Then, f is defined by the equation,

$$f = (A_o/L_o)/(A/L) \qquad (3\text{-}5)$$

Since the influence of fixed charges in the membrane on the activities

and mobilities is diminished when the concentration of the external solution is high compared with the fixed charge density, X, the value of f can be determined from the limiting value of the concentration of the external solution. Then Eq.(3-6) follows from Eq.(3-4) when the cold ion concentration in the membrane C_k approaches the solution concentration C.

$$f = \frac{A_o}{L_o} \frac{(CPM)_2}{VS} \frac{RT}{F} u_k^o \qquad (3\text{-}6)$$

Here u_k^o is the mobility of ion species k in the bulk solution at a concentration C. This factor is assumed to be constant irrespective of the concentration and species of ions in the membrane so far as the membrane is not swollen by the variation of salt concentration as encountered in the present study. Once the value of f is evaluated for a given combination of a membrane and an electrolyte , the mobility of ion species k in the membrane can be evaluated from Eq.(3-4) by using the data for C_k in the membrane at a given concentration of the external salt solutions.

For determination of the mobilities of ion species whose radioactive isptopes are not readily available, e.g. K^+, Li^+, the following method has been employed.

Fig. 3-2 shows a schematic diagram of the system for the determination of mobilities of small ions in the membrane. A negatively

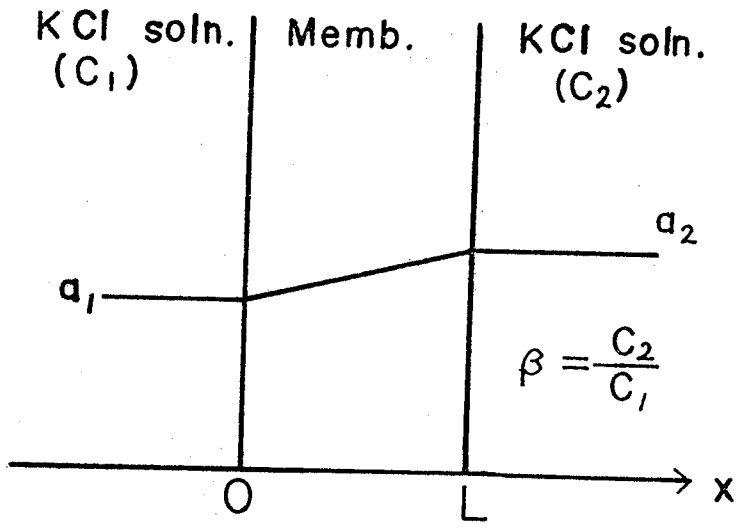

Fig. 3-2. System used for the determination of u_+C_+ and u_-C_- in the membrane.

ionized membrane of uniform thickness separates two large compartments containing solutions of 1:1 type electrolyte of different concentrations C_1 and C_2 $(C_1 < C_2)$, and their activities are denoted by a_1 and a_2, respectively. The temperature and pressure are assumed to be constant throughout the system and the two solutions are stirred vigorously to maintain the concentration in each compartment uniform. Following to Schlögl et al,[12] the steady state values of salt flux J_s and membrane potential $\Delta\varphi$ for the system mentined above can be represented by Eqs.(3-7) and (3-8).

$$\Delta\varphi = -\frac{RT}{F}\int_{a_1}^{a_2}\frac{u_+C_+ - u_-C_-}{u_+C_+ + u_-C_-}\,d\ln a + \int_0^L \frac{(C_+^* - C^*)\,U_m}{u_+C_+ + u_-C_-}\,dx \qquad (3\text{-}7)$$

$$J_s = -\frac{2RT}{FL}\int_0^L \frac{u_+C_+\,u_-C_-}{u_+C_+ + u_-C_-}\,\frac{d\ln a}{dx}\,dx + \frac{U_m}{L}\int \frac{u_+C_+C^* - u_-C_-C_+^*}{u_+C_+ + u_-C_-}\,dx \qquad (3\text{-}8)$$

As will be discussed in detail in the following chapter, the contributions of mass movement to $\Delta\varphi$ and J_s, which is represented by the second terms in the right hand side of Eqs.(3-7) and (3-8) are evaluated to be less than several percent. Therefore, this term is neglected in the subsequent analysis. The error stemming from this neglection of U_m terms for the evaluated u_+ and u_- will be less than 10 %.

In Eqs.(3-7) and (3-8) the quantity a is the geometrical mean of the activities of cation and anion defined by $(a_+a_-)^{1/2}$ at an arbitrary

point in the membrane. By the definition of a, the activity of the electrolyte component is continuous throughout the system considered, i.e. the Donnan equilibrium condition $a^2 = a_+ a_-$ is maintained at the membrane-solution interface (see Eq.3-1). Note that a is a function of x in the membrane.

The case will now be considered for the ratio of concentrations in two bulk solutions close to unity. In the following, β stands for the ratio of concentration, i.e.

$$\beta = C_2/C_1 \tag{3-9}$$

Expanding Eqs.(3-7) and (3-8) in powers of $(\beta - 1)$, we obtain

$$\Delta\varphi = -\frac{RT}{F}\left(\frac{u_+c_+ - u_-c_-}{u_+c_+ + u_-c_-}\right)_{a=a_1} \ln\beta + A(a_1)(\beta - 1 - \ln\beta) + \cdots \tag{3-10}$$

$$J_s = -\frac{2RT}{F}\left(\frac{u_+c_+u_-c_-}{u_+c_+ + u_-c_-}\right)_{a=a_1} \ln\beta + B(a_1)(\beta - 1 - \ln\beta) + \cdots \tag{3-11}$$

where $A(a_1)$ and $B(a_1)$ are constants depending only on the activity of the electrolyte component in the bulk solution of one side of the membrane. When β is close to unity, $\ln\beta$ is of the order of $(\beta - 1)$, while $(\beta - 1 - \ln\beta)$ is of the order of $(\beta - 1)^2$, and then ΔJ_s and $\Delta\varphi$ depend linearly on $\ln\beta$ when $\beta \cong 1$. Combining Eqs.(3-10) and (3-11), the following equations are obtained,

$$-[(RT/F)\ln\beta + \Delta\varphi]/LJ_s = (u_+C_+)^{-1}_{a=a_1} + C(a_1)(\beta-1) + O(\beta-1)^2 \quad (3\text{-}12)$$

$$-[(RT/F)\ln\beta - \Delta\varphi]/LJ_s = (u_-C_-)^{-1}_{a=a_1} + D(a_1)(\beta-1) + O(\beta-1)^2 \quad (3\text{-}13)$$

where $C(a_1)$ and $D(a_1)$ are constant independent of β, and $(u_iC_i)_{a=a_1}$ ($i = +, -$) is the value of u_iC_i in the membrane immersed in an electrolyte solution of activity a_1. Eqs.(3-12) and (3-13) imply that the values of (u_+C_+) and (u_-C_-) in the membrane which is contiguous with an electrolyte solution of activity a_1 and hence of concentration C_1, can be determined from the ordinate intercepts of

$$-[(RT/F)\ln\beta \pm \Delta\varphi]/LJ_s$$

plotted against $(\beta - 1)$ at a fixed value of C_1. Since the values of C_+ and C_- in the membrane at concentration C_1 are obtained by chemical analysis as mentioned above, the absolute values of u_+ and u_- in the membrane can be determined.

Fig. 3-3 illustrates schematically the cell and apparatus for measurements of membrane potential. The emf arisen between two aqueous solutions separated by a membrane was conducted to a high input-impedance electrometer (Takeda Riken Co. Model TR-8651) through a pair of KCl saturated salt bridge. The bulk solutions were agitated vigorously by a pair of magnetic stirrers so as to eliminate the contribution of a stagnant layer adhered to the membrane surface. The emf measurement

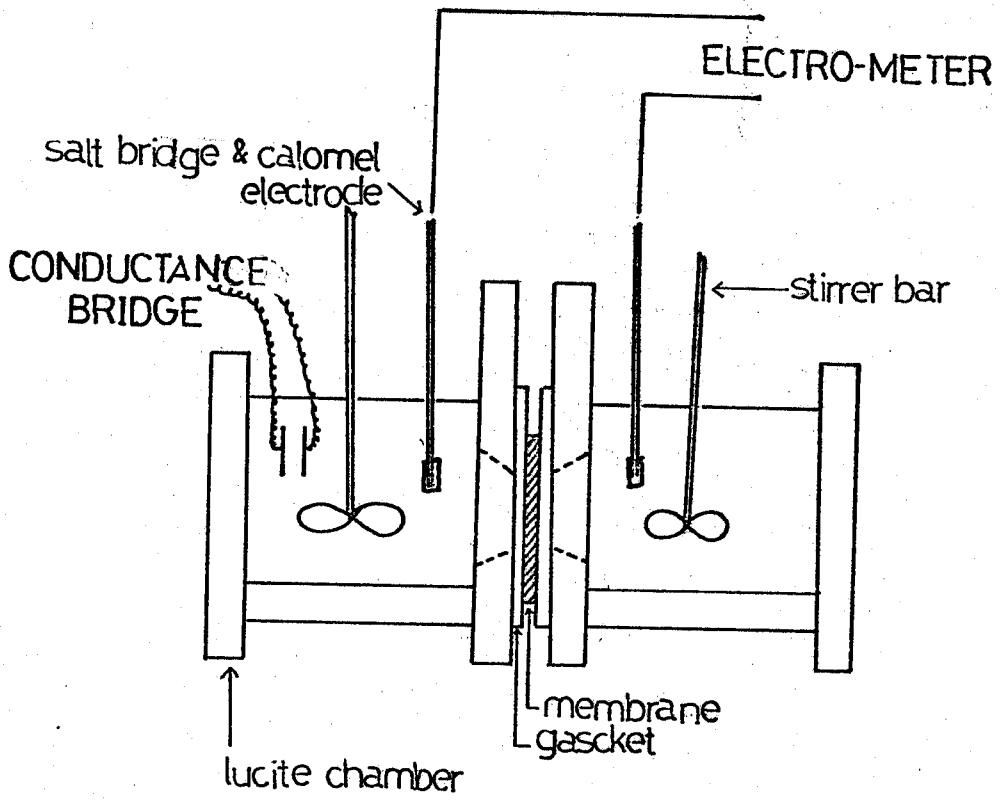

Fig. 3-3. Schematic diagram for a cell and an apparatus of measuring a membrane potential and salt flux.

was repeated two or three times at a given condition, and the averaged value was taken as a value of membrane potential at that combination of solutions. The meaurements of J_s were done using the essentially same cell depicted in Fig. 3-3. The variation of salt concentration on either side of the membrane was followed as a function of time by means of the conductometric method. The solutions in two compartments were stirred vigorously by a pair of magnetic stirrers. Before starting the measurement of salt flux for a given pair of C_1 and C_2, the membrane was allowed to stand over-night with the same pair of solutions to be measured. The conductance of the solution in either side of the membrane was found to change linearly with time from the onset of each run. When the slope of this linear portion of the conductance vs. time plot is denoted by θ, the steady flux of the electrolyte J_s can be calculated by the relation[13]

$$J_s = -VC_1\theta/A\Lambda_1^\circ \qquad (3\text{-}14)$$

where V is the volume of the solution contained in the test compartment, Λ_1°, the initial conductance of the solution, and A, the effective area of the membrane. Upon introduction of Eq.(3-14) into Eqs.(3-12) and (3-13), the ratio of the effective area and thickness of the membrane, f appear in the resulting equations. (see Eq.3-5) The value of f may be obtained from the data of fu_i/u_i° at the concentrated

limit. The value of f thus obtained must be independent of ion species i for a given pair of membrane and an electrolyte component. Actually, the value of f obtained from co-ion and counter-ion agreed each other within 3 %. The experiments were performed in an air oven regulated at 30° C.

Results and Discussion

Activity coefficients of small ions.

The results of analysis of C_+ and C_- in the membranes are presented in tables 3-3 and 3-4 at various concentrations of the external NaCl and KCl solution. Strictly speaking, instead of Eq.(3-2) the Donnan condition is written as follows

$$\begin{aligned} \gamma_+\gamma_- / (\gamma_\pm^\circ)^2 &= (c^2/c_+c_-)\exp\{-v_s(c_+ + c_- - 2c)\} \\ &\cong (c^2/c_+c_-)\{1 - v_s(c_+ + c_- - 2c) + \cdots\} \end{aligned} \qquad (3\text{-}15)$$

Here v_s stands for the partial molar volume of salt and the van't Hoff equation for the osmotic pressure difference is used. The calculation of the second term of r.h.s. of Eq.(3-15) using the data given in Tables 3-3 and 3-4 reveals that the value of correction term caused by the osmotic pressure difference is at most 0.03, which is negligibly small than unity. Hence, Eq.(3-2) is employed for the present analysis. By introducing C_- and C_+ ($C_+ = C_- + X$) determined experimentally as described above into Eq.(3-2) the value of $\gamma_+\gamma_-/(\gamma_\pm^\circ)^2$

Table 3-3. Experimental values of C_-, $\gamma_+\gamma_-/(\gamma_\pm)^2$, u_+ and u_- for various concentrations of external NaCl solutions

Membrane	C (N)	C_- (N)	$\gamma_+\gamma_-/(\gamma_\pm)^2$	$u_+ \times 10^4$ *)	$u_- \times 10^4$ *)
PS-1	0.0039	0.0003	0.22	0.53	8.45
(X=	0.0078	0.0013	0.21	0.87	
0.224)	0.0156	0.0041	0.26	1.23	6.55
	0.0313	0.0129	0.32		6.80
	0.0625	0.0376	0.40	2.17	6.70
	0.125	0.0944	0.52		7.72
	0.250	0.214	0.67	3.52	6.23
	0.500	0.445	0.84		6.17
PS-2	0.0039	0.0008	0.16	0.975	8.08
(X=	0.0078	0.0024	0.21	1.13	7.80
0.116)	0.0156	0.0072	0.27	1.63	8.35
	0.0313	0.0210	0.34	1.95	7.15
	0.0625	0.0506	0.46		7.35
	0.125	0.112	0.61	3.32	7.35
	0.250	0.234	0.76		7.73
	0.500	0.468	0.92	4.25	7.53
PS-3	0.0039	0.0012	0.28	1.70	
(X=	0.0078	0.0041	0.31	2.05	
0.0438)	0.0156	0.0109	0.41		
	0.0313	0.0255	0.55		
	0.0625	0.0563	0.69	4.32	
	0.125	0.118	0.82	4.58	
	0.250	0.240	0.92		
	0.500	0.480	0.99	6.63	

*) In units of $cm^2 \cdot sec^{-1} \cdot volt^{-1}$.

Table 3-4. Experimental values of C_-, $\gamma_+\gamma_-/(\gamma_\pm)^2$, u_+ and u_- for various concentrations of external KCl solutions

membrane	C (N)	C_- (N)	$\gamma_+\gamma_-/(\gamma_\pm)^2$	$u_+ \times 10^4$ *)	$u_- \times 10^4$ *)
PS-1	0.0039	0.0009	0.08	0.255	6.1
	0.0078	0.0025	0.11	0.712	6.59
	0.0156	0.0050	0.21	1.19	8.60
	0.0313	0.0151	0.27	2.05	8.39
	0.0625	0.0440	0.33	2.68	7.50
	0.125	0.104	0.46	3.78	6.60
	0.250	0.220	0.64	4.77	6.58
	0.500	0.466	0.78	5.41	6.75
PS-2	0.0039	0.0014	0.09	0.93	6.11
	0.0078	0.0031	0.16	1.23	6.93
	0.0156	0.0107	0.18	2.10	6.21
	0.0313	0.0243	0.29	2.74	6.78
	0.0625	0.0528	0.48	4.18	7.82
	0.125	0.230	0.60	5.12	7.30
	0.250	0.234	0.76	6.15	7.13
	0.500	0.474	0.89	6.86	7.59
PS-3	0.0039	0.0023	0.14	1.32	6.25
	0.0078	0.0048	0.26	1.83	7.45
	0.0156	0.0119	0.37	3.11	7.65
	0.0313	0.0265	0.53	3.67	7.36
	0.0625	0.0581	0.66	5.02	7.15
	0.125	0.121	0.78	5.72	7.02
	0.250	0.245	0.88	5.93	6.94
	0.500	0.488	0.96	6.25	6.73

*) in units of $cm^2 sec^{-1} volt^{-1}$.

can be evaluated. Fig. 3-4 shows the data for $\gamma_+\gamma_-/(\gamma_\pm^\circ)^2$ as a function of C/X in various pairs of NaCl or LiCl and three membranes having different values of X. The similar plots of KCl are shown in Fig. 3-5. It is seen that the observed points for different pairs of X and C follow a single curve when plotted against log (C/X) for every electrolytes studied.

In the field of polyelectrolyte solution studies, it has been widely accepted that the activity coefficents of counter- and co-ions are represented by an empirical equation known as the "additivity rule"[14]. The charged groups are localized on the polymer chains not only in a polyelectrolyte solution but also in the membrane matrix. Therefore, it is reasonable to use the same functional form both in polyelectrolyte solution and membranes to describe the non-ideality of the activity of small ions in the membrane[13]. The additivity rule can be written for the present system as follows;

$$\gamma_+ = \gamma_\pm^\circ (c_- + \phi x)/(c_- + x)$$
$$\gamma_- = \gamma_\pm^\circ \qquad (3\text{-}16)$$

where ϕ $(0<\phi<1)$ is a characteristic constant for the membrane-electrolyte combination considered, and represents the fraction of counter ions not tightly bound to the polymer skeletons constituting the membrane. ϕX may be referred to as the thermodynamically effective charge density of a membrane.

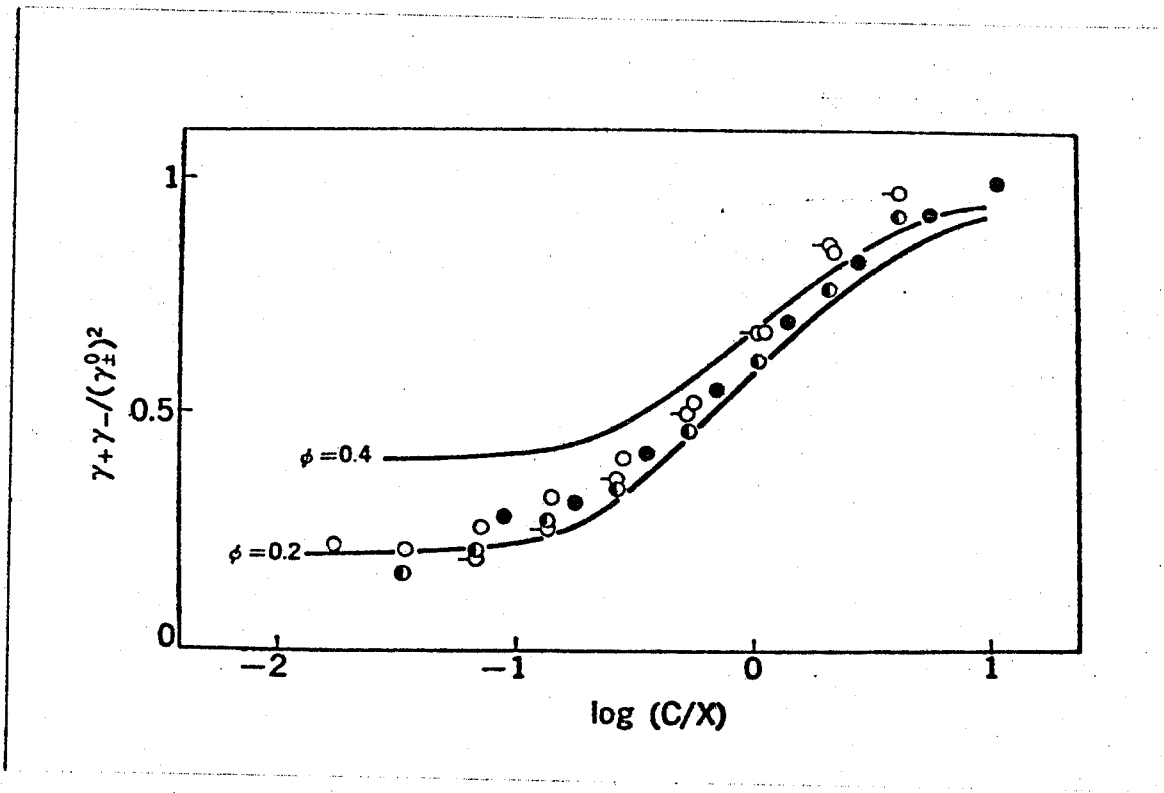

Fig. 3-4. Plots of $\gamma_+\gamma_-/(\gamma_\pm)^2$ against log(C/X).

○, PS-1; ◑, PS-2; ●, PS-3 for NaCl; -○, PS-2 for LiCl. Solid lines represent calculated values using Eq.(3-17) with ϕ = 0.2 and 0.4, respectively.

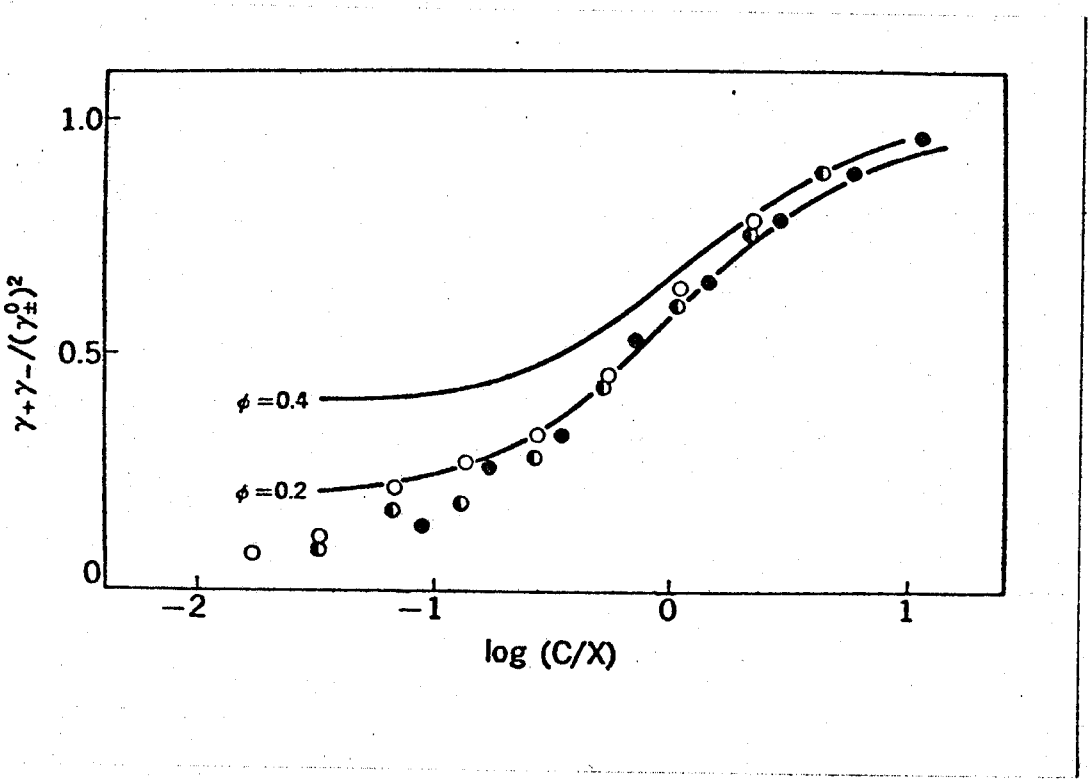

Fig. 3-5. Plots of $\gamma_+\gamma_-/(\gamma_\pm)^2$ in various concentrations of KCl solution. ○, PS-1; ◑, PS-2; ●, PS-3. Solid lines represent calculated values using Eq.(3-17) with ϕ = 0.2 and 0.4, respectively.

Combining Eqs.(3-2) and (3-16), we obtain the following equation which expresses $\gamma_+\gamma_-/(\gamma_\pm^0)^2$ as a function of C/X and ϕ.

$$\frac{\gamma_+\gamma_-}{(\gamma_\pm^0)^2} = \frac{\phi + \sqrt{\phi^2 + 4(C/X)^2}}{2-\phi + \sqrt{\phi^2 + 4(C/X)^2}} \qquad (3\text{-}17)$$

Expanding the above equation under the condition that $C \gg \phi X$ yields

$$\gamma_+\gamma_-/(\gamma_\pm^0)^2 = 1 - [(1-\phi)X]/C + O(\tfrac{1}{C})^2$$

This equation means that the slope of the plots of $\gamma_+\gamma_-/(\gamma_\pm^0)^2$ against X/C gives the value of $(1-\phi)$. The value of ϕ thus obtained was 0.4 ± 0.05. Introducing the value of ϕ determined above into Eq.(3-17), $\gamma_+\gamma_-/(\gamma_\pm^0)^2$ can be calculated as a function of C/X, and compared with the experimental results given in Figs.3-4 and 3-5. The data points deviate appreciably in a dilute solution from the calculated curve when ϕ is taken as constant of 0.4. This implies that the value of ϕ decreases with decreasing salt concentration C when C is less than X. When we put the value of C/X into zero the value of Eq.(3-17) takes ϕ, which indicates that ϕ may be evaluated in the region of very dilute concentration in external solutions. Figs. 3-4 and 3-5 give $\phi = 0.2$ for dilute concentration region, while $\phi = 0.4$ for the concentrated region as described above. The values of ϕ thus obtained for different pairs of X and C were found to follow a single sigmoid-shaped curve when plotted against log (C/X) and the curve approached 0.4 and 0.2 at the upper and the lower limits of log (C/X), respectively.

Mobilities of small ions

The radioactivity of the cold compartment increased proportionally with time after about 20 min from the onset of each run. The linear portion of this plot is used for the determination of the flux of the isotope. The experimental error in determination of the slope was less than ± 5 %. Fig. 3-6 illustrates determination of the tortuosity factor f in accordance with Eq.(3-6). The ordinate of the figure represents $(F/RT)(C_o/A_o)\ SV/(CPM)_2 u_k^o$, and the abscissa is 1/C. The ordinate intercept of this plot yields the value of 1/f. As seen in the figure, f is a constant irrespective of ion species i for a given membrane-electrolyte pair.

As for the determination of mobility of K^+ ion, the membrane potential data obtained with membrane PS-2 at various fixed values of C are plotted against log β in Fig. 3-7. Fig. 3-8 illustrates the linear relations between fLJ_s $(=-L_o V C_1 S/A_o \lambda_1^o)$ and log β for the same system as in Fig. 3-7. Note that the values indicated in Fig. 3-8 used the geometrical values of L and A, and hence the data include the tortuosity factor f. Fig. 3-9 shows the linear relations between $-[(RT/F)\ln\beta + \Delta\varphi]/fLJ_s$ and $-[(RT/F)\ln\beta - \Delta\varphi]/(fLJ_s)$ against $(\beta - 1)$ for membrane PS-2 in KCl solution of C = 0.0625 N. Similar results were obtained for other combinations of membrane and electrolyte. In both plots, the data points follow the corresponding straight line at any pair

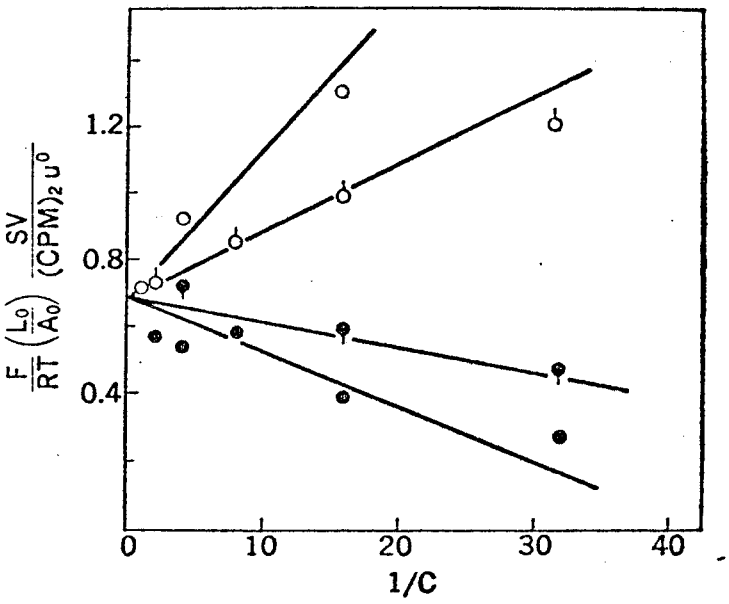

Fig. 3-6. Determination of the tortuosity factor f for systems of two kinds of membranes and ^{22}Na and ^{36}Cl. Results of ^{22}Na, ○, PS-1; ♁, PS-2. Results of ^{36}Cl, ●, PS-1; ⚲, PS-2.

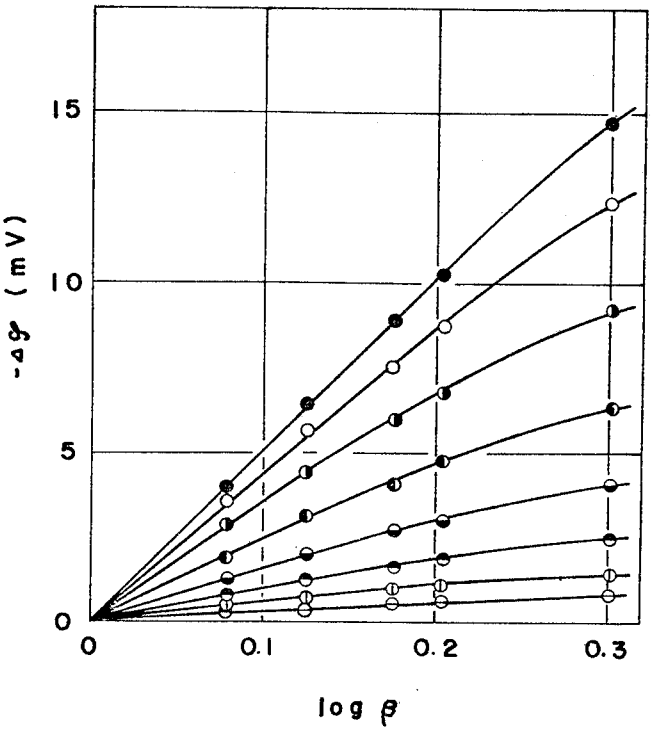

Fig. 3-7. Dependence of membrane potential on log β for the system of PS-2 and KCl at various fixed values of C_1. ●, C_1 = 0.0039 N; ○, 0.0078 N; ◑, 0.0156 N; ◐, 0.0313 N; ◒, 0.0625 N; ◓, 0.125 N; ⊕, 0.250 N; ⊖, 0.500 N.

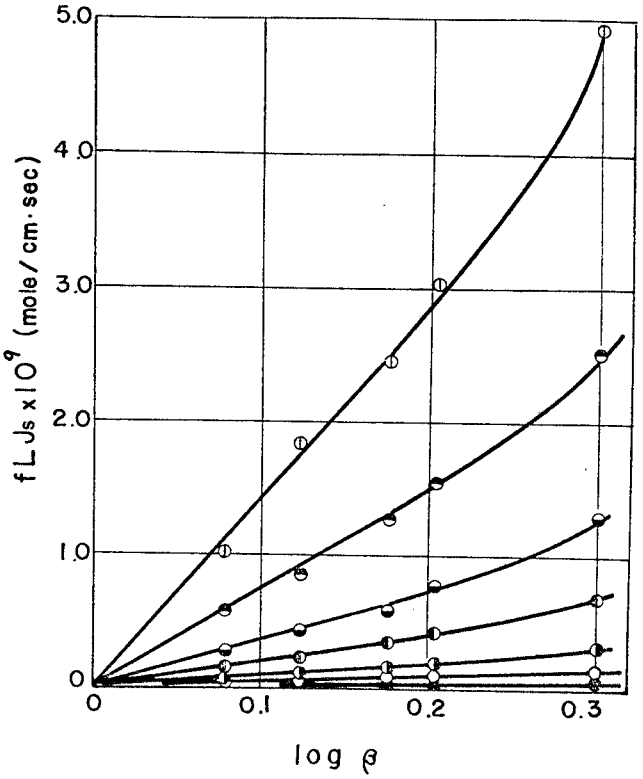

Fig. 3-8. Plots of fLJ_s against log β for the same system in Fig. 3-7 at various fixed values of C_1. Notations are the same as in Fig. 3-7.

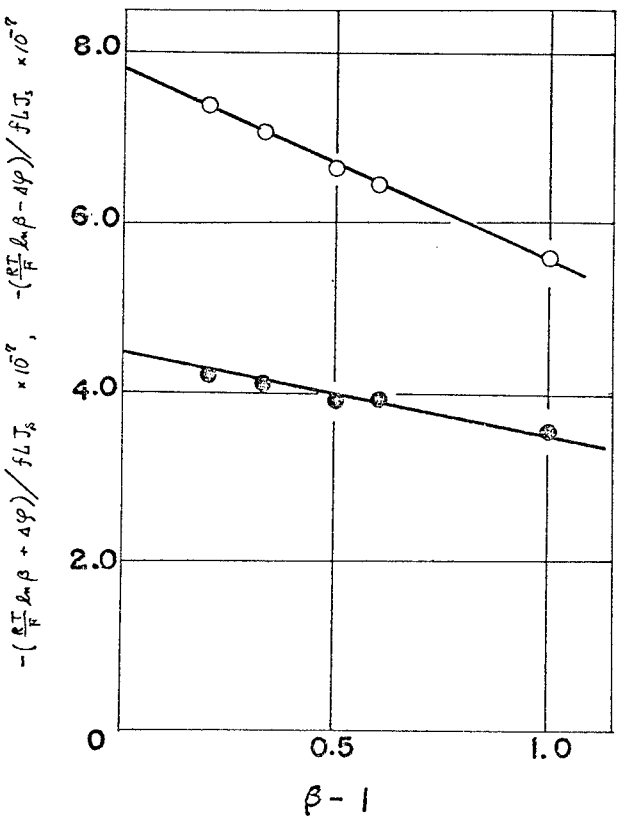

Fig. 3-9. Plots of $-[(RT/F) \ln \beta + 4\varphi]/(fLJ_s)$ and $-[(RT/F) \ln \beta - 4\varphi]/(fLJ_s)$ against $(\beta - 1)$ for the system of PS-2 and KCl at C_1 = 0.0625 N.

○, $-[(RT/F) \ln \beta - 4\varphi]/(fLJ_s)$; ●, $-[(RT/F) \ln \beta + 4\varphi]/(fLJ_s)$.

of membrane and salt concentration studied. The values of fu_+C_+ and fu_-C_- are determined from the ordinate intercepts of these straight lines by means of Eqs.(3-12) and (3-13). As noted above the absolute values of u_+ and u_- in the membrane can be evaluated by introducing the values of C_+ and C_- at the corresponding external salt concentration, together with the value of f for each membrane. Combining the values of u_iC_i, C_i and f determined above, we can evaluate u_+ and u_- in the charged membrane at an arbitrary salt concentration in the external solution. They are listed in Tables 3-3 and 3-4. In Figs. 3-10 and 3-11, u_+/u_+° and u_-/u_-° for NaCl and KCl are plotted against log(C/X) for three membranes.

It is noted that u_- (coions in the present case) in the membrane is approximately constant and is equal to the mobility in bulk solution over the entire concentration range indicated. In contrast, u_+/u_+° decreases with decreasing C/X. It is interesting to note that the concentration dependence of u_+/u_+° is practically the same as that of $\gamma_+\gamma_-/(\gamma_\pm^\circ)^2$ given in Figs. 3-4 and 3-5, for the respective systems. The data points closely follow the solid line, and therefore, it may be reasonable to express the concentration dependence of mobility as

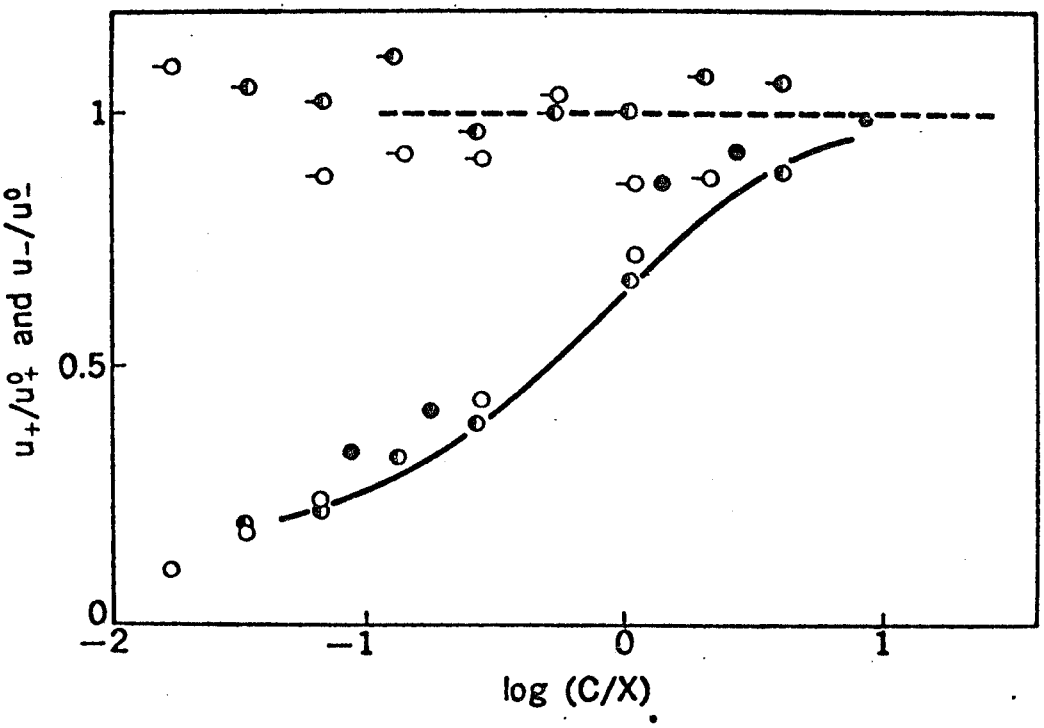

Fig. 3-10. Concentration dependence of u_+/u_+° and u_-/u_-° in NaCl solution. Results of u_-/u_-°, ○, PS-1; ◑, PS-2; ●, PS-3. Results of u_+/u_+°, ○, PS-1; ◑, PS-2; ●, PS-3. Solid line represents the experimental curve of $\gamma_+\gamma_-/(\gamma_\pm)^2$ shown in Fig. 3-4.

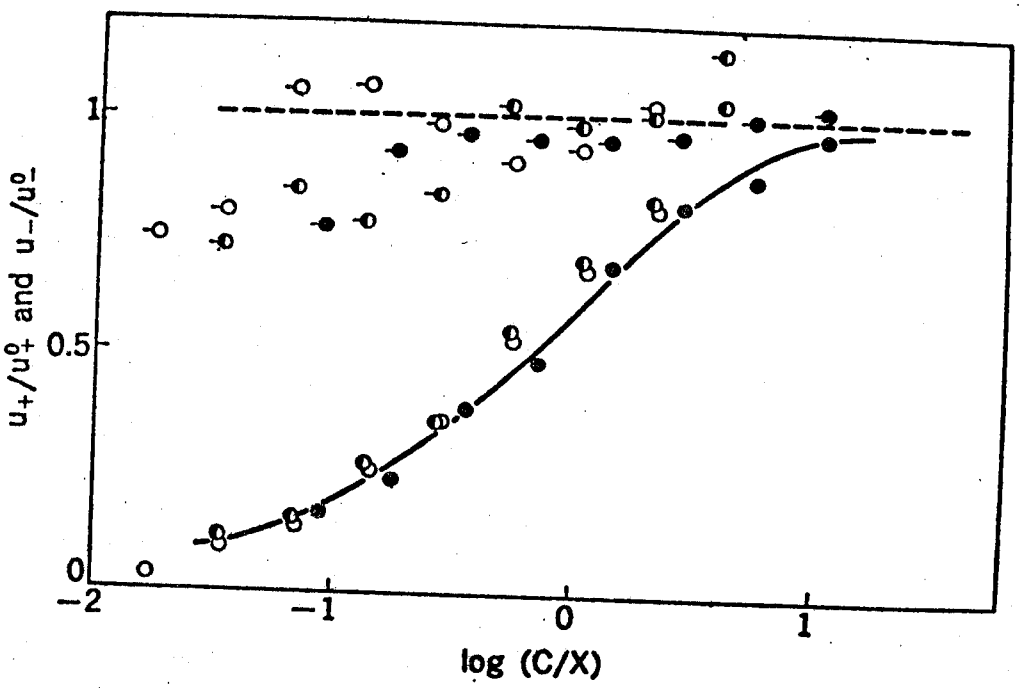

Fig. 3-11. Concentration dependence of u_+/u_+° and u_-/u_-° in KCl solution. Notations are the same as in Fig. 3-10. Solid line represents the experimental curve of $(\gamma_+\gamma_-)/(\gamma_\pm)^2$ shown in Fig. 3-5.

$$u_+ = u_+^\circ \frac{c_- + \phi X}{c_- + X} \qquad u_- = u_-^\circ \tag{3-18}$$

which is analogous to Eq.(3-16) for activity coefficients.

The agreement between concentration dependences of mobilities and activity coefficients of small ions in the membrane leads to the following flux equation for species k rather than Eq.(2-9), assuming $\gamma_\pm^\circ = 1$.

$$FJ_k = -u_k^\circ a_k (\partial \tilde{\mu}_k / \partial x) + FC_k^* U_m \tag{3-19}$$

This representation for the flux of species k was used intuitively by previous investigators for the analysis of membrane phenomena[15]. The factors involved in the flow processes of ions are different from those in thermodynamic or static problems, as seen in Debye-Hückel's and Ongager's theories for activities and mobilities of ions in electrolyte solutions. Thus the coincidence of ϕX in Eqs (3-25) and (3-27) for the whole range of salt concentrations seems rather fortuitous although this agreement leads to a great simplification in the theoretical analysis of membrane phenomena, as will be discussed later. The theoretical consideration of Eq.(3-19) will be given in the subsequent chapter.

References

1) T. Teorell, Proc. Soc. Exptl. Biol., 33, 282 (1935).

2) K. H. Meyer and J. F. Sievers, Helv. Chim. Acta., 19, 649, 665, 987(1936).

3) A. J. Staverman, Trans. Faraday Soc., 48, 176 (1952).

4) G. Scatchard, Discussions Faraday Soc. 21, 30 (1956).

5) N. Lakshminarayanaiah and V. Subrahmanyan, J. Polymer Sci., A2, 4491(1964).

6) Y. Kobatake, N. Takeguchi, Y. Toyoshima, and H. Fujita, J. Phys. Chem., 69, 3981(1965).

7) R. Schlögl, Z. Elektrochem. 57, 195(1953).

8) G. J. Hills, P. W. M. Jacobs and N. Lakshminarayanaiah, Proc. Roy. Soc. A262, 257(1961).

9) R. Neihof, J. Phys. Chem., 58, 916(1954).

10) M. Kato, T. Nakagawa and H. Akamatsu, Bull. Chem. Soc. Japan 33, 322(1960).

11) N. Lakshminarayanaiah, "Transport Phenomena in Membranes" Academic Press, New York (1969).

12) R. Schlögl and F. Helfferlich, Z. Physik. Chem. 162, 346 (1932).

13) Y. Toyoshima, Y. Kobatake and H. Fujita, Trans. Faraday Soc., 63, 2814 (1967).

14) A. Katchalsky, Z. Alexandrowicz, and O. Kedem, "Chemical Physics of Ionic Solutions", p.296, John Wily and Sons, Inc., New York(1966).

15) M. Nagasawa and I. Kagawa, Discussions Faraday Soc., 21, 52(1956).

Chapter 4. Theoretical Consideration on the Relation between Mobilities and Activity Coefficients of Small Ions

In chapter 3, it was shown that the activity coefficients and mobilities of small ions in a charged membrane can be expressed by Eqs. (3-16) and (3-18), respectively. This conclusion has been confirmed also in a polyelectrolyte solution by measuring the self-diffusion of small ions in an aqueous solution of poly-styrenesulfonic acid[1]. Then, we have

$$\gamma_i/\gamma_i^{\circ} = u_i/u_i^{\circ} \qquad (i = +, -) \qquad (4\text{-}1)$$

which implies that the concentration dependences of mobility of a small ion in the membrane agree with that of activity coefficent Several authers[2-7] attemped to derive theoretically the self-diffusion constant, but their results did not accord with the experimental data shown in the previous chapters.

In this chapter, the relation between the activity and mobility of small ions in charged membrane and/or in polyelectrolyte solution will be derived theoretically by using a cell model. The result obtained is in line with the conclusion drawn from the experimental studies.

Basic Equation for Mobilities of Small Ions

The macro-ions constituting the membrane are located in the membrane phase. It is assumed that a macroion is localized periodically in the membrane phase with forming a cubic lattice of a lattice constant, 2d. In other words, the membrane phase is subdivided into unit cell containing a macro-ion, which is regarded as the central ion in the unit cell. In any unit cell, the condition of the electro-neutrality is assumed to be satisfied. Then, it is sufficient to confine our consideration to an arbitrary unit cell for calculating the flux of small ions. The electrostatic potential at a point in the cell caused by central ion is denoted by φ. The symmetry requirement of the electrostatic potential at the peripheral surface, R, can be written as

$$(\nabla\varphi)_R = 0 \qquad (4\text{-}2)$$

Following the treatment of Katchalsky et al.[8], it may be assumed that

$$\varphi^R = 0 \qquad (4\text{-}3)$$

since the choice of the reference point of potential is arbitrary. The concentration of i-ion at the surface of a cell is denoted by n_i^R, which is equivalent to the activity of i-ion[9]. The distribution of small ions in a cell is represented by Boltzmann's equation, and the concentration of i-ion at point $\mathbf{r}$, n_i is given by

$$n_i = n_i^R \exp(-z_i e\varphi/kT) = n_i^R \exp(-z_i \varepsilon) \tag{4-4}$$

where ε is the reduced electric potential defined by

$$\varepsilon = e\varphi/kT \tag{4-5}$$

Here, z_i stands for the valence of i-ion and e, electronic charge, k, Boltzmann constant, T, the absolute temperature, respectively.

When a constant electric field **E**(E, 0, 0) is applied in the direction of the x-axis, the local electric potential ε and local concentration of i-ion, n_i, are changed to ε_E and n_i^E, respectively. Flow of i-ion, J_i can be represented by[5,6]

$$J_i = -(kT/\gamma_i)[\nabla n_i^E + n_i^E z_i \nabla \varepsilon_E + z_i n_i^E E/kT] \tag{4-6}$$

where γ_i is the friction constant of an i-ion and assumed to be constant irrespective of salt concentration. When the perturbed quantities, ε_E and n_i^E are linealized as

$$\varepsilon_E = \varepsilon(1 + gE) \tag{4-7}$$

$$n_i^E = n_i^R \exp(-z_i \varepsilon)(1 + f_i E) \tag{4-8}$$

Eq.(4-6) is transformed to give

$$J_i = -(n_i^R/\gamma_i) \exp(-z_i \varepsilon)[\nabla h_i + z_i \mathbf{K}] E \tag{4-9}$$

under the approximation that the higher order terms of E are neglected. In Eq.(4-9), **K** is the unit vector in the direction of the x-axis and h_i is defined as follows:

$$h_i = -kT(f_i + z_i \varepsilon g) \tag{4-10}$$

To clarify the meaning of h_i, it is instructive to derive the relation between n_i^E and ε_E. Eliminating ε from Eqs.(4-7) and (4-8) with use of approximations that $gE \ll 1$ and $z_i \varepsilon_E gE \ll 1$, we obtain the following equation;

$$\begin{aligned} n_i^E &= n_i^0 \exp[-z_i \varepsilon_E (1 - gE)] \; (1 + f_i E) \\ &\simeq n_i^0 \exp(-z_i \varepsilon_E)\,[1 - (h_i/kT)E] \end{aligned} \tag{4-11}$$

Since the system is not in equilibrium owing to the externally applied electric field, E, the Boltzmann relation no longer retains between the local concentration, n_i^E and the local electric potential, ε_E, and the function h_i represents the degree of deviation of n_i^E from the Boltzmann relation at the statistical equilibrium. Since the functions f_i and g are periodic, the value of h_i is repeated in every unit cell, which in turn means that h_i is continuous at any point on the peripheral surface of a cell. Then, the following boundary condition must be satisfied for h_i;

$$h_i(d,0,0) = h_i(-d,0,0) \tag{4-12}$$

The condition of the steady state of the flux of i-ions is given by the equation; $\nabla \cdot \mathbf{J}_i = 0$ (4-13)

which leads to the relation between h_i and ε as follows;

$$-z_i(\nabla \varepsilon) \cdot (\nabla h_i) - z_i \frac{\partial \varepsilon}{\partial x} + \nabla^2 h_i = 0 \tag{4-14}$$

Derivation of Mobility for i-Ion from the Basic Equations

For simplicity of mathematical analysis, we replace the cubic unit cell by a sphere of radius d. The center of a spherically coiled macro-ion is taken as the coordinate origin of a cell. Defining q_i by Eq.(4-15),

$$q_i = h_i + z_i x \tag{4-15}$$

and introducing Eq.(4-15) into Eq.(4-), we obtain

$$-z_i(\nabla\varepsilon)\cdot(\nabla q_i) + \nabla^2 q_i = 0 \tag{4-16}$$

Considering the symmetrical requirement, we may write

$$q_i = R_i(r)Q_i(\theta) \tag{4-17}$$

where r is $(x^2+y^2+z^2)^{1/2}$ and θ, the angle between x-axis and the vector $\mathbf{r}$. Introducing Eq.(4-17) into Eq.(4-16) and rearranging, we obtain the following two equations for θ and r;

$$\frac{d^2Q_i}{d\theta^2} + \cot\theta\frac{dQ_i}{d\theta} = -l(l+1)Q_i \tag{4-18}$$

$$-z_i r^2\frac{d\varepsilon}{dr}\frac{dR_i}{dr} + r^2\frac{d^2R_i}{dr^2} + 2r\frac{dR_i}{dr} = l(l+1)R_i \tag{4-19}$$

where $l(l+1)$ is a separating constant. The solution to Eq.(4-18) is given by $P_l(\cos\theta)$ when $P(\xi)$ is the Lagrangian function of l-th order. Then, q_i can be written by $\sum_l R_{il} P_l(\cos\theta)$. Comparing this equation with Eq.(4-15), i.e. $q_i = h_i(r, \cos\theta) + z_i r\cos\theta$, the value of l must be 0 or 1. When $l = 0$, h_i is given by $-z_i r\cos\theta$ since $P_0(\cos\theta) = 1$. Introducing the relation that $h_i = -z_i\cos\theta$ into Eq.(4-9), however, yields that $J_{ix} = 0$, which is trivial solution. Then, Eq.(4-17) is recasted as follows;

$$q_i = R_i(r)\cos\theta \tag{4-20}$$

and Eq.(4-9) is reduced to

$$-z_i \frac{d\varepsilon}{dr}\frac{dR_i}{dr} + \frac{d^2R_i}{dr^2} + \frac{2}{r}\frac{dR_i}{dr} - \frac{2R_i}{r^2} = 0 \qquad (4\text{-}21)$$

Boundary condition of Eq.(4-12) requires that

$$R_i(d) = z_i d \qquad (4\text{-}22)$$

In order to solve Eq.(4-21), another boundary condition is necessary which is not known a priori. But, it is certain that the boundary condition is independent of the variation of n_i^R. Near the sperical surface, R, ε is approximately equal to zero. Then, Eq.(4-21) can be adequately approximated by Eq.(4-23) at the neighbour of the boundary of a cell, R.

$$-z_i \frac{d\varepsilon}{dr}\frac{dR_i}{dr} - z_i\varepsilon\frac{d^2R_i}{dr^2} + \frac{d^2R_i}{dr^2} + \frac{2}{r}\frac{dR_i}{dr} - \frac{2R_i}{r^2} = 0 \qquad (4\text{-}23)$$

Integration of Eq.(4-23) yields

$$-z_i\varepsilon\frac{dR_i}{dr} + \frac{dR_i}{dr} + 2\left(\frac{R_i}{r}\right) = A_i \qquad (4\text{-}24)$$

where A_i is an integration constant. It is noted that the value of A_i is not depending on n_i^R, since the integration constant is determined only from the boundary condition which is independent of n_i^R as mentioned above.

The total amount of i-ions, T_i, which is passing through the boundary sperical surface, R, of $x>0$ in the direction to x-axis is represented as follows;

$$T_i = \int_0^{\pi/2} J_{ix}(r=d)\, 2\pi d^2 \sin\theta\, d\theta$$

$$= -\left(\frac{2\pi}{3} d^2\right)\left(n_i^R/\gamma_i\right)\left[\frac{dR_i}{dr} + 2\frac{R_i}{r}\right]_{r=d} E \qquad (4\text{-}25)$$

Introducing Eqs.(4-24) and (4-3) into the above equation, we obtain

$$T_i = -(2\pi d^2/3)\left(n_i^R/\gamma_i\right) A_i E \qquad (4\text{-}26)$$

Since the cross-sectional area of a unit cell perpendicular to the x-axis is πd^2, the flow of i-ion, J_i, which is defined as the flux of i-ion per unit area is expressed by

$$J_i = T_i/(\pi d^2) = -(2/3)\left(n_i^R/\gamma_i\right) A_i E \qquad (4\text{-}27)$$

The mobilities of i-ion, u_i, is defined by Eq.(2-9), and hence, comparison between Eqs.(2-9) and (4-27) leads to the following relation.

$$u_i z_i = (2/3) A_i \gamma_i u_i^o \qquad (4\text{-}28)$$

In the derivation of the above relation, $u_i^o = 1/\gamma_i$ and $\gamma_i = n_i^R/C_i$ are used since n_i^R is equal to the activity of i-ion as is insisted by Katchalsky et al.[9] and by Oosawa[10]. They showed that the chemical potential of i-ion, μ_i, is represented by

$$\mu_i = \mu_i^o + RT \ln n_i^R$$

from the mathmatical analysis of the Poisson-Boltzmann equation, where μ_i^o stands for the standard chemical potential. Eq.(4-28) implies that the depression of mobility of counter-ions is proportional to that of activity coefficients irrespective of added salt concentration.

Comparing the experimental results given by Eq.(4-1) with Eq.(4-28), A_i is equal to $(3z_i)/2$ provided that $\gamma_{\pm}^{\circ} = 1$.

References

1) T. Ueda and Y. Kobatake, J. Phys. Chem. 77, 2995 (1973).

2) S. R. Coriell and J. L. Jackson, J. Chem. Phys. 39, 2418(1963).

3) S. Lifson and J. L. Jackson, J. Chem. Phys., 36, 2410 (1962).

4) J. L. Jackson and S. R. Coriell, J. Chem. Phys. 38, 959 (1963).

5) G. S. Manning, J. Chem. Phys., 46, 2324 (1967).

6) G. S. Manning, J. Chem. Phys., 51, 934 (1969).

7) G. M. Bell, Trans, Faraday Soc., 60, 1752(1964).

8) Z. Alexandrowics and A. Katchalsky, J. Polymer Sci., A1, 3231 (1963).

9) A. Katchalsky and Z. Alexandrowics, J. Polymer Sci., A1, 2093 (1963).

10) F. Oosawa, "Polyelectrolytes" p.33, Marcel Dekker, New York 1971.

Chapter 5. Thermodynamically Effective Charge Density of a Membrane

It has been shown in the preceeding chapters that the activity coefficients and mobilities of counter- and co-ions in charged membranes are represented by Eqs.(3-16) and (3-18) with a characteristic parameter ϕX. In contrast to the empirical additivity rule of polyelectrolyte studies[1], ϕX depended slightly upon the external salt concentrations. Once ϕX is evaluated from the data of any membrane phenomena, the other transport phenomena in which the mass movement does not play a decisive role can be predicted theoretically. In this chapter a simple method is proposed for determining ϕX of a membrane in a solution of arbitrary salt concentration, and the usefulness of ϕX thus determined will be emphasized.

Theoretical

A simple method for evaluation of ϕX in membrane

The membrane potential $\Delta\varphi$ which arises between two solutions of a 1:1 type electrolyte at different concentrations C_1 and C_2 on the two sides of the membrane is represented by Eq.(3-7). The effect of mass flow is neglected as before (second term in Eq.3-7) and Eqs.(3-16) and (3-18) for activity coefficients and mobilities of small ions in the membrane are introduced into Eq.(3-7). Substituting α as in

Eq.(5-1),

$$\alpha = \frac{u_+^\circ}{u_+^\circ + u_-^\circ} \qquad (5\text{-}1)$$

and integrating across the membrane, Eq.(5-2) is obtained.

$$\Delta\varphi = -\frac{RT}{F}\left[\ln\frac{C_2}{C_1} + (2\alpha-1)\ln\frac{\sqrt{\kappa C_2^2+\phi^2X^2}+(2\alpha-1)\phi X}{\sqrt{\kappa C_1^2+\phi^2X^2}+(2\alpha-1)\phi X} - \ln\frac{\sqrt{\kappa C_2^2+\phi^2X^2}+\phi X}{\sqrt{\kappa C_1^2+\phi^2X^2}+\phi X}\right] \qquad (5\text{-}2)$$

In the derivation of Eq.(5-2), the contribution of the unstirred liquid film was neglected.[2-4] Eq.(5-2) has the same functional form as that given by the Teorell-Meyer-Sievers theory[5,6] for the membrane potential except that the thermodynamically effective charge density ϕX of the membrane is used in place of the stoichiometric fixed charge density X. When $\phi = 1$, Eq.(5-2) is reduced to the TMS membrane potential theory. Eq.(5-2) is valid when the dependence of ϕX on salt concentration is not great and the difference in concentraions in the two bulk solutions is small. Even if a constant ϕ $(0<\phi<1)$ is used, agreement between theory and experiments is improved considerably. As an example, in Fig. 5-1 a comparison is made using a constant ϕ of 0.2. In actual calculations of the membrane potentials, the value of ϕ at the average concentration $C = (C_1 + C_2)/2$ must be used when the value of ϕX is known as a function of C. Since, it is somewhat troublesome to determine ϕX at an arbitrary external concentration from the observed membrane potential $\Delta\varphi$ using Eq.(5-2),

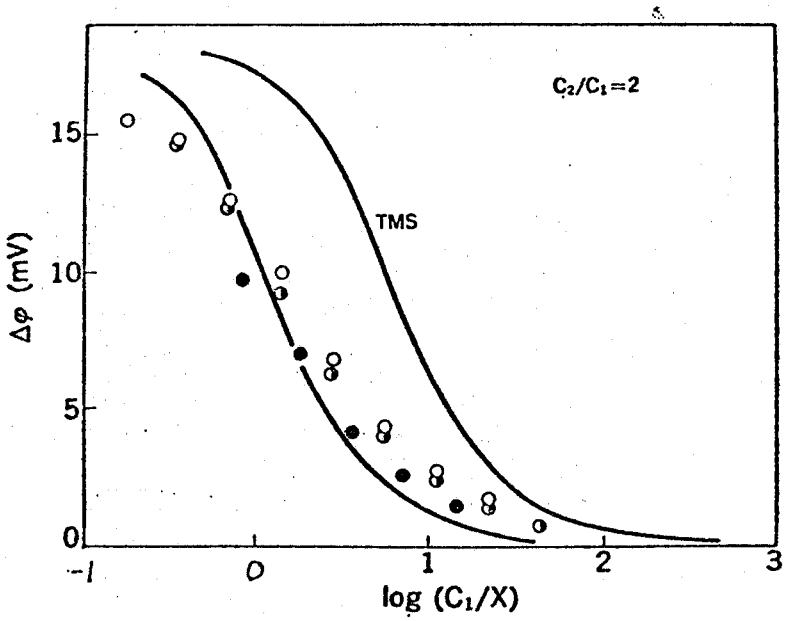

Fig. 5-1. Comparison between TMS theory and experimental data of $\Delta\varphi$. Notations are the same as in Fig. 3-4. The solid line on the left represents the theoretical curve of Eq.(5-2) with $\phi = 0.2$.

a simple method of high precision is proposed.

Defining the apparent transference number of coions in the membrane $\bar{t}_{app}$ by the Nernst equation,

$$\Delta\varphi = -(RT/F)(1-2\bar{t}_{app})\ln(c_2/c_1) \qquad (5\text{-}3)$$

equating Eq.(5-3) with Eq.(5-2) and using Eq.(3-11), we obtain the following expression for $\bar{t}_{app}$.

$$\bar{t}_{app} = \left(\frac{1-2\alpha}{2}\right)\frac{\ln\left(\frac{\sqrt{\kappa\xi_2^2+1}+2\alpha-1}{\sqrt{\kappa\xi_1^2+1}+2\alpha-1}\right)}{\ln\beta} + \frac{\ln\left(\frac{\sqrt{\kappa\xi_2^2+1}+1}{\sqrt{\kappa\xi_1^2+1}+1}\right)}{2\ln\beta} \qquad (5\text{-}4)$$

$$\xi = c/\phi X \qquad (5\text{-}5)$$

where ξ is the reduced concentration defined by Eq.(5-5). Fig.5-1 shows the relation between $\bar{t}_{app}$ and $\log(C/\phi X) = \log[(C_1 + C_2)/2\phi X]$ when the ratio of concentrations $C_2/C_1 = \beta$ is fixed at 1.5 and 2 for KCl and NaCl solutions, respectively. In the figure, α is assumed to be 0.5 for KCl and 0.4 for NaCl. It is noted that in plotting $\bar{t}_{app}$ the values are practically independent of the ratio of concentrations β, as long as β is not large within the range of conconcentrations indicated.

On the other hand, the mass fixed transference number of coions in a membrane immersed in an electrolyte solution of concentration C is defined by

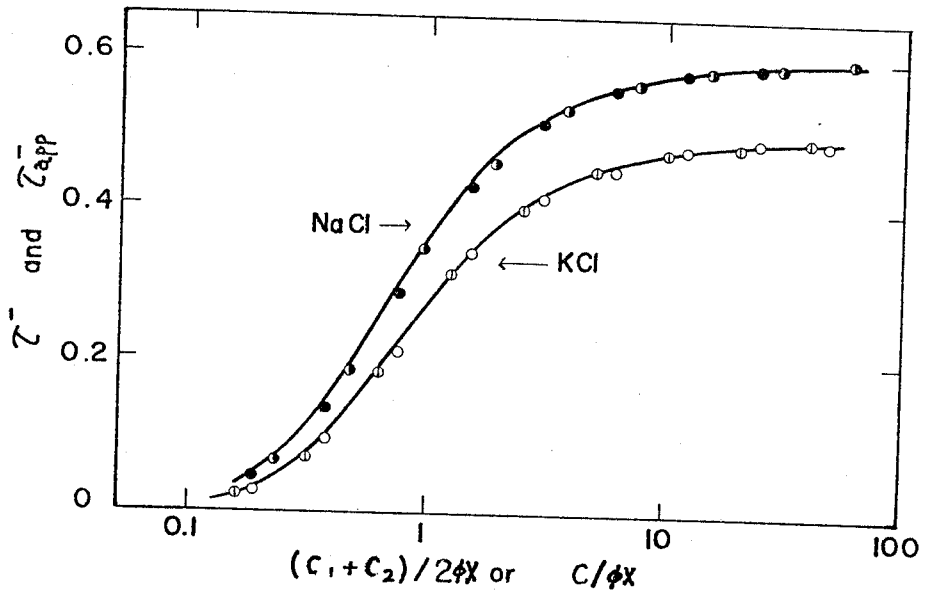

Fig. 5-2. The relation between $\bar{\nu}_{app}$ and $\log(C/\phi X) = \log (C_1 + C_2)/2\phi X$ ○, $\beta = 2$ for KCl; ⊖, $\beta = 1.5$ for KCl; ●, $\beta = 2$ for NaCl; ◐, $\beta = 1.5$ for NaCl. Solid lines are $\bar{\nu}$ calculated from Eq.(5-6) as a function of C/ X for KCl and NaCl.

$$\bar{t} = u_- c_- / (u_+ c_+ + u_- c_-) \qquad (5\text{-}6)$$

This equation is transformed to

$$\bar{t} = 1 - \alpha \frac{\sqrt{\kappa\xi^2 + 1} + 1}{\sqrt{\kappa\xi^2 + 1} + (2\alpha - 1)} \qquad (5\text{-}7)$$

Here, Eqs.(3-16) and (3-18) for the activity coefficients and mobilities of small ions in membranes and the equilibrium condition, Eq.(3-1), have been introduced. The solid line in Fig. 5-2 shows the values of $\bar{t}$ given by Eq.(5-7) plotted against $\log(C/\phi X)$. The difference between $\bar{t}_{app}$ and $\bar{t}$ is found to be less than 2% over the entire range of salt concentrations for both KCl and NaCl systems. The plots shown in Fig.5-1 are valid even when the value of ϕ varies with the salt concentration in so far as $\bar{t}$ and $\bar{t}_{app}$ are plotted as a function of $C/\phi X$. In other words, the apparent transference number $\bar{t}_{app}$ evaluated from the membrane potential data(see Eq.5-3) permits the determination of the effective charge density ϕX of the membrane at a given averaged salt concentration C by the following equation derived from Eq.(5-7);

$$\phi X = C \frac{1 - \bar{t}_{app} - \alpha}{\sqrt{\alpha \bar{t}_{app} (1-\alpha)(1-\bar{t}_{app})}} \qquad (5\text{-}8)$$

When the concentration of the external salt solution is large with respect to the effective charge density ϕX, i.e. when $C_1/\phi X =$

$\xi_1 \gg 1$, Eq.(5-4) can be expanded to give

$$1/\bar{\tau}_{app} = 1/(1-\alpha) + [(\beta-1)/(C\beta\lambda_\beta)][\alpha/(1-\alpha)](\phi X/C_1) + \mathcal{O}(1/C_1)^2 \qquad (5\text{-}9)$$

Eq.(5-9) indicates that the plot of $1/\bar{\tau}_{app}$ against $1/C_1$ with a fixed $\beta(=C_2/C_1)$ should produce a strainght line, and that the values of α and ϕX in the concentrated solution for a given combination of membrane and electrolyte can be determined from the ordinate intercept and the slope of the line. The value of α thus determined for the membrane used is approximately equal to that in the bulk solution.

Characterization of membrane-electrolyte systems

It has been shown in the preceeding chapter that the effective charge density ϕX of the membrane is a characteristic parameter of the system in question. However, each ionic species has its respective mobility in the bulk solution, and this leads to different values of the observed membrane phenomena with each species of electrolyte, even if the value of ϕX for a membrane is independent of electrolyte used. Therefore, it may be worthwhile to develop a general method of characterization of membrane-electrolyte systems, which is applicable to any system irrespective of the electrolyte species involved. This will be done by introducing a parameter representing the permselectivity of the membrane.

When the external salt concentration C is large with respect to ϕX, i.e. $C \gg \phi X$, Eq.(5-2) reduced to

$$\Delta\varphi = -(RT/F)(2\alpha-1)\ln\beta \qquad (5\text{-}10)$$

This equation is just a diffusion potential of an electrolyte in the bulk solution, i.e. the membrane has no permselectivity[7]. In other words, the effects of the fixed charges of the membrane are completely eliminated when the salt concentration is high enough. On the other hand, when $C \ll \phi X$, Eq.(5-2) reduces to the following simple form

$$\Delta\varphi = -(RT/F)\ln\beta \qquad (5\text{-}11)$$

which is the maximum potential difference across a charged membrane for a system with a given value of β. When the membrane potential is in accord with Eq.(5-11), the membrane is referred to as a perfectly permselective membrane. Comparing Eqs.(5-10) and (5-11) with Eq.(5-3), one may conclude that $\bar{\tau}_{app}$ takes a value between zero and $(1-\alpha)$ due to the external condition of the membrane and to the electrolyte pair. The situation where $\bar{\tau}_{app} = 0$ corresponds to a perfectly permselective negatively charged membrane. Hence, the value of $\bar{\tau}_{app}$ may be considered to be a measure of permselectivity. However, $\bar{\tau}_{app}$ depends strongly on the mobilities of the ionic species used. Rearrangement of Eq.(5-7) leads to

$$\frac{1}{(4\xi^2+1)^{1/2}} = \frac{1-\bar{z}-\alpha}{\alpha-(2\alpha-1)(1-\bar{z})} \quad (\equiv P_s) \qquad (5\text{-}12)$$

The left-hand side of the above equation approaches to unity when $C \ll \phi X$, and zero when $C \gg \phi X$, and depends only on the relative concentration $\xi = C/\phi X$. The right-hand side of Eq.(5-12) can be calculated from a simple measurement of the membrane potential when $\bar{z}$ is set equal to $\bar{z}_{app}$. Hence, the qunatity $(1-\bar{z}_{app}-\alpha)/[\alpha-(2\alpha-1)(1-\bar{z}_{app})]$ may be referred to as the degree of permselectivity of the membrane, and is denoted by P_s.

Experimental

The procedures and apparatus for the measurements of the membrane potential were the same as those employed in Chapter 3. The membranes used here were four different kinds of charged membranes. They were; (1) three oxidized collodion membranes having different fixed charge densities (designated as M-1, M-2 and M-3), (2) two collodion-based polystyrene sulfonic acid membranes used in the previous chapter, (PS-1 and PS-3), (3) collodion-based protamine membrane prepared according to the method reported by Sollner[8] (PR membrane), and (4) dextrane sulfate incorporated collodion membrane which was prepared by the method same as that of protamine collodion membranes (DS membrane). The salts used as electrolyte component were LiCl, KCl, NaCl, KF, and KIO_3. Each of analytical grade reagent was used as delivered. Water used was prepared by passing distilled water through both cation

and anion exchanger resin column. The carbon dioxide dissolved in water was not degassed and the pH of the water was 5.5.

Fig. 5-3 shows a block diagram of the apparatus used for the D.C resistance measurements. In the figure, E_1 and E_4 are a couple of Ag-AgCl plate electrodes through which the direct current is delivered to the system from a battery, E_2 and E_3 are a couple of feeler electrodes[9, 10] made of a silver wire of 50 μ in diameter, which were chloridized in a HCl solution of 0.1 N with a 0.1 mA of electric current for 10 min. These wire electrodes were mounted in contact with the membrane surface. The two bulk solutions were agitated vigorously with a magnetic stirrer to prevent the polarization at the membrane-solution interfaces[11]. The direct current delivered in the system was measured with a calibrated ammeter (Yokogawa Works Co., Type 2011) and the potential difference across the membrane surface was measured with a vibrating reed electrometer (Takeda Riken Co., Type TR-84B). Plots of the measured $E = E_2 - E_3$ against the applied current strength gave a straight line passing through the coordinate origin. The desired electrical resistance of the membrane was calculated from the slope of this plots.

Results and Discussion

By way of an example, in Fig. 5-4, the membrane potential data obtained with two PS-membranes in various 1:1 electrolytes are plotted as functions of $\log(C_1 + C_2)/2$, where the ratio of concentrations, β

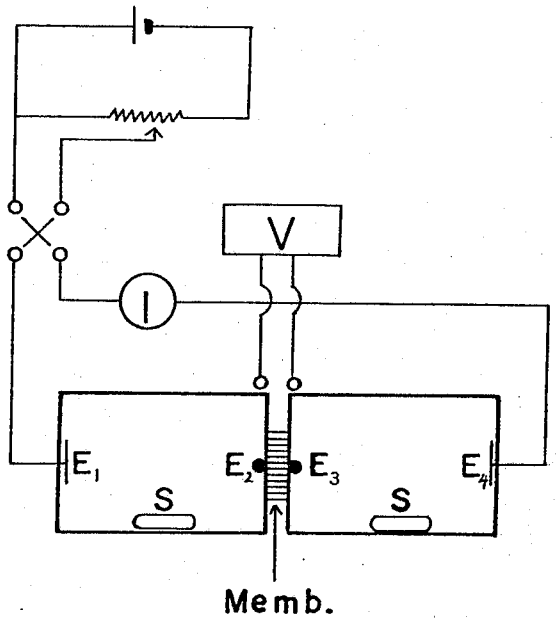

Fig. 5-3. Block diagram of the apparatus used for the D.C. resistance measurements. E_1, E_4, silver-silver chloride plate electrodes; E_2, E_3, silver-silver chloride feeler electrodes; Memb., test membrane; V, vibrating reed electrometer; I, d. c. micro- or milli-ammeter; S, stirrer chip.

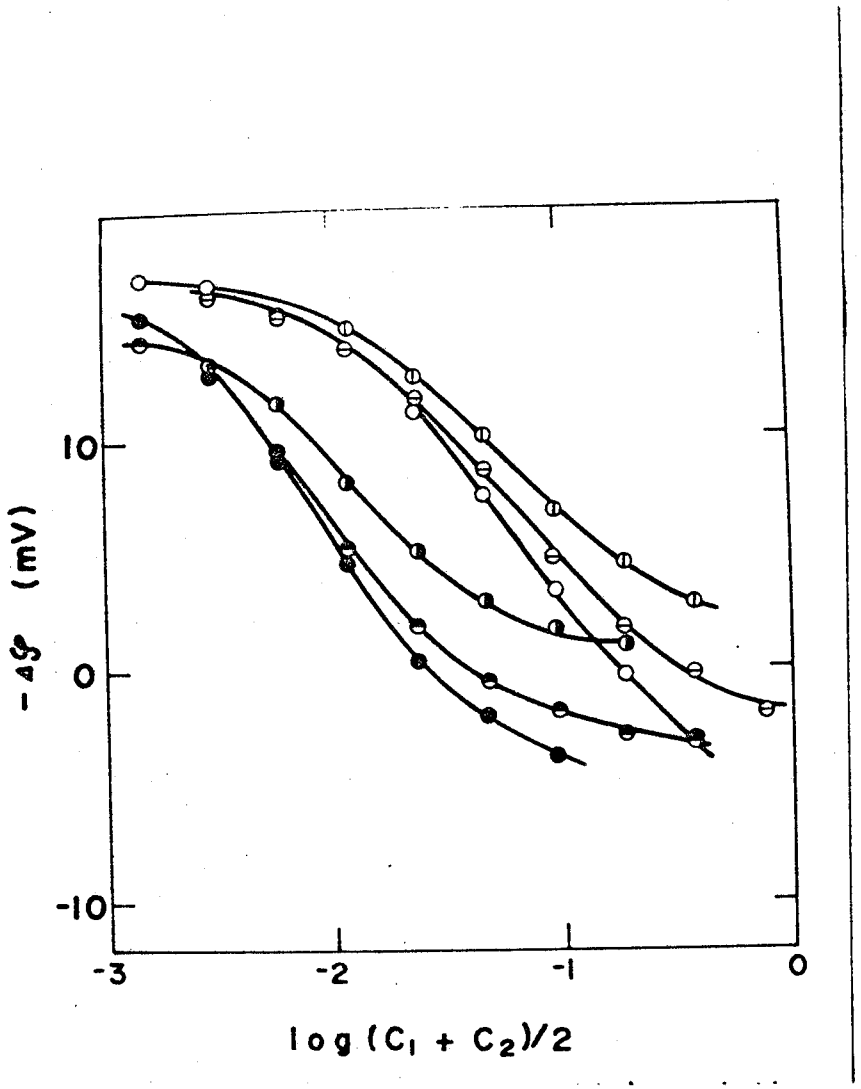

Fig. 5-4. Plots of observed membrane potential, $\Delta\varphi$, against log $(C_1 + C_2)/2$ for combinations of PS-1 and PS-3 membranes and LiCl, NaCl, KCl. The concentration ratio of two external solutions is kept constant at 2.

○, LiCl for SP-1; ⊖, NaCl for SP-1; ⊕, KCl for SP-1;

●, LiCl for SP-3; ◓, NaCl for SP-3; ◑, KCl for SP-3.

($=C_2/C_1$) is fixed at 2. The results at other values of β were essentially simillar to this graph. This figure illustrates that the membrane potential, $\Delta\varphi$, depends on the electrolyte species or on the transference number of electrolyte in bulk solution. As shown in Fig. 5-5, this difference due to the mobilities of ions is eliminated when P_s defined by Eq.(5-12) is plotted against $\log(C_1 + C_2)/2$, where the data points for various ion species are reduced to a single curve for the respective membrane unless the effective fixed charge density of the system depends strongly on the species of electrolyte component. When the average concentration $C = (C_1 + C_2)/2$ is equal to the effective fixed charge density ϕX, i.e. $C/\phi X = 1$, the value of P_s must give $1/\sqrt{5} = 0.448$. In other words, from the data of P_s plotted as a function of C, it is possible to determine the value of the effective fixed charge density of a given pair of membrane and electrolyte.(see dotted lines in Fig.5-5)

In Table 5-1, the value of ϕX determined from both P_s vs. C plots and Eq.(5-9) for various combinations of membrane and electrolytes. The agreement between values of ϕX obtained by two different methods is satisfactory, although we have not evaluated the small variation of ϕX due to ion species in the present study.

Using values of ϕX predetermined by the method proposed above, the permselectivity P_s of all systems are replotted as a function of

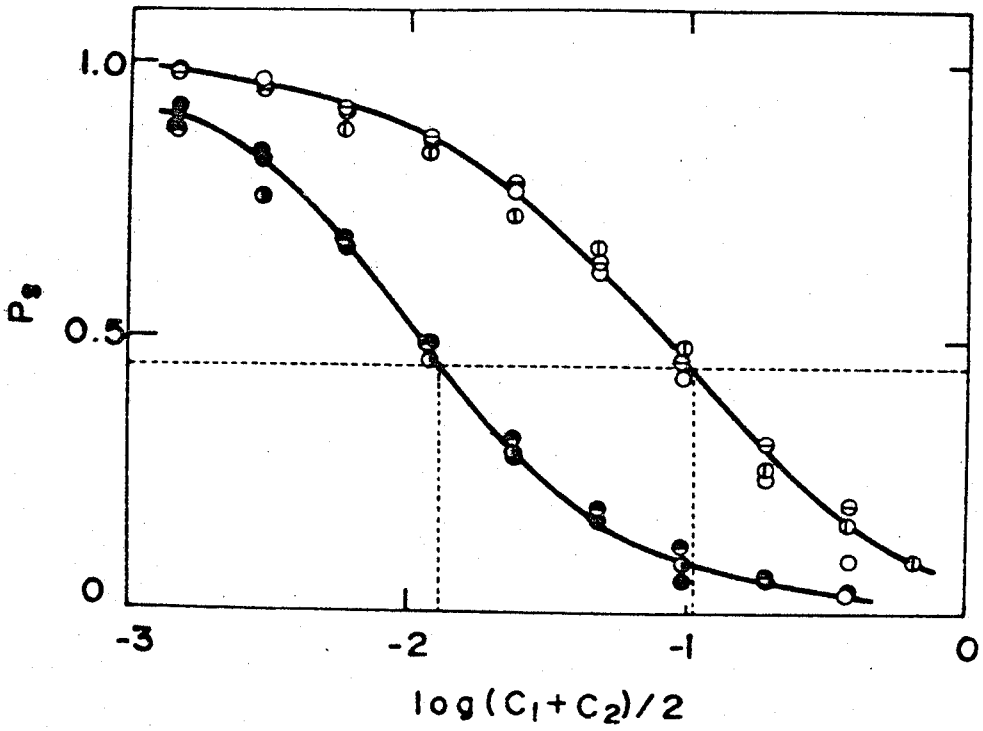

Fig. 5-5. Plots of P_s defined by Eq.(5-12) against $\log(C_1 + C_2)/2$ for the same system as in Fig. 5-4. Dotted horizontal line shows $P_s = 1/\sqrt{5}$, and the vertical line gives the value of ϕX for the corresponding membrane. Notations are the same as in Fig. 5-4.

Table 5-1. Comparison between X determined from P_s and from Eq.(5-9)

Membrane		ϕX determined from P_s (mole/l)	ϕX determined *) from Eq.(5-9) (mole/l)
PSSA -collodion	PS-1	0.091	0.082 ~ 0.092
	PS-3	0.014	0.015 ~ 0.009
Oxidized -collodion	M-1	0.005	0.0044 ~ 0.0058
	M-2	0.014	0.0158 ~ 0.0168
	M-3	0.021	0.023 ~ 0.027
Dextrane sulfate -collodion	DS	0.0029	0.0025 ~ 0.0027
Protamine -collodion	PR	0.038	0.018 for LiCl 0.024 for KF 0.034 for NaCl, KCl

*) Deviation of ϕX values in this column depends on the electrolyte species used.

$(1 + 4\xi^2)^{-1/2}$ in Fig. 5-6. Here the straight line of unitary slope is the theoretical line with the assumption that the value of ϕX of each respective system is independent of the salt concentration. In the case where a positively charged membrane is used such as protamine-collodion membranes, P_s must be defined as $[\bar{z}_{app} - (1-\alpha)]/[1-\alpha-(1-2\alpha)\bar{z}_{app}]$ instead of Eq.(5-12). All data studied here approximately follow a single curve which deviates systematically from the straight line of slope unity in a dilute salt solution. As discussed in the previous chapters, the degree of unbound counterions depends slightly on the external salt concentration when the external concentration decreases in comparison with ϕX. Thus the deviation of the data points from the straight line stems from the concentration dependence of ϕX. Fig. 5-6 shows the dependence of ϕX on the external salt concentration is approximately equal for all combinations of membranes and electrolytes studied here. It is noted that for the system with protamine-collodion membrane in LiCl the data deviate appreciably from the straight line in the concentrated region. This is also seen in Table 5-1 where the value of ϕX determined from P_s vs log C plots is much smaller than that obtained from the other method in a concentrated region of LiCl, and that the value of ϕX for LiCl is much larger than those for KCl or NaCl.

Once ϕX of a membrane in an electrolyte solution is determined

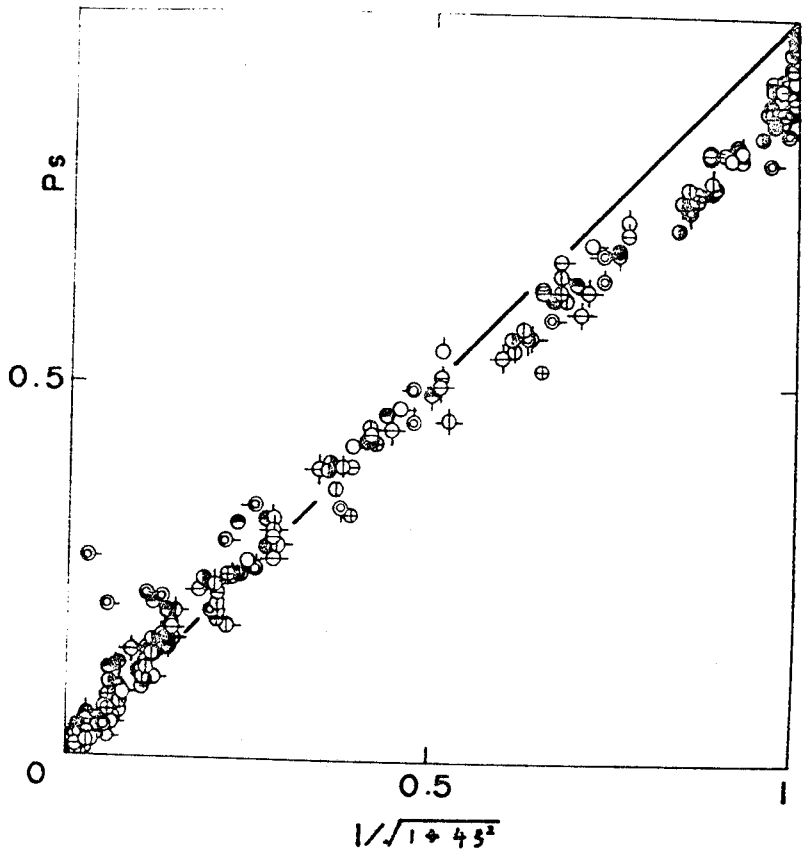

Fig. 5-6. Plots of P_s agaist $1/(1+4s^2)^{1/2}$ for various combinations of membrane and electrolyte.

oxidized collodion	⊙, KCl for M-1; ○, LiCl for M-1; ⊖, NaCl for M-1; ⊕, KIO_3 for M-1; ϕ, KCl for M-2; ♁, LiCl for M-2; ⊖, NaCl for M-2; ⊕, KIO_3 for M-2; ⊙–, KCl for M-3; ○–, LiCl for M-3; ⊖–, NaCl for M-3; ⊕–, KIO_3 for M-3;
PSSA collodion	⊙, KCl for PS-1; ○, LiCl for PS-1; ⊖, NaCl for PS-1; ♀, KCl for PS-3; ♀, LiCl for PS-3; ♀, NaCl for PS-3;
Dextrane sulfate collodion	–⊕–, KCl for DS; –⊕–, NaCl for DS;
Protamine collodion	◎, KCl for PR; ◎–, LiCl for PR; ◎, NaCl for PR; –◎, KF for PR.

from the observed membrane potential at an arbitrary concentration C, the values of other transport phenomena, e.g. DC resistance, salt flux, transference number, etc. can be calculated. A comparison with corresponding experimental data may be made to check the validity of the theory and also the applicability of the concept of the effective fixed charge density, ϕX. The electrical resistance r of the membrane may be taken as an example. Under the assumption that the effect of mass movement is ignored , the electrical resistance r is represented by

$$r = L/[AF(u_+C_+ + u_-C_-)] \qquad (5\text{-}13)$$

The contribution of the mass flow to the DC resistance is less than a few percent for the system studied here, as is shown later. Introducing Eqs.(3-16) and (3-18) into Eq.(5-13), and rearranging, Eq.(5-14) is obtained

$$r = \frac{2L}{AF\Lambda^\circ} \frac{1}{\sqrt{4C^2 + \phi^2X^2} + (2\alpha - 1)\phi X} \qquad (5\text{-}14)$$

where Λ° stands for $(u_+^\circ + u_-^\circ)$, whose value can be taken from an appropriate table[12]. Comparison between the calculated and the observed value of r is made in Fig. 5-7, for the systems of membrane SP-1, SP-2 and SP-3 in various concentrations of KCl, RbCl, and LiCl solution. As seen in the figure, the agreement between calculated and the observed values is satisfactory within the limits of experimental errors.

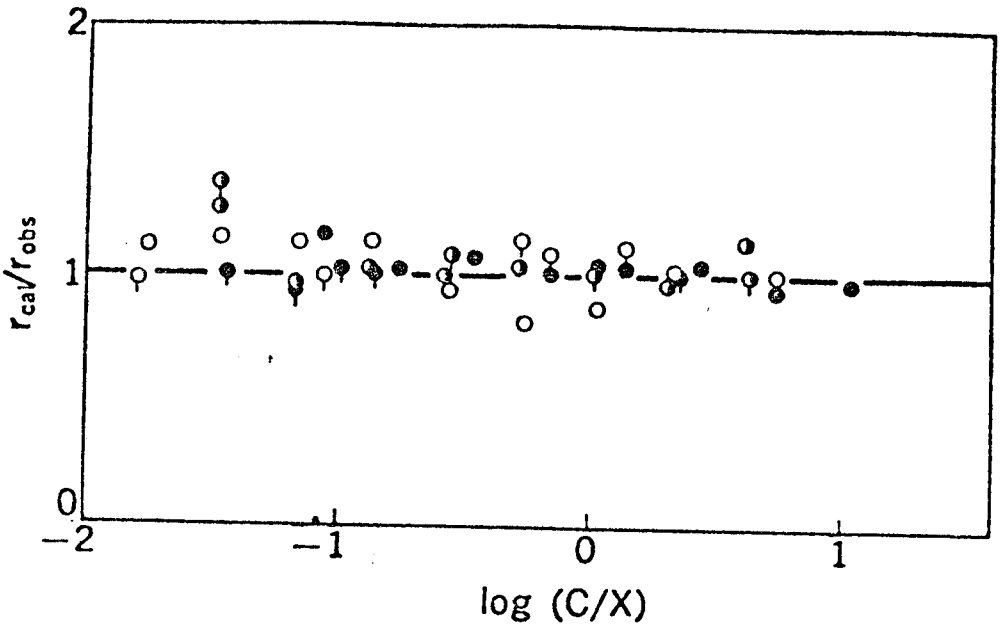

Fig. 5-7. Comparison between observed and calculated values of electric resistance in various combinations of membranes and electrolytes. ○, PS-1 KCl; ◑, PS-2 KCl; ●, PS-3 KCl; ◕, PS-3 RbCl; ⚲, PS-1 RbCl; ⚲, PS-2 LiCl.

In the above discussion, the difference of the standard chemical potential, μ_i° between the aqueous and the membrane phases is ignored since the water content of the membrane is as high as 80 %. For the more compact membrane, however, this difference must be taken into consideration. Actually, Toyoshima et al.[13] stated that the membrane of low water contents prepared from the collodion exhibits the ionic selectivity. Here, the term "ionic selectivity" is defined as follows; the values of the permselectivity defined by Eq.(5-12) at the same concentration are dependent on the ionic species used. The liquid membrane prepared by dissolving a certain ion-exchanger into organic solvents shows highly ionic selectivity. In order to expound the ionic selectivity, it is necessary to introduce the difference of the standard chemical potential between the aqueous and the membrane phases.

The electrochemical potential of species i in the membrane is expressed by

$$\tilde{\mu}_i = \mu_i^{\circ}(m) + RT \ln a_i + z_i F \psi' \qquad (5\text{-}15)$$

while that in the bulk aqueous solution which is contiguous with the membrane is represented by

$$\tilde{\mu}_i = \mu_i^{\circ} + RT \ln a + z_i F \psi \qquad (5\text{-}16)$$

Here, z_i is the valence of ions, i.e. +1 or -1. Note that the

standard chemical potential of an ion species in the membrane, $\mu_i^{\circ}(m)$ is different from that in the aqueous solution, μ_i°. When the thermodynamic equilibrium holds between the membrane and solution phases, Eqs.(5-15) and (5-16) must be equal to each other. Then we have

$$[\mu_i^{\circ}(m) - \mu_i^{\circ}] + RT \ln (a_i'/a) + z_i F(\psi' - \psi) = 0 \qquad (5\text{-}17)$$

Elimination of $(\psi' - \psi)$ from the equations for the cation and anion species given by Eq.(5-17) leads to

$$a_+ a_- = a^2 (K_m^{\circ})^2 \qquad (8\text{-}18)$$

where K_m° is defined by the following equation,

$$\frac{1}{2}\{(\mu_+^{\circ}(m) + \mu_-^{\circ}(m)) - (\mu_+^{\circ} + \mu_-^{\circ})\} = -RT \ln K_m^{\circ} \qquad (5\text{-}19)$$

and represents the difference in solubilities of the electrolyte component between the membrane and the aqueous phases. The value of K_m° is a constant irrespective of the salt concentration of the external solution for a given combination of membrane and electrolyte components under consideration. Making use of Eq.(3-16) for the activity coefficients of i-ion in the membrane, C_- is given by

$$C_- = \frac{-\phi X + \sqrt{(\phi X)^2 + 4(K_m^{\circ})^2 c^2}}{2} \qquad (5\text{-}20)$$

Introducing Eq.(5-20) into Eq.(3-7) and integrating between the two bulk solutions across the membrane with use of Eq.(3-18), we obtain the following equation:

$$\Delta\varphi = -\frac{RT}{F}\left[\ln\frac{c_2}{c_1} + (2\alpha-1)\ln\frac{\sqrt{\kappa c_2^2+\chi^2}+(2\alpha-1)\chi}{\sqrt{\kappa c_1^2+\chi^2}+(2\alpha-1)\chi}\right.$$

$$\left. -\ln\frac{\sqrt{\kappa c_2^2+\chi^2}+\chi}{\sqrt{\kappa c_1^2+\chi^2}+\chi}\right] \qquad (5\text{-}21)$$

where χ is defined as $\phi X/K_m^{\circ}$ and the term of U_m in Eq.(3-6) is neglected as before. This equation is identical to Eq.(5-2) except that the effective fixed charge density ϕX is replaced by χ. Then, the above discussion is also applicable to the membrane potential data even when the difference of the standard electrochemical potential must be taken into consideration.

References

1) A. Katchalsky, Z. Alexandrowics and O. Kedem, "Chemical Physics of Ionic Solution", P. 296 (John Wily, New York, 1966).

2) D. Mackay and P. Mears, Kolloid. Z. 167 37(1959)

3) Y. Toyoshima, Y. Kobatake and H. Fujita, Trans. Faraday Soc., 63, 2814 (1967)

4) N. Lakshminarayanaiah, "Transport Phenomena in Membranes" p. 132 (Academic Press, New York and London, 1969).

5) T. Teorell, Proc. Soc. Exptl. Biol., 33, 282 (1935).

6) K. H. Meyer and J. F. Sievers, Helv. Chim. Acta, 19, 649 (1936).

7) D. A. MacInnes, "The Principles of Electrochemistry" p. 225 (Dover Publications, Inc. New York, 1961).

8) M. Lewis and K. Sollner, J. Electrochem. Soc., 106, 347 (1959).

9) Y. Toyoshima, M. Yuasa, Y. Kobatake and H. Fujita, Trans. Faraday Soc., 63 2803 (1967).

10) G. J. Hills, A. O. Jakubovic and J. A. Kitchener, J. Polymer Sci. 19, 382 (1956).

11) N. Lakshminarayanaiah, J. Phys. Chem., 72, 3699 (1968).

12) Landolt-Börnstein Tabellen, II-7, 6-th ed., (Berlin-Heidelberg, Springer,1960).

13) Y. Toyoshima and H. Nozaki, J. Phys. Chem., 74, 2704 (1970).

Chapter 6. Charge Density Effects on Hydrodynamic Properties of Membrane

As seen in the basic equations given in Chapter 2, the flux of each movable species relative to the membrane is represented by the sum of two terms, one relative to the local center of mass, and the other associated with mass movement. The term related to the mass movement in Eq.(2-9) was neglected in the analysis developed in the previous chapters. This is reasonable, as will be seen at the end of this chapter. In transport phenomena related to a volume flow, however, the mass movement plays a decisive role, and no satisfactory interpretation may be made unless the effect of mass flow is taken into consideration. For this reason, mass flow in the membrane is thoroughly investigated in this chapter. The effects of fixed charges on the hydrodynamic properties of the membrane are also investigated. The charge density influencing the hydrodynamic properties of the membrane will be determined as a function of salt concentration using electroosmotic flow and streaming potential data, and the effect of mass movement on the membrane potential and on the ion permeability of the membrane will be discussed.

Theoretical

The system considered here consists of a negatively charged membrane which separates two aqueous solutions of a 1:1 type electrolyte with identical concentrations and temperature. When differences in electrical potential and pressure is applied across the membrane, electrical current I and volume flow J_v occur through the membrane. Starting from the flux equation, Eq.(2-9), I and J_v are represented by[1)]

$$I = -(u_+c_+ + u_-c_-)F(d\varphi/dx) - (v_+^* u_+ c_+ - v_-^* u_- c_-)(dp/dx) + F(c_+^* - c_-^*)U_m \tag{6-1}$$

$$J_v = -(v_+^* u_+ c_+ - v_-^* u_- c_-)(d\varphi/dx) - (1/F)(v_+^{*2} u_+ c_+ + v_-^{*2} u_- c_-)(dp/dx) + U_m \tag{6-2}$$

Here, v_k^* is defined by

$$v_k^* = v_k - (m_k/m_o)v_o \qquad (k = +, -) \tag{6-3}$$

with v_k, m_k, v_o, and m_o, the partial molar volume and the molecular weight of ion species k and the solvent, respectively. $d\varphi/dx$ and dp/dx are the gradients of electrical potential and pressure.

As noted above, the total number of small ions which is conveyed by the mass movement, C_k^* is not necessarily equal to the averaged or stoichiometric amount of small ions C_k in the membrane phase. Then, the quantity $F(C_+^* - C_-^*)U_m$, the last term on the right-hand side of

Eq.(6-1) is written as in $F\psi XU_m$ for the subsequent analysis.

$$F(c_+^* - c_-^*)U_m = F\psi X U_m \qquad (6\text{-}4)$$

Here, ψ is a dimensionless positive parameter less than unity ($0<\psi<1$) which represents the effect of fixed charges on the hydrodynamic properties of the membrane at a given concentration.

The motion of the local centre of mass in the membrane U_m, should be obtained by the solution of a hydrodynamic equation. Since the rigorous equation of mass motion is not amenable to an analytical solution for membrane systems in general, an approximation is used in the expression of U_m in the subsequent analysis[2]. Any volume element in the membrane phase is subject to two kinds of external forces under the experimental conditions considered here, i.e. the negative gradient of pressure, $-dp/dx$, and of electrical potential, $-F\psi' X(d\varphi/dx)$. Here, $\psi' X$ represents the excess charges in the membrane which can transmit the external electric field acting on them to their surrounding liquid medium. Again, $\psi' X$ is not necessarily equal to X, ϕX or ψX. In this chapter, the values of $\psi' X$, ψX, and ϕX will be compared with one another for given system. In mechanical equilibrium, the sum of the above mentioned forces must balance with the viscous stress produced in the volume element considered. As a first approximation, this stress may be taken to

be $-(1/k)U_m$. Then,

$$U_m = -k(dp/dx) - kF\psi' X(d\varphi/dx) \tag{6-5}$$

where k is a constant which depends on the fluidity of the solution, the compactness and the other structual characteristics of the membrane. Introducing Eq.(6-5) into Eqs.(6-1) and (6-2), and integrating the resulting equations under the condition that the system is in a steady state, i.e. $dI/dx = dJ_v/dx = 0$, Eq.(6-6) is obtained

$$\begin{aligned} I &= -\omega_{11}(\Delta\varphi/L) - \omega_{12}(\Delta p/L) \\ J_v &= -\omega_{21}(\Delta\varphi/L) - \omega_{22}(\Delta p/L) \end{aligned} \tag{6-6}$$

where the phenomenological coefficients ω_{ij} are given by

$$\omega_{11} = (u_+c_+ + u_-c_-)F + \kappa F^2\psi\psi' X^2 \tag{6-7}$$

$$\omega_{12} = (V_+^* u_+ c_+ - V_-^* u_- c_-) + \kappa F\psi X \tag{6-8}$$

$$\omega_{21} = (V_+^* u_+ c_+ - V_-^* u_- c_-) + \kappa F\psi' X \tag{6-9}$$

$$\omega_{22} = (V_+^{*2} u_+ c_+ + V_-^{*2} u_- c_-)(1/F) + \kappa \tag{6-10}$$

Note that ω_{ij} (i,j = 1, 2) are composed of two terms as in Eq.(2-9). ω_{11} represents the electrical conductance of the membrane, which is obtained experimentally as

$$\omega_{11} = -L(I/\Delta\varphi)_{\Delta p=0} = (L/A)(1/r) \tag{6-11}$$

where r is the observed electric resistance. The streaming potential and the electroosmosis are defined by

$$-(\Delta\varphi/\Delta p)_{I=0} = \omega_{12}/\omega_{11} \tag{6-12}$$

$$(J_v/I)_{\Delta p=0} = \omega_{21}/\omega_{11} \tag{6-13}$$

Combining Eq.(6-11) with Eqs.(6-12) and (6-13), the value of ω_{12} or ω_{21} may be determined at a given concentration of the external solution. Finally, ω_{22} is calculated to give

$$\omega_{22} = -L(J_v/\Delta p)_{\Delta\varphi=0} \tag{6-14}$$

Since it is difficult to measure the volume flow under the condition that $\Delta\varphi = 0$, the values of ω_{22} may be obtained as follows. With the external condition that I = 0, the hydraulic permeability $(J_v/\Delta p)_{I=0}$ is given by

$$(J_v/\Delta p)_{I=0} = [(\omega_{12}\omega_{21}/\omega_{11}) - \omega_{22}](1/L) \tag{6-15}$$

when the values of ω_{11}, ω_{12}, and ω_{21} are known for a given system, the value of ω_{22} can be evaluated.

As shown in the previous chapters, u_+C_+ and u_-C_- have been determined over a wide range of salt concentraiions, and hence the values of k, ψX, and $\psi' X$ which appear in Eqs.(6-7)~(6-10) can be evaluated when the values of v_+^* and v_-^* defined by Eq.(6-3) are known.

Experimental

The membranes used in this study were PS-1 and PS-2 membrane, characteristics of which are listed in table 3-1.

Fig. 6-1 is a schematic diagram of the apparatus used for the measurement of streaming potential, electroosmosis and velocity of volume flow through membranes. The external electrolyte solutions on both sides of the membrane were stirred vigorously by a pair of magnetic stirrers in order to prevent the concentration polarization at the membrane-solution interfaces. (see Chapter 8). L-shaped capillaries were connected vertically to each compartment in such a manner that the horizontal arms of the two capillaries came to be the same level. In the measurement of streaming potential, one of the capillaries was opened to air; the other was connected to the bomb for nitrogen gas with a manometer by which the difference of hydrostatic pressure between two solution, Δp was measured. In the figure, E_1 and E_2 are silver-silver chloride reversible electrodes through which the electromotive force arising between the bulk solutions was measured. The plots of the observed electromotive forces against Δp gave proportional relation passing through the origin and values of ω_{21}/ω_{11} were calculated from the slope of the plot.

For the measurements of electroosmosis, the direct electric

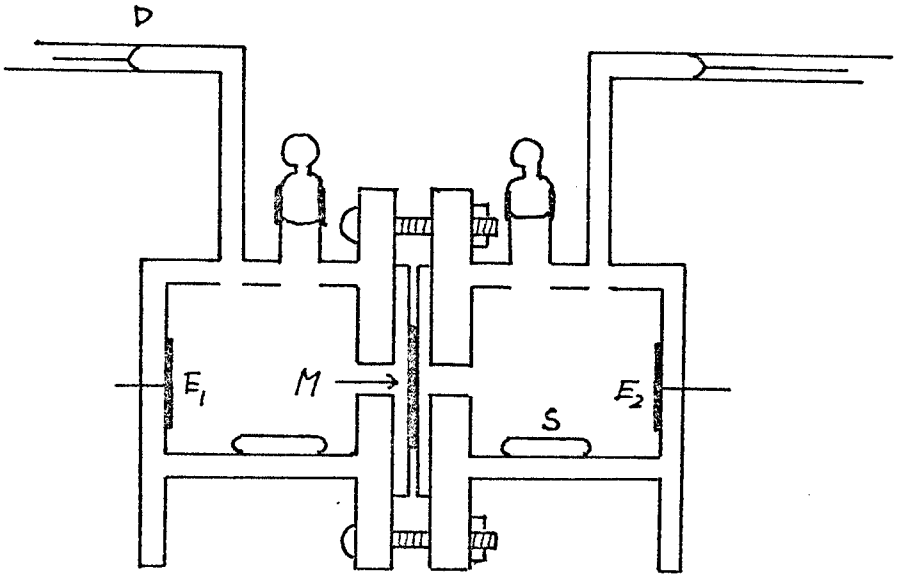

Fig. 6-1. Schematic diagram of the cell used for measurements of streaming potential, electroosmosis and velocity of volume flow. M, membrane; E_1 and E_2, Ag-AgCl plate electrodes; S, stirrer bar; D, capillary.

current was delivered to the membrane from a battery through E_1 and E_2. A variable resistor was connected in series to adjust the current strength, which was measured with a calibrated micro- or milli-ammeter. The rate of volume flow associated with the passage of current was calculated by the movement of the meniscus in the capillary. The displacement of the meniscus was followed as a function of time by a traveling microscope. After some interval of time from the onset of each run, plots of the displacement of meniscus against time became linear. The slope of this linear portion multiplied by a factor λ ($= S_c/S_m$) was taken as the steady-state value of the velocity of volume flow, J_v, where S_c denotes the cross section of the capillary and S_m the area of the membrane. Data were taken as a function of current strength, I. Plots of J_v against I gave straight line passing through the origin and the values of ω_{21}/ω_{11} were evaluated from the slope of these plots.

In measurements of hydraulic permeability, the hydrostatic pressure difference between two solutions was applied by putting L-shaped capillaries at different height. The rate of volume flow was measured by the same way as described above. Data were taken at various Δp and the value of hydraulic permeability can be evaluated from the slope of the plots for J_v against ΔP.

Results and Discussion

Fig. 6-2 shows the data of streaming potential $F(\Delta\varphi/\Delta p)_{I=0}$, and the ratio of the electroosmosis $(J_v/I)_{\Delta p=0}$ to the streaming potential, i.e. ω_{21}/ω_{12}, in various concentrations of the external KCl solution for membrane PS-1. It is noted that the Saxén relation[3] ($\omega_{12} = \omega_{21}$) holds for the present membrane system in the whole range of KCl concentration studied. The other membranes studied also satisfy this relation. Thus, tracing back Eqs.(6-8) and (6-9), the excess charges carried by the mass movement ψX appeared in Eq.(6-4) and charges which transmit the electrical field to the surrounding fluid medium $\psi' X$ defined by Eq.(6-5) are equal to each other for the present systems. Hereafter, ψ' is not discriminated from ψ.

Since the value of ω_{11} for the system is known for a given concentration of KCl as discussed in Chapter 5, the value of ω_{12} $(=\omega_{21})$ can be determined by combining Eqs.(6-11) and (6-12) or (6-13). The values of ω_{12} obtained are plotted as functions of log (C/X) for PS-1 and PS-3 membranes in Fig.6-3. As seen in Eqs.(6-8) and (6-9), ω_{12} and ω_{21} are composed of two terms; one associated with the movement of individual ion species relative to the local centre of mass, and the other with the mass movement. The first term $(v_+^* u_+ C_+ - V_-^* u_- C_-)$ can be evaluated by using $u_+ C_+$ and $u_- C_-$ determined in the previous chapter together with an appropriate value of v_i^* determined from

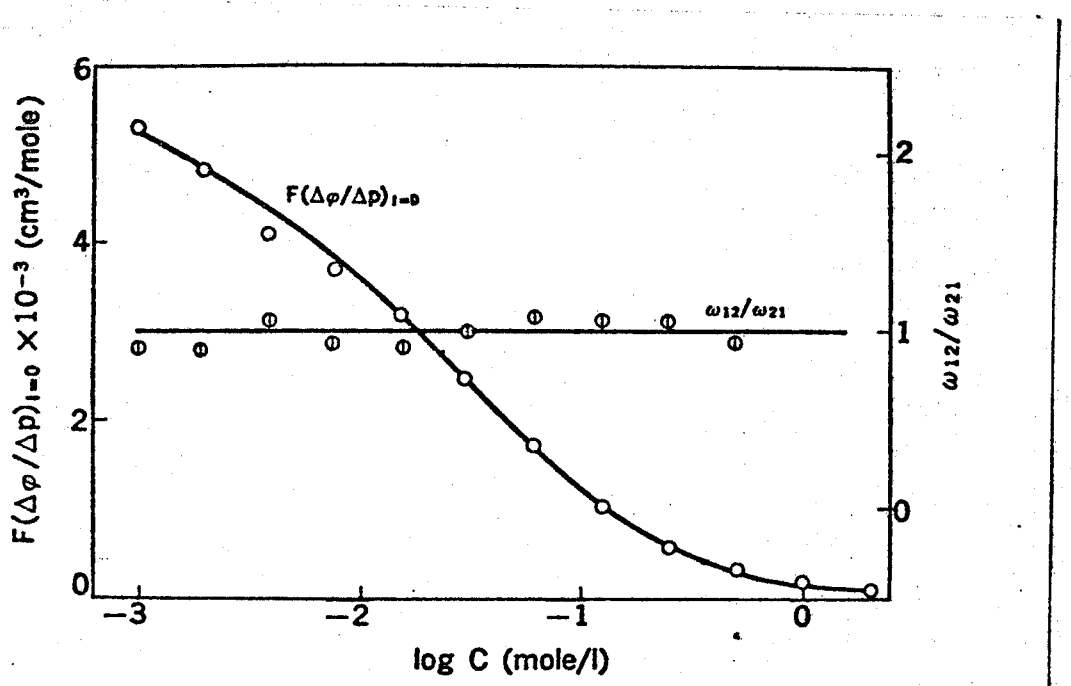

Fig. 6-2. Plots of $F(\Delta\varphi/\Delta P)_{I=0}$ against log C and the comparison between electroosmosis data, ω_{12} and streaming potential data, ω_{21} for the system of membrane PS-1 and KCl. ○, $F(\Delta\varphi/\Delta P)_{I=0}$; ⊙, ω_{12}/ω_{21}.

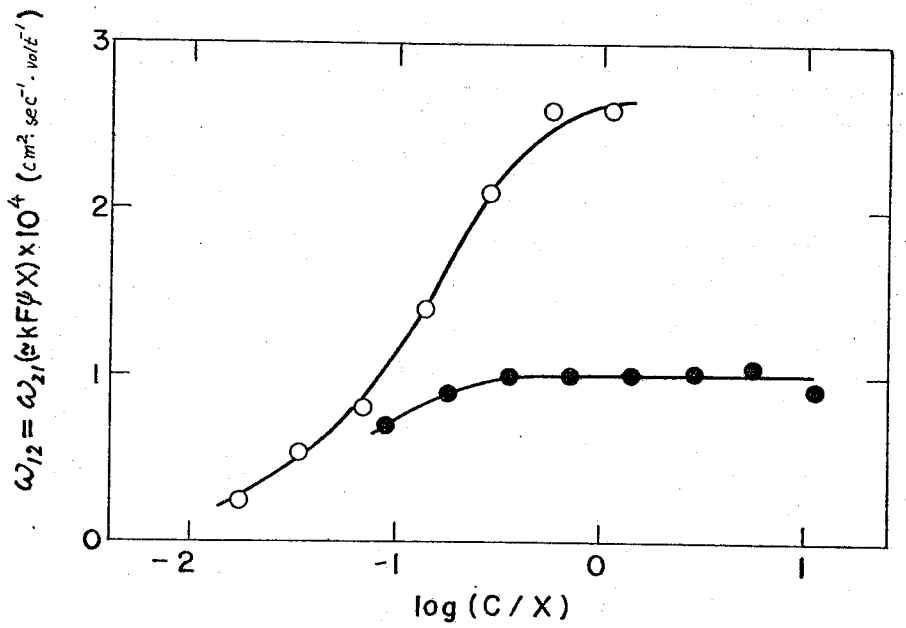

Fig. 6-3. ω_{12} as a function of log(C/X) for membranes PS-1 and PS-3 with KCl. ○, PS-1; ●, PS-3.

the Stokes radius of individual ion species calculated from the mobility data of ions in free solution[2,4]. For K^+ and Cl^- ions they were $v_k^* = -19.6$ cc/mole, and $v_c^* = -17.3$ cc/mole, respectively. When C = 0.5 N, u_+C_+ and u_-C_- were evaluated as 36.82×10^{-8} and 31.77×10^{-8} mole cm^{-1} sec^{-1} $volt^{-1}$. Then, $(v_+^* u_+C_+ - v_-^* u_-C_-)$ gives -0.02×10^{-4} cm^2 sec^{-1} $volt^{-1}$ at C = 0.5 N. The value of ω_{12} obtained experimentally was 2.13×10^{-4} $cm^2 sec^{-1}$ $volt^{-1}$ at the same salt concentration. Then the contribution of the first term of Eq.(6-8) or (6-9) was evaluated to be only 1 % of the observed value. This may be valid even when u_+C_+ and u_-C_- determined in the previous chapter contain some experimental errors. Since the contribution of the first term decreases with decrease of the external salt concentration, the observed values of ω_{12} and ω_{21} mainly stem from the mass movement represented by $kF\nabla X$ in Eq.(6-8) or (6-9).

Since the values of ω_{12} and ω_{21} are known for the system at a given salt concentration, we can evaluate the value of ω_{22} from the data of hydraulic permeability given by Eq.(6-15). When the external salt concentration was 0.5 N, ω_{11} and ω_{12} were 6.59×10^{-2} ohm^{-1} cm^{-1} and 2.13×10^{-4} $cm^2 sec^{-1} volt^{-1}$, respectively. Then, $\omega_{12}^2/\omega_{11} = 0.69 \times 10^{-13}$ cm^4 $dyne^{-1} sec^{-1}$, while the observed value of the hydraulic permeability was 3.80×10^{-11} cm^4 $dyne^{-1}$ sec^{-1}. The contribution of the first term in Eq.(6-15) decreases with decrease

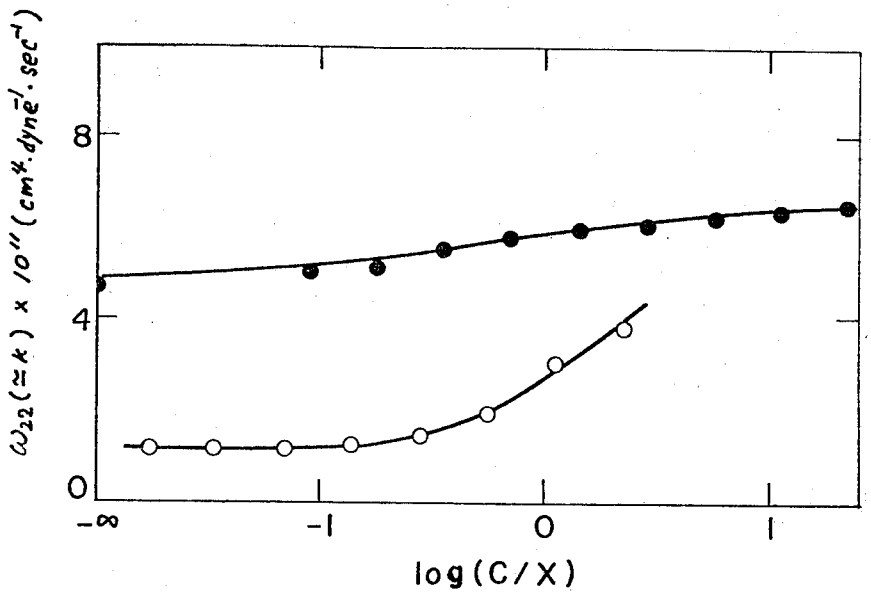

Fig. 6-4. ω_{22} as a function of log(C/X) for membranes PS-1 and PS-3 with KCl. ○, PS-1; ●, PS-3.

of the salt concentration. Thus, the observed hydraulic permeability is practically equal to ω_{22} in the whole range of salt concentration. Fig. 6-4 shows the relation between ω_{22} and the reduced external concentration (C/X) for membranes PS-1 and PS-3. As seen in Eq.(6-10) ω_{22} is also composed of two terms. The first term given by $(v_+^{*2} u_+ C_+ + v_-^{*2} u_- C_-)/F$ was evaluated to be 2.5×10^{-16} cm^4 dyne^{-1}sec^{-1} at concentration 0.5 N, which is compared with the observed ω_{22} at the same concentration, i.e. 3.80×10^{-11} cm^4 dyne^{-1} sec^{-1}. The first term of ω_{22} which represents the contribution of flux of individual ions relative to the local center of mass movement is then negligibly small compared with that of the mass movement represented by k in Eq.(6-10). Thus we have $(J_v/\Delta p)_{I=0} = (J_v/\Delta p) \cong kL^{-1}$. As noted in the theoretical section the magnitude of k depends on the compactness of the membrane and the fluidity of the liquid in the membrane. Kobatake et al. showed that the values of k for oxidized collodion membrane were independent of the salt concentration[1]. In the present system, however, the hydraulic permeability and hence k of the membrane increases appreciably for the case of membrane PS-1 with increase of external salt concentration although, as noted in the previous chapter, the membranes used were not swelling in the whole range of salt concentration. It is noted that the concentration dependence of k is increased with increase of amounts of polyelectrolyte impregnated in the membrane. Thus, the

variation of k due to the external salt concentration probably stems from the shrinkage of the macro-molecules which are stuck to the cellulose skeleton of the collodion when the concentration of the added salt is increased. Since no variation of analytical value of X was observed more than two years, the macroions did not leak out from the membrane.

The values of k and ψX for a given combination of membrane and KCl in variety of its concentration were determined. Then the contribution of the second term in the right hand side of Eq.(6-7) for the membrane conductance, i.e. $kF^2(\psi X)^2$, can be evaluated. For membrane PS-1 with 0.0039 N of KCl, the value of $kF^2(\psi X)^2$ is evaluated to be 5.4×10^{-6} cm^{-1} ohm^{-1}, while the observed ω_{11} was 5.51×10^{-4} cm^{-1} ohm^{-1} at the same condition. Thus, the contribution of the second term in ω_{11} was about 1 %. With increase of the concentration of the external solution, the magnitude of $(u_+C_+ + u_-C_-)$ increases while the value of $kF^2(\psi X)^2$ stays approximately constant. Therefore, the second term in the right hand side of Eq.(6-7), i.e. $kF^2(\psi X)^2$ is neglected with a good approximation in the whole range of the external salt concentration.

Values of ψ

By use of values of $k(=\omega_{22})$ and $kF\psi X(=\omega_{12}=\omega_{21})$ determined above the value of ψ can be evaluated, since the value of X is de-

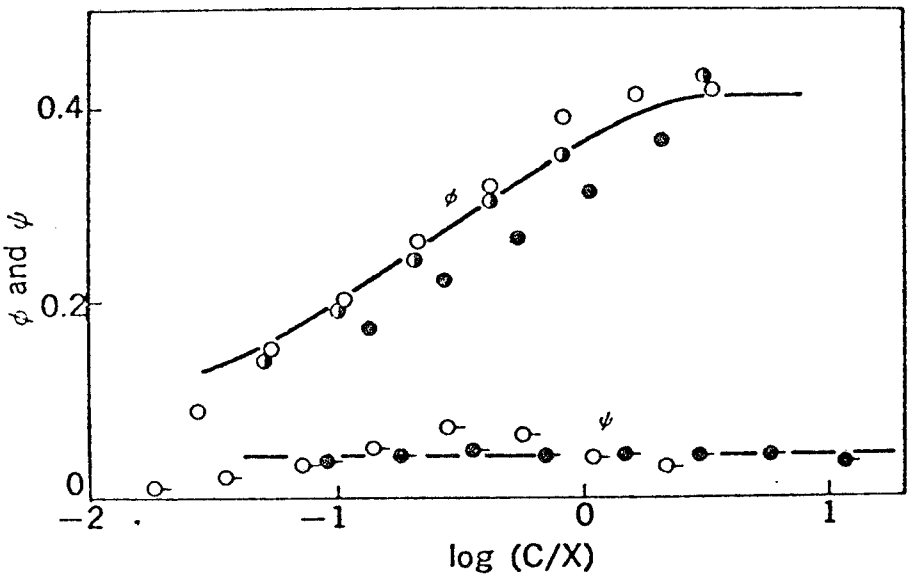

Fig. 6-5. Plots of ϕ and ψ against log(C/X). The values of ϕ are calculated in accordance with Eq.(5-8).

○, ϕ for PS-1; ◑, ϕ for PS-2; ●, ϕ for PS-3;

○-, ψ for PS-1; ●-, ψ for PS-3 in KCl solution.

termined for a given pair of membrane and KCl. The values of ψ thus obtained for membranes PS-1 and PS-3 in various KCl concentrations are plotted as function of log(C/X) in Fig.6-5. It is noted that the value of χ is approximately constant for different membranes, and that χ is much smaller than ϕ as shown in the figure. A method for obtaining ϕ for a given membrane in an arbitrary salt concentration has been described in Chapter 5. The value of χ was about 10 % of the value of ϕ in the whole range of salt concentration. The similar result was partially obtained for oxidized collodion membranes by previous authers[1,4].

Contribution of U_m to the membrane potential and salt flux.

At this stage, it is worthwhile to evaluate the contribution of the mass flow to the observed membrane potential and salt flux. Utilizing Eq. (6-4), Eqs. (3-7) and (3-8) for $\Delta\varphi$ and J_s can be rewritten as follows;

$$\Delta\varphi = -\frac{RT}{F}\int_0^L \frac{u_+C_+ - u_-C_-}{u_+C_+ + u_-C_-}\frac{d\ln a}{dx}dx + U_m\int_0^L \frac{\psi X}{u_+C_+ + u_-C_-}dx \qquad (6\text{-}16)$$

$$J_s = -\frac{2RT}{FL}\int_0^L \frac{u_+C_+u_-C_-}{u_+C_+ + u_-C_-}\frac{d\ln a}{dx}dx \qquad (6\text{-}17)$$

$$+\frac{U_m}{L}\int_0^L \left(\frac{u_-C_-\psi X}{u_+C_+ + u_-C_-} + C^*\right)dx$$

With the restriction of zero electric current through the membrane, the rate of volume flow, J_v is represented by the equation,

$$J_v = v_+ J_+ + v_- J_- + v_o J_o = v_s J_s + v_o J_o \qquad (6\text{-}18)$$

In the above equation, $v_i (i = s, o)$ is the partial molar volume of species i, where subscripts s and o stand for the electrolyte component and the solvent, respectively. The velocity of mass movement U_m is obtained by

$$m_s J_s + m_o J_o = \rho_o U_m \qquad (6\text{-}19)$$

where ρ_o is the density of the fluid in the membrane, and m_s and m_o are the molecular weight of the salt and water. Combining the above two equations, and assuming the density of solution, ρ_o, approximately equal to that of the pure solvent, Eq.(6-20) is obtained.

$$J_v = (v_s - m_s v_o / m_o) J_s + U_m \qquad (6\text{-}20)$$

Here $(v_s - m_s v_o/m_o)$ is equivalent to $(v_+^* + v_-^*)$ defined in

Eq.(6-3). Then, if the volume flow J_v and salt flux J_s are measured under the same external condition, the value of U_m at a given pair of salt concentrations C_1 and C_2 can be evaluated. Besides, the second term in the right-hand side of Eq.(6-16) can be approximated to give

$$\int_0^L \frac{\not{X}\, U_m}{u_+C_+ + u_-C_-}\, dx = L \frac{[\not{X}]_c}{[u_+C_+ + u_-C_-]_c} U_m \qquad (6\text{-}21)$$

where subscript C represents the value of the quantity in the brackets at the averaged concentration defined by $C = (C_1 + C_2)/2$. Introducing the value of U_m, $[\not{X}]_c$ and $[u_+C_+ + u_-C_-]_c$ in the above equation, one can evaluate the contribution of mass movement to the observed membrane potential, which is tabulated in table 6-1 for the combination of PS-1 membrane and KCl solution. This contribution was calculated to be less than 3% for the membranes studied.

The transference number of the counterions $u_+C_+/(u_+C_+ + u_-C_-)$ is always less than unity, and C_-^* is not very different from the average concentration of coions in the membrane C_- as will be discussed in the subsequent chapter. Thus, the second term in the right-hand side of Eq.(6-17), i.e. $(1/L)\int_0^L [u_+C_+ \not{X}/(u_+C_+ + u_-C_-) + C_-^*] U_m\, dx$ should be less than $(\not{X} + C_-)_c U_m$. Here subscript c represents again the value of $\not{X} + C_-$ at a given concentration C. With the value of

Table 6-1. Contribution of Mass Movement to Membrane Potential

C_1 -- C_2	$[u_+C_+ + u_-C_-]_c \times 10^8$ (equiv.cm^{-1}sec^{-1}volt^{-1})	$[\psi X]_c \times 10^5$ (equiv. cm^{-3})	$[U_m]_c \times 10^6$ (cm sec^{-1})	values of Eq.(6-21) (mV)	Observed membrane potential (mV)
1/256 - 1/128	1.21	0.353	8.46	0.44	15.51
1/128 - 1/64	2.47	0.608	11.9	0.52	14.85
1/64 - 1/32	4.66	0.947	13.85	0.50	12.62
1/32 - 1/16	8.33	1.33	14.10	0.23	9.99
1/16 - 1/8	14.90	1.46	9.00	0.46	6.82
1/8 - 1/4	27.46	1.15	5.00	0.037	4.37
1/4 - 1/2	52.20	0.74	1.05	0.0015	2.77

U_m obtained above, the contribution of U_m term in Eq.(6-17) was evaluated to be less than 10 % for membrane PS-1 when the external salt concetrantion was between 0.0039 N and 0.0625 N, and decreases with increase of the salt concentration. Therefore, it may be concluded that the values of u_+ and u_- determined in the previous chapter using the experimental data of membrane potential and salt flux with neglecting the contribution of mass movement were valid within 10 %.

References

1) Y. Kobatake, M. Yuasa and H. Fujita, J. Phys. Chem. 72, 1752 (1968)

2) Y. Toyoshima, Y. Kobatake and H. Fujita, Trans. Faraday Soc., 63, 2828 (1967).

3) U. Saxén, Ann. Physik, 47, 46 (1892).

4) Y. Toyoshima, H. Nozaki, J. Phys. Chem., 73, 2134 (1969).

Chapter 7. Transference Numbers of Small Ions in Charged Membrane

In chapter 3, the activity coefficients and mobilities of small ions in charged membranes were determined with use of the membrane potential and ion permeability for the systems of collodion based polystyrene sulfonic acid membrane immersed in aqueous solution of KCl and NaCl. The results were; 1)the mobility of coions in charged membrane is approximately equal to that in free solution, 2) both the activity coefficient and mobility of counterion are much smaller than those in bulk solution when the concentration of the external solution C is lower than the stoichiometric density of charges fixed in the membrane, X, and 3) the dependence of mobility of counterions in membrane on the external salt concentration is approximately equal to that of activity coefficient of the counterions in the membrane. These facts imply that the behaviour of coions is not affected materially by the presence of fixed charges, while that of counterions is affected very much by the immovable charges in the membrane when C/X is smaller than unity.

Chapter 6 described the charge density which governs the hydrodynamic properties of the membrane by analyzing the experimental data of electroosmosis and streaming potential. The charge density governing the mass movement was found to be about 10 % of that for mobility and

activity of small ions for the same system, and was less than 4 % of the stoichiometric charge density of the membrane, X. Furthermore, it has been shown that the Saxén relation[1] holds experimentally for the system studied for whole range of salt concentration, i.e. the electroosmosis and streaming potential are equal each other in an arbitrary salt concentration within the experimental error. This fact implies that the difference between the amounts of counterions and coions carried by the mass flow must be equal to the excess charges inside the membrane which can transmit the external electrical force acting on them to the fluid medium in the membrane. However, any interpretation on the mechamism of marked depression of the fixed charge density of the membrane governing the mass movement has not been given.

This chapter purports to study the physicochemical mechamism for the remarkable depression of the charge density governing the hydrodynamical properties of the membrane by analyzing the trasference numbers of co-and counterions in the membrane.

Theoretical

The electrical transference number of cations or anions in charged membrane is defined as the ratio of the electricity transported by cation or anion species to the total electric current when the external electic field is applied across the membrane with no differences in

concentration and in hydrostatic pressure in two sides of the membrane. In the system in problem, Eq.(2-9) is represented by Eq.(7-1),

$$\begin{aligned} J_+ &= -u_+ c_+ (d\varphi/dx) + c_+^* U_m \\ J_- &= u_- c_- (d\varphi/dx) + c_-^* U_m \end{aligned} \tag{7-1}$$

while the equation of U_m, Eq.(6-5) can be simplified to give

$$U_m = -kF\psi X(d\varphi/dx), \tag{7-2}$$

under the present external condition. Here the conclusion that $\chi = \psi'$ drown in Chapter 6 has been used. Starting from these equations, the transference number of cation in the membrane, t^+, is calculated to give

$$t^+ = [u_+ c_+ + c_+^* kF\psi X]/[u_+ c_+ + u_- c_- + kF(\psi X)^2] \tag{7-3}$$

and that of anion, t^- is given be

$$t^- = [u_- c_- - c_-^* kF\psi X]/[u_+ c_+ + u_- c_- + kF(\psi X)^2] \tag{7-4}$$

As shown in chapter 6, in the electroosmosis experiments the observed rate of the volume flow J_v mainly stems from the movement of the local center of mass, and is proportional to the current density, I. The slope of J_v vs. I plot is given by

$$F(J_v/I)_{\Delta p=0} = kF\psi X/[u_+ c_+ + u_- c_- + kF(\psi X)^2] \tag{7-5}$$

Combination of Eqs.(7-3) and (7-5), or (7-4) and (7-5) leads to

$$t^+ = \frac{u_+ c_+}{u_+ c_+ + u_- c_- + kF(\psi X)^2} + c_+^* F(J_v/I) \tag{7-6}$$

or $$t^- = \frac{u_- c_-}{u_+ c_+ + u_- c_- + kF(\psi X)^2} - c_-^* F(J_v/I)$$

The term of $kF(\psi X)^2$ in the denominator of Eq.(7-6) can be neglected compared with the preceeding two terms in the present membrane-electrolyte system. Then, Eq.(7-6) is simplified to give

$$\text{or} \quad \begin{aligned} t^+ &= \bar{t}^+ + c_+^* F(J_v/I) \\ t^- &= \bar{t}^- - c_-^* F(J_v/I) \end{aligned} \qquad (7\text{-}7)$$

Here, $\bar{t}^+$ and $\bar{t}^-$ are the mass fixed transference numbers of cations and anions in the membrane, and are given by (cf. Eq. 5-6)

$$\bar{t}^+ = u_+ c_+ / (u_+ c_+ + u_- c_-) \quad \text{and} \quad \bar{t}^- = u_- c_- / (u_+ c_+ + u_- c_-) \qquad (7\text{-}8)$$

Since we have determined the values of $u_+ C_+$ and $u_- C_-$ in the membranes in various concentrations of KCl, the values of $\bar{t}^+$ and $\bar{t}^-$ are evaluated at an arbitrary KCl concentration. Besides, $\bar{t}^+$ and $\bar{t}^-$ can also be evaluated by the membrane potential as shown in Chapter 5. Eq.(7-7) implied that the measurements of t^+ and J_v/I allow to determine the values of C_+^* and C_-^* separately.

Experimental

Materials The membranes studied here are one of three membranes used in Chapter 3 and an oxidized collodion membrane (M-2) used in Chapter 5. KCl is used as the solute for all experiments reported here.

Measurements of transference number The cell used for measurements

of the transference number is schematically shown in Fig.7-1. Each half cell had 15 ml in volume, and a large Ag-AgCl plate electrode was installed in it. The solution in the cell was stirred vigorously with a pair of plastic fans to prevent the concentration polarization[4]. All experiments were perfomed in an air oven regulated at 25° C. As illustrated in Fig. 7-2, the observed transference number of cation t^{+}_{obs} at a given current strength was independent of the speed of stirring when the speed was faster than 180 r.p.m. Hence all experiments were performed at 360 r.p.m. in stirring speed. Prior to measurements, KCl solution of a given concentration was filled in the cell and allowed to stand overnight to equilibrate the membrane-electrolyte system. After the solution was drained away through the stop cock, the cell and electrodes were washed by ion exchanged water and wiped with filter papers. Exactly measured volume of KCl solution of a given concentration was introduced into each compartment of the cell with a burette. Slight unbalance of the solution levels in two compartments, that is a small difference in hydrostatic pressure gave no detectable influence on the measured transference number. The electric current was delivered in the cell from batteries (60 V) through the pair of Ag-AgCl electrodes. The current strength was kept constant manually with a variable resistor, and measured with a calibrated milliammeter. The period of passage of electric current was measured with a stop-watch to determine the total electricity Q delivered for a given period of time with a constant current strength,I, the solution in

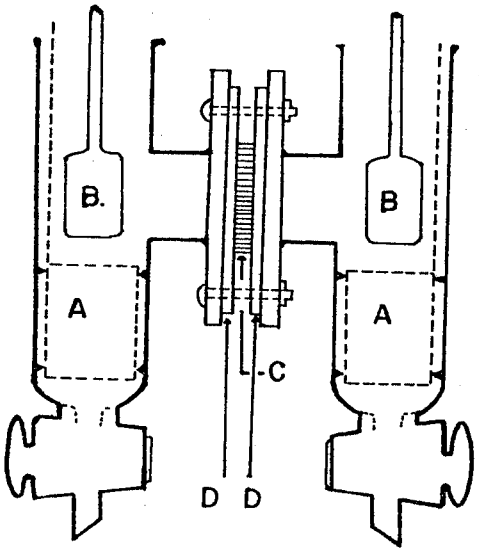

Fig. 7-1. Diagram of the cell used for the measurements of the transference number. A, Ag-AgCl electrode; B, Plastic fan; C, Membrane; D, Silicon rubber gasket.

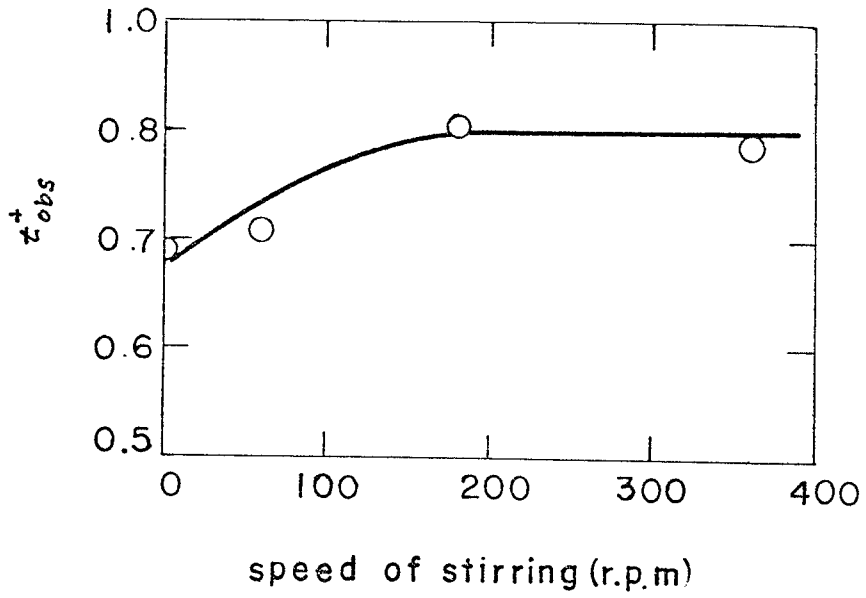

Fig. 7-2. Effect of the rate of stirring on the transference number.

each half cell was drained into an Erlenmeyer flask. The electrode and the cell were washed carefully with ion exchanged water so that no ions remained in the cell. The total amounts of Cl^- ions in each half cell was evaluated by titration with a standard $AgNO_3$ solution. Since the initial concentration and the volume of KCl solution in each compartment were known, the total amounts of elecrolyte transported by the passage of electricity, Δn, were able to be determined. The measured Δn in the two compartments agreed each other within 2 %. The change in concentrations before and after the passage of electicity in each half cell was less than 15 %. The transference number of potassium ion t^+_{obs} is calculated by the equation,

$$t^+_{obs} = F\Delta n/Q \qquad (7\text{-}9)$$

As pointed out by previous investigators[5-7], notably Lakshminarayanaiah, the following two points should be taken into accounts to obtain the meaningful transference number of cations t^+ in a charged membrane; a) the concentration polarization at the membrane-solution interfaces, and b) the back diffusion due to concentration difference in the two compartments caused by the passage of electricity. As shown in the next chapter, when these effects are properly considered, the observed transference number of cation t^+_{obs} can be represented by the following equation,

$$t^+_{obs} = [t^+ - (FRT/L)\,g(c)H(c)][1 - \tfrac{1}{2}D(c)S + O(S^2)]$$

$$D(c) = (RT/LV)A[1 + h(c)] \cdot H(c) \qquad (7\text{-}10)$$

Here, t^+ is the transference number defined by Eq.(7-3), and L, A, and V are the effective thickness and areas of the membrane, and the volume of solution in the two compartments, respectively. In Eq.(7-10), g(C) h(C) and H(C) are functions of the initial salt concentration C and of parameters characteristic to the pair of membrane and electrolyte, and S is the period of time for the passage of electricity. The term (FRT/L)g(C)H(C) represents the effect of concentration polarization at the membrane-electrolyte solution interfaces. This term becomes negligibly small compared with t^+ when two sides of the membrane are stirred vigorously. Eq.(7-10) indicates that the plot t^+_{obs} against S must give a staright line irrespective of the current strength I, and the ordinate intercept gives the desired value of the transference number t^+ provided that the solutions are agitated vigorously.

Results and Discussion

Transference number. By way of example, Fig.7-3 shows t^+_{obs} against S relations in accordance with Eq.(7-10). Lakshiminarayanaiah and Subrahmanyan[6] discussed the effect of back diffusion, and proposed two methods for eliminating this effect for obtaining the desired transference number t^+. The first method is that a high density of

electric current is passed through the membrane to bring the change in concentration amenable for accurate measurements within a very short period of time. The second method is that the initial concentrations in the two compartments are so chosen that on completing the experiment, the concentrations in the two compartments are reversed. Thus the mean value of concentration difference between two bulk solutions with respect to time would be close to zero, and the effect of the back diffusion through the membrane might vanish on the average. The procedure of extrapolation to S = 0 corresponds to the first method described above. The value of t^+ thus determined is confirmed experimentally by comparing with that obtained by the second method. The transference number obtained by the second method was independent of the current strength, and agreed well with the extrapolated value of t^+_{obs} to S = 0 as illustrated in Fig.7-3. Therefore, we may use either method for obtaining the transference number at a given salt concentration C. In Fig.7-4 is shown t^+ for membrane PS-1 in KCl solution as a function of log C (O marks).

Mass fixed transference number ζ^+ or ζ^- The temperature at which u_+C_+ and u_-C_- had been determined was 30°C as described in chapter 3. It is considered, however, that the mass fixed transference number of cation in the membrane defined by Eq.(7-8) is almost independent of

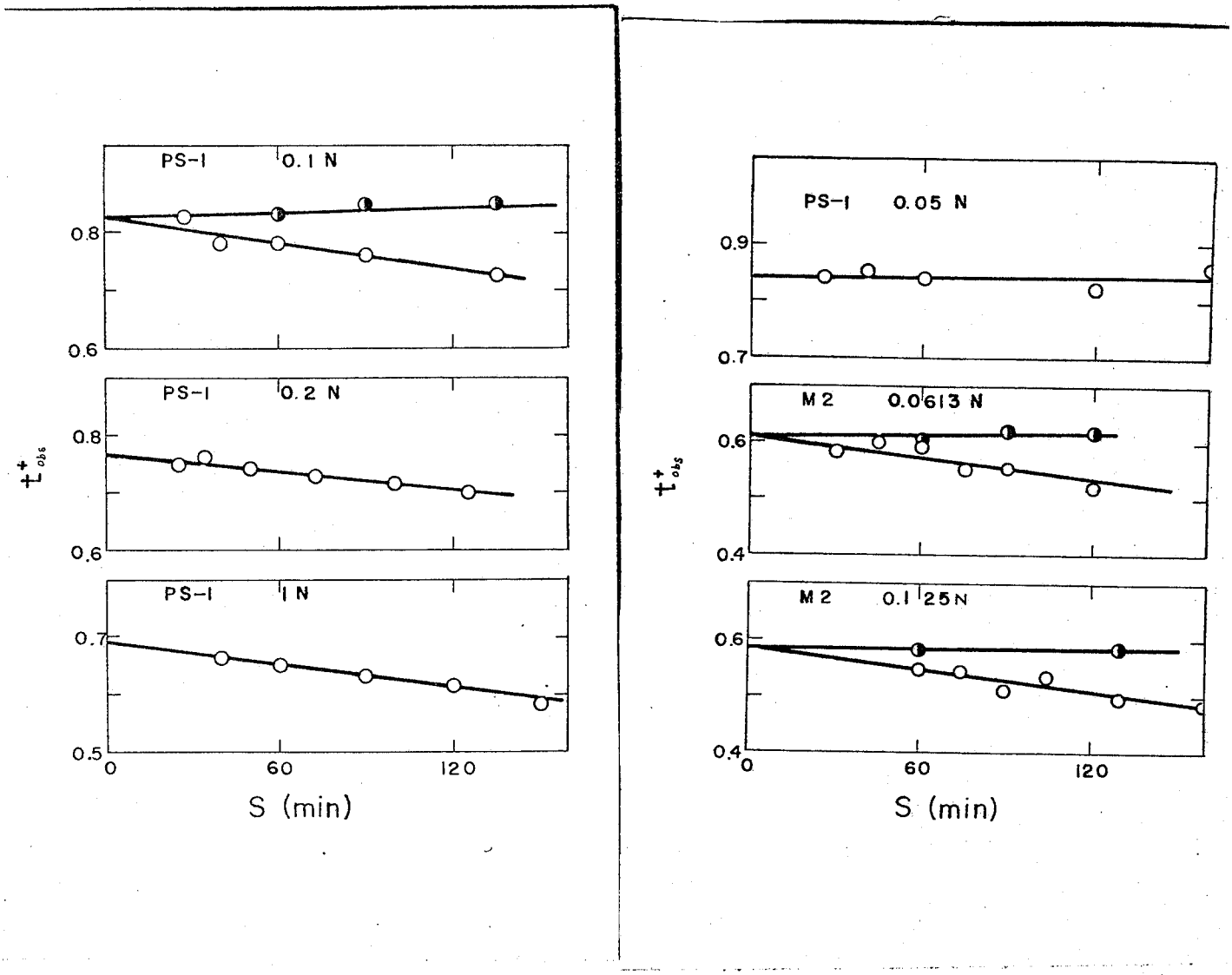

Fig. 7-3. Plots of t^+_{obs} against S in various KCl concentrations. ○, first method, i.e. based on Eq.(7-10); ◑, second method, i.e. adjusting the initial concentration in two compartments so as to cancel the back-diffusion effects.

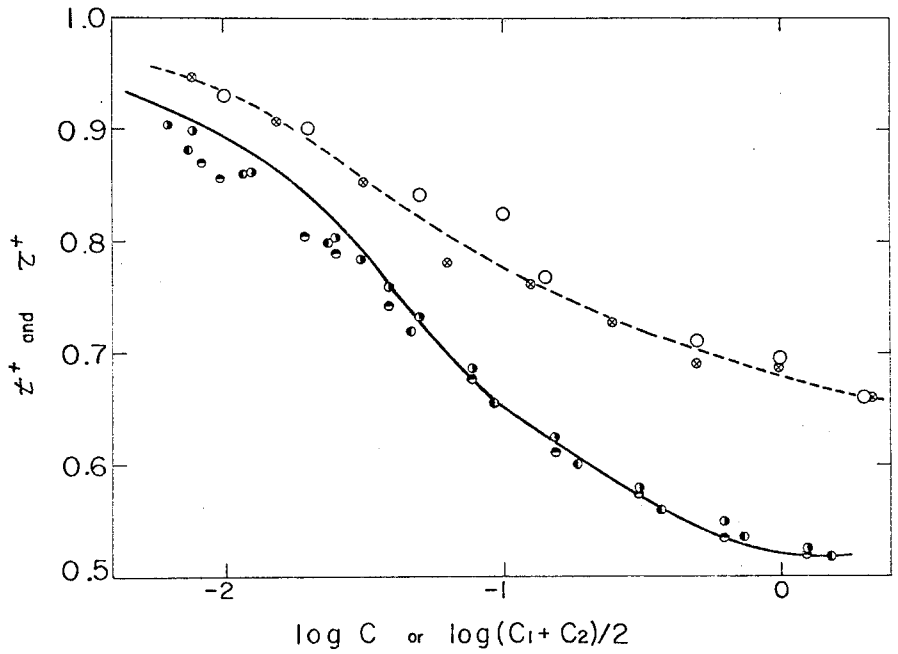

Fig. 7-4. Plots of t^+ and $\bar{t}^+$ against log C for membrane PS-1 in KCl solution. ○, observed transference numbers of cation; ⊗, calculated by Eq.(7-7) with assumption of $C_-^* = C_-$; ◑, ◐, ◒ are $\bar{t}_{app}$ calculated from the membrane potential data and Eq.(5-3) at β = 4, 2, and 1.5, respectively.

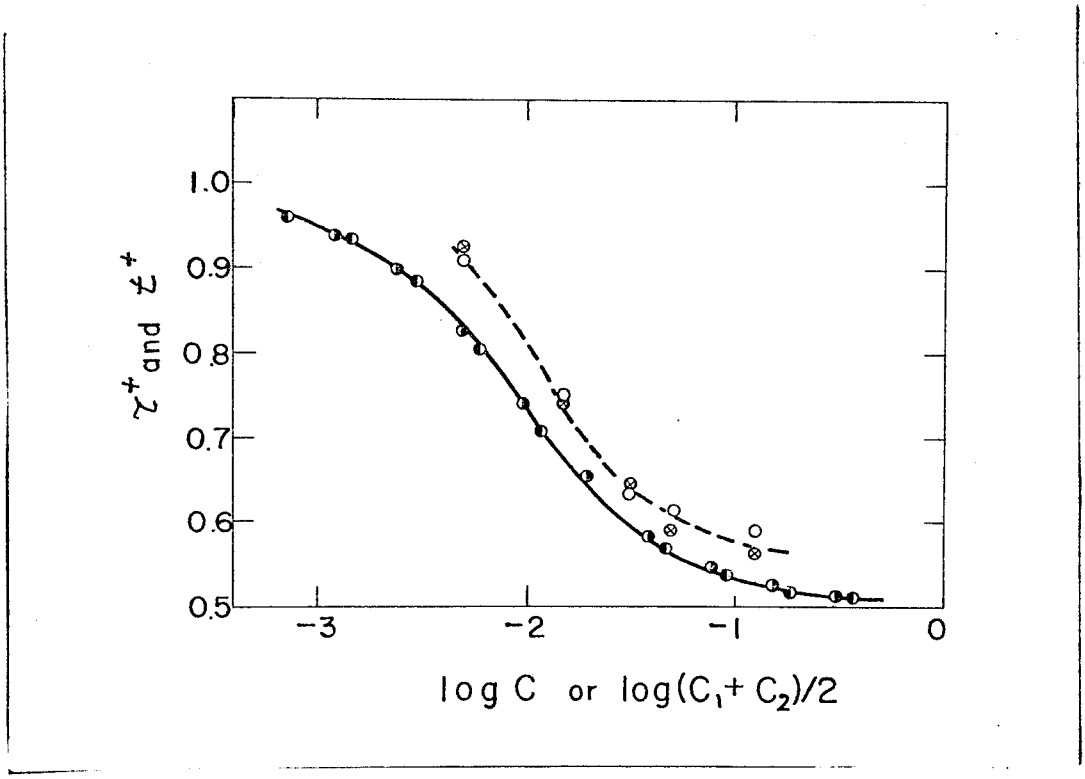

Fig. 7-5. Plots of t^+ and $\mathcal{T}^+$ against log C for membrane M-2 in KCl solution. Notations are the same as in Fig. 7-4.

temperature at least between 25° C and 30° C, because that the transference number in a free aqueous solution scarecely depends on the temperature[8], that the Donnan uptake of small ions in the membrane equilibrated with a given concentration of an electrolyte solution has been found to be independent of temperature within experimental error, and that the dependence of electrical resistance of membrane on temperature is approximately equal to that in a free solution. Therefore, we may use the values of $u_i C_i$ ($i = +, -$) which were determined at 30° C and described in Chapter 3 (see table 3-2). The values of τ^+ are shown by a solid line in Fig. 7-4 and compared with the values of t^+ determined above. It is noted that the difference between τ^+ and t^+ becomes appreciable when the concentration of the external salt C exceeds the stoichiometric charge density X fixed in the membrane[9,10]. This diffrence between t^+ and τ^+ is the contribution of the mass movement in the membrane represented by the second term in the right hand side of Eq.(7-7). The comparisons between τ^+_{app} and t^+ were made for an oxidized collodion membrane (M-2) in KCl solution, and the results were shown in Fig.7-5.

Evaluation of C^*_+ and C^*_- Taking the difference between t^+ and τ^+, and introducing the experimental data of the electroosmosis $(J_v/I)_{\Delta p=0}$ at a given KCl concentration C, the value of C^*_- or C^*_+ is determined. The relevant data for the electroosmosis were given in Fig.6-3. The value of C^*_- thus obtained were compared with the analytical

value of C_- in the membrane at a given concentration C of the external KCl solution which were presented in Table 3-4 of Chapter 3. The ratio of C_-^*/C_- was found to be 1.05 ± 0.05 when the external salt concentration C is higher than the stoichiometric charge density of the membrane, X. As noted in Eq.(6-4), the difference between C_+^* and C_-^* was represented by ψX from the analysis of the electroosmosis and the streaming potential data in various KCl concentration, where ψ was found to be 0.04 ~ 0.05. Assuming C_-^*/C_- is equal to unity, indtroducing the values for $\bar{t}^+$, ψX, together with the experimental data for $(J_v/I)_{\Delta p=0}$ into Eq.(7-7), t^+ at an arbitrary concentration of KCl solution can be evaluated. The results are plotted against log C for membrane PS-1 in Fig.7-4(⊗ marks), and compared with the corresponding experimental data of t^+ (○ marks). The calculated values agree quite satisfactorily with the experimental data in wide range of KCl concentration studied. Then, the amounts of co-and counter-ions in the membrane carried by the mass movement may be represented as follows in the whole range of salt concentration studied

$$\begin{aligned} C_-^* &= C_- \\ C_+^* &= C_- + \psi X. \end{aligned} \qquad (7\text{-}11)$$

Since the condition of the electroneutrality is represented by $C_+ = C_- + X$, the ratio C_+^*/C_+ and C_-^*/C_- (denoted by Γ_+ and Γ_-) are expressed as $\Gamma_+ = (C_- + \psi X)/(C_- + X)$ and $\Gamma_- = 1$ (7-12)

where $\psi = 0.04 \sim 0.05$.

These expressions are similar to those found in Chapter 3 for activity coefficients and mobilities of small ions in the membrane(see Eqs. 3-16 and 3-18).

Eqs.(7-12), (3-16) and (3-18) imply that all coions in the membrane are active both thermodynamically and hydrodynamically, while the counterions behave quite non-ideally in the membrane phase, i.e. only a part of the counterions dissociated from the polyelectrolyte skeletons are active for mobility and activity, and a much smaller part of the counterions are effective for the hydrodynamical properties of the membrane. Qualitatively, these facts may be interpreted as follows when the spatial distributions of small ions and of the local center of mass movement in the membrane are considered. The coions are restricted by repulsion to the region where no electric effect of the fixed charges on the membrane skeletons is reached. The velocity of the local center of mass movement must be small in the vicinity of the membrane skeletons due to the hydrodynamical interaction between the fixed membrane matrix and the surrounding fluid. Then the averaged mass flow in the membrane U_m is mainly attributed to the mass movement in the region which is far apart from the polymer skeletons in the membrane. A larger part of the coins may be localized in the same region in the membrane. These regions comprise the predominant

parts of the membrane phase when the water contents of the membrane is very large (about wt. 80 %) as encountered here. Thus the amounts of coions carried by the mass flow is not materially different from that of the average concentration of coions in the membrane. On the contrary, a larger proportion of the counterions dissociated from the polyelectrolyte skeletons of the membrane is immobilized in the vicinity of the fixed charges of the polymer chain, where the velocity of the local center of mass flow is also small. This part of the mass movement does scarcely contribute to the averaged rate of mass flow in the membrane U_m. Therefore, the concentrations of counterions C_+^* carried by the mass flow U_m is much smaller than the stoichiometric density of the counterions dissociated from the membrane skeletons. Final justification of Eq.(7-12) or the reason of marked depression of the hydrodynamically effective charge density $\not{X}$ of the membrane is left for future theoretical work.

References

1) U. Saxén, Ann. Physik. 47, 46(1892)

2) Y. Kobatake, M. Yuasa and H. Fujita, J. Phys. Chem., 72, 1752(1968)

3) Y. Toyoshima, Y. Kobatake and H. Fujita, Trans. Faraday Soc., 63, 2814(1967).

4) N. Lakshminarayanaiah, J. Phys. Chem., 72, 3699(1968).

5) T.R.E. Kressman and F.L. Tye, Disc. Faraday Soc., 21, 185 (1956)

6) N. Lakshminarayanaiah and V. Subrhmanyan, J. Polymer Sci. A2, 4491 (1964)

7) D.K. Hale and D.J. McCaulay, Trans. Faraday Soc., 57, 135 (1961)

8) Landolt-Börmstein Tabellen, II-7, p247, 6th ed.,(Berlin-Heidelberg, Springer, 1960)

9) N. Lakshminarayanaiah, J. Phys. Chem., 73, 97 (1969).

10) Y. Oda and Y. Yawataya, Bull. Chem. Soc. Jap., 29, 673 (1956).

Chapter 8. Concentration Polarization at the membrane surface

It is well known that various transport phenomena across a charged membrane are affected very much by the rate of stirring of the external solutions.[1,2] This stems from the unstirred liquid film remainig at the membrane-solution interface. This layer is referred to as the stagnant layer and is caused by the hydrodynamic interaction between the liquid and the solid membrane surface. Considering the cause of the layer, the layer remains even if the solution is stirred vigorously[3]. Then, the presence of the layer must be taken into consideration for a quantitative analysis of membrane phenomena. The effect of the layer to the membrane phenomena observed when the current is passed through the membrane is often called as concentration polarization. This chapter aims to discuss the concentration polarization and shows that the effect of the presence of the layer can be diminished to be negligibly small compared to the observed value of membrane phenomena when the solution are stirred vigorously as employed in the previous chapters. Then, to check the validity of the theoretical implications, the experiments are performed uner the condition both of vigorous stirring and of no stirring.

Theory

Let us consider a system in which two electrolyte solutions are separated by a membrane bounded between x = 0 and x = L. A steady electric current normal to the membrane surface is passing the membrane through a pair of electodes reversible to the anion used. The solution in the cathode compartment occupies the region $x>L$, and the solution in the anode compartment lies in the region $x<0$. Before the current is delivered in the system, the concentration in the two bulk solutions are assumed to be the same, and which is denoted by C.

The concentration of the electrolyte component in the cathode compartment increases with the passage of electricity due to the ion transport and the electrode reaction. The change in salt concentration ΔC is expressed as follows;

$$\Delta C = \int_0^S (A/V)(J_+)\, dS'$$

where A, V, and S are the effective area of the membrane, the volume of the solution in the cathod compartment, and the period of time for the passage of the electric current, respectively. Strictly, the above representation for ΔC is not accurate because the volume in

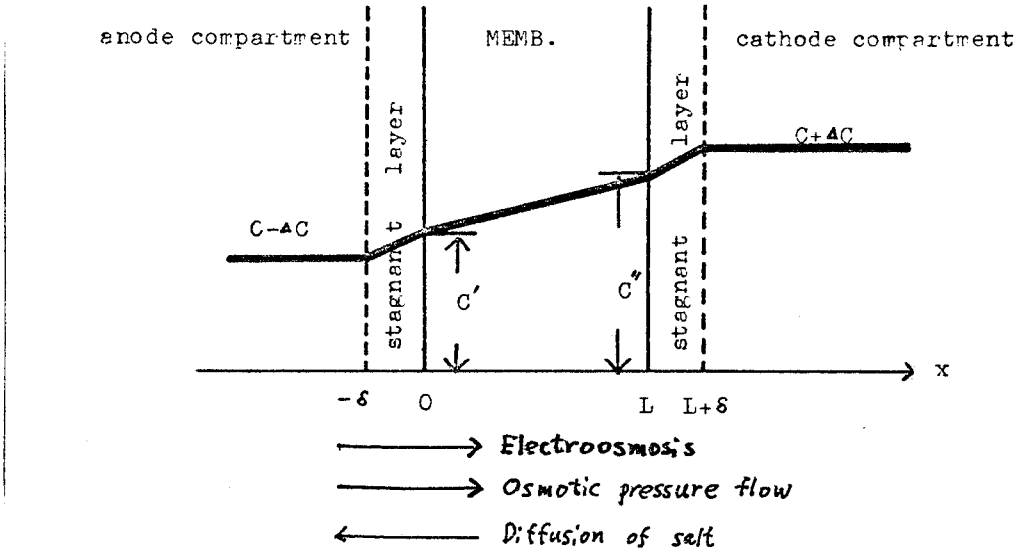

Fig. 8-1. Schematic diagram of the system considered. The symbols are defined in the text.

each compartment changes due to the electroosmosis which takes place with the passage of electricity. This volume change due to the electroosmotic flow, however, can be neglected in comparison with the initial volume of the solution in actual experimental set up.

The thickness of the stagnant layer is assumed to be the same in two sides of the membrane and is denoted by δ. The concentration profile in the system is illustrated schematically in Fig.8-1 where the ordinate represents the concentration of the electrolyte component, and the abscissa represents the distance x in the direction of the current. The concentration at x = 0 is denoted by C', and that at x = L by C''. The deviation of C' or C'' from the initial concentration C is attributed to the concentration polarization at the membrane surface, i.e. to the electrolyte accumulation or depression in the bulk solution. The concentration polarization is a function of the density of electric current I. Then, C' and C'' can be expanded in powers of I, and given by

$$\begin{aligned} C' &= C - \Delta C + f(c)\, I + O(I^2) \\ C'' &= C + \Delta C - f(c)\, I + O(I^2) \end{aligned} \qquad (8\text{-}1)$$

Here f(C) is a function only of C. To proceed further, the following assumptions must be taken into considerations; (1) Fluxes of all species are steady in the range $-\delta < x < L + \delta$, although the concentration of the electrolyte component in the bulk solution changes with time. (2) The period of time necessary to attain the equilibrium at the membrane surface is short enough compared with the speed of concentration variation in bulk solutions. In otherwords, the condition of the Donnan equilbrium at the membrane surface is applicable. (3) The partial molar volume of species i, v_i is assumed to be constant in all phases considered. Due to these assumtions, the volume flow $J_v = v_+J_+ + v_-J_- + v_oJ_o$ and the electric current density, I, must stay constant in the range $-\delta < x < L+\delta$. Introducing Eq.(2-9) into the above equation for J_v and rearranging, we obtain

$$J_v = -\frac{RT}{F}(\nu_+^* + \nu_-^*)\frac{u_+c_+u_-c_-}{u_+c_+ + u_-c_-}\frac{d\ln a^2}{dx}dx + \frac{\nu_+^*u_+c_+ - \nu_-^*u_-c_-}{u_+c_+ + u_-c_-}\frac{I}{F} + \left[1 - \frac{\nu_+^*u_+c_+ - \nu_-^*u_-c_-}{u_+c_+ + u_-c_-}(4X)\right]U_m, \quad (8\text{-}2)$$

Since the term $(4X)[v_+^*u_+C_+ - v_-^*u_-C_-]/(u_+C_+ + u_-C_-)$ in the above equation is negligibly small compared with unity in the present membrane-electrolyte system (see chapter 6), Eq.(8-2) is simplified to give

$$J_v = -\frac{RT}{F}(\nu_+^* + \nu_-^*)\frac{u_+c_+u_-c_-}{u_+c_+ + u_-c_-}\frac{d\ln a^2}{dx} + \frac{\nu_+^*u_+c_+ - \nu_-^*u_-c_-}{u_+c_+ + u_-c_-}\frac{I}{F} + U_m \quad (8\text{-}3)$$

Making use of equations for mobilities and activities of small ions in the membrane given by Eqs.(3-16) and (3-18) together with three presumptions described above, Eq.(8-3) can be integrated to give

$$J_v L = -\frac{RT}{F}(\nu_+^* + \nu_-^*)\frac{u_+^\circ u_-}{u_+^\circ + u_-^\circ}\left[Z(C'') - Z(C') - (2\alpha-1)\phi X \ln\frac{Z(C') + (2\alpha-1)\phi X}{Z(C') + (2\alpha-1)\phi X}\right] + \frac{I}{F}\int_0^L \frac{\nu_+^* u_+ c_+ - \nu_-^* u_- c_-}{u_+ c_+ + u_- c_-}dx + L U_m \qquad (8\text{-}4)$$

(for $0 < x < L$)

and

$$J_v \delta = -\frac{RT}{F}(\nu_+^* + \nu_-^*)\frac{2u_+^\circ u_-^\circ}{u_+^\circ + u_-^\circ}(C' - c + \Delta c) + [\nu_+^* \alpha - \nu_-^*(1-\alpha)]\frac{I}{F}\delta + \delta U_m \qquad (8\text{-}5)$$

(for $-\delta < x < 0$ or $L < x < L+\delta$)

where Z(C) stands or $(\phi^2 X^2 + 4C^2)^{1/2}$. In the derivation of Eq. (8-5), the thermodynamically effective charge density of the membrane, ϕX, was assumed to be constant irrespective of the salt concentration C. This assumption is not unreasonable when the concentrations in the two compartments, C' and C'' are close each other as encountered here. Due to the three presumptions described above, J_v must be continuous at the interfaces between the membrane and stagnant layers at x = 0 or x = L. Therefore, substituting Eq.(8-1) into Eqs.(8-4) and (8-5), expanding in powers of I, and

eliminating J_v from the resulting equations, we obtain the following relation for f(C) defined in Eq.(8-1)

$$f(c) = g(c) - h(c)\Delta C/I \qquad (8-6)$$

with

$$g(c) = \frac{2(u_+^\circ + u_-^\circ)\nu}{RT\, u_+^\circ u_-^\circ} \cdot \frac{\tau^+ - \alpha}{1 - \dfrac{\delta\nu C}{\bar{z}(c) + (2\alpha-1)\phi X}}$$

and

$$h(c) = \delta\nu C / [\bar{z}(c) + (2\alpha-1)\phi X - \delta\nu C]$$

where ν is the relative thickness of the stagnant layer defined by $\nu = \delta/2L$. The above relations hold to be valid so far as the higher order terms of I in Eq.(8-1) are neglected.

The equation for U_m is given by

$$U_m = -\kappa(d\rho/dx) - \kappa F \phi X (d\varphi/dx) \qquad (8-7)$$

where dp/dx represents the gradient of pressure caused by the osmotic pressure difference at the membrane surfaces. This osmotic pressure difference at the membrane surface is approximately expressed as follows;

$$(\Delta p)_{x=L} = RT[(C_+ + C_-)_{x=L_-} - 2C''] \qquad (8-8)$$

$$(\Delta p)_{x=0} = RT[(C_+ + C_-)_{x=0_+} - 2C']$$

Integrating Eq.(8-7) with respect to x, introducing Eq.(8-8) for the pressure difference at the membrane interfaces, and eliminating the potential by using the expression for the electric current I in the membrane, and rearranging the resulting equation, we obtain

$$L_{11} U_m = \left[\frac{\kappa F \Delta X}{u_+ C_+ + u_- C_- + \kappa F (\Delta X)^2} \right]_{I=0} \frac{I}{F} L_{11}$$

$$+ 2(2\alpha - 1) \frac{\Delta C [\Delta C - f(c) I]}{\bar{Z}(c) [\bar{Z}(c) + (2\alpha - 1) \Delta X + \gamma]} + \kappa RT \left[\chi - \frac{\beta C}{\bar{Z}(c)} \right] (\Delta C - f(c) I)$$

(8-9)

where γ stands for $2KF(\psi X)^2 / (u_+^0 + u_-^0)$. The flux equation for J_+ is written as follows;

$$J_+ = - u_+ C_+ [d\varphi/dx + (RT/F) d \ln a_+ / dx] + C_+^* U_m$$

Elimination of $d\varphi/dx$ from this equation by using the expression for $I = F(J_+ - J_-)$, substitution of Eq.(8-9) for U_m, and rearrangment leads to

$$J_+ = t^+ I/F - (RT/L_{11}) g(c) H(c) I - (RT/L_{11}) A [1 + h(c)] H(c) \int_0^S J_+ \, ds.$$

(8-10)

Here H(C) is given by

$$H(c) = \frac{1}{F}\frac{u_+^\circ u_-^\circ}{u_+^\circ + u_-^\circ}\frac{\partial c}{z(c)} - \frac{1}{F}\frac{(2\alpha-1)\phi x\ \partial c}{z(c)\left[z(c)+(2\alpha-1)\phi x\right]}\frac{u_+^\circ u_-^\circ}{u_+^\circ + u_-^\circ}$$

$$-4(c_+^* - z^+\phi x)_{I=0}\left[2(2\alpha-1)\kappa\phi x\frac{c}{z(c)\left[z(c)-\phi x\right]} + \kappa - \kappa\frac{2c}{z(c)}\right]$$

(8-11)

The solution to the above integral equation (8-10) is

$$J_+ = \left[\left(It^+/F\right) - (RT/\Delta)g(c)H(c)I\right]\exp\left[D(c)s\right] \qquad (8-12)$$

where D(C) is given by

$$D(c) = (RTA/\Delta V)\left[1 + h(c)\right]H(c) \qquad (8-13)$$

Thus the observed transference number t^+_{obs} is represented by the equation

$$t^+_{obs} = F\int_0^s J_+\,ds' \Big/ \int_0^s I\,ds'$$

$$= \left[t^+ - (FRT/\Delta)g(c)H(c)\right]\left[1 - \tfrac{1}{2}D(c)s + O(s^2)\right] \qquad (8-14)$$

This is identical to Eq.(8-10) in the previous chapter.

Vigorous stirring of the external solutions decreases the thickness of the stagnant layer $\hat{\delta}^a$, which in turn the decrease of g(C)

term. As seen in the above derivation, g(C) represents the effect of concentration polarization. The correction for the concentration polarization (FRT / L)g(C)H(C) is approximately 0.003 when ν is put equal to 0.01[3] under the condition that $\phi X < C$.

In order to check the applicability of Eq.(8-6), the effect of concentration polarization on another membrane phenomena will be considered. The electroosmosis is chosen as an example. According to the above equations, the rate of electroosmosis is given by

$$J_v = \omega_{12} I - \frac{4k}{L} RT \left\{ 1 - \frac{2C}{\Sigma(c)} \right\} f(c) \qquad (8\text{-}15)$$

where ω_{12} is defined by Eq.(6-8) and the term concerned with the back diffusion is omitted.

Experimental

The membrane used in this study was a collodion based polystyrene sulfonic acid membrane designated as PS-1. The physicochemical characteristics of the membrane have been determined in our previous studies, and the relevant characteristics are tabulated in Table 8-1. The cell used and procedures for the measurement of electroosmosis were the same as those employed in the previous chapter. The geometrical area of the membrane was 1.70 cm^2, and the cross sectional area of the capillary for the measurements of the volume flow was 0.0096 cm^2. The bulk solutions were stirred by a pair of magnetic stirrers at a

Table 8-1 Some characteristics of membrane used

X	0.224	equiv. /l
ϕX	0.089	equiv. /l
water content	78	wt %
L	0.053	cm
k	1.16×10^{-11}	$cm^4\ dyne^{-1}\ sec^{-1}$

speed of about 400 r.p.m. unless otherwise noted. KCl used as the solute was purified by repeated crystallization of the analytical grade of the salt. The water was obtained by passing distilled water through both cation and anion exchangers.

Results and Discussion

Figs 8-2 and 8-3 show the effects of stirring on the rate of the electroosmotic flow in various KCl concentrations. Fig.8-2 illustrates the linear relations between J_v (cc $cm^{-2}min^{-1}$) and current density I (mA cm^{-2}) hold in the case where the KCl concentration is high in comparison with the effective fixed charge density of the membrane ϕX. This linear relations hold for both cases with and without stirring of the external solutions. It is noticed that the effect of stirring on J_v diminishes with increase of the external salt concentration C, i.e. no effect of the stirring is observed in 1/4 M KCl, while J_v with no stirring is much larger than that with vigorous stirring in 1/128 M KCl solution. As seen in Eq.(8-12), when the concentration in the external solution C is sufficiently high in comparison with ϕX, the value of $\{1 - 2C/\Sigma(c)\}$ diminishes. Hence, the effect of the stagnant layer on J_v is neglected even if the unstirred film is remained at the membrane surface. With decrease of the external salt concentration, the

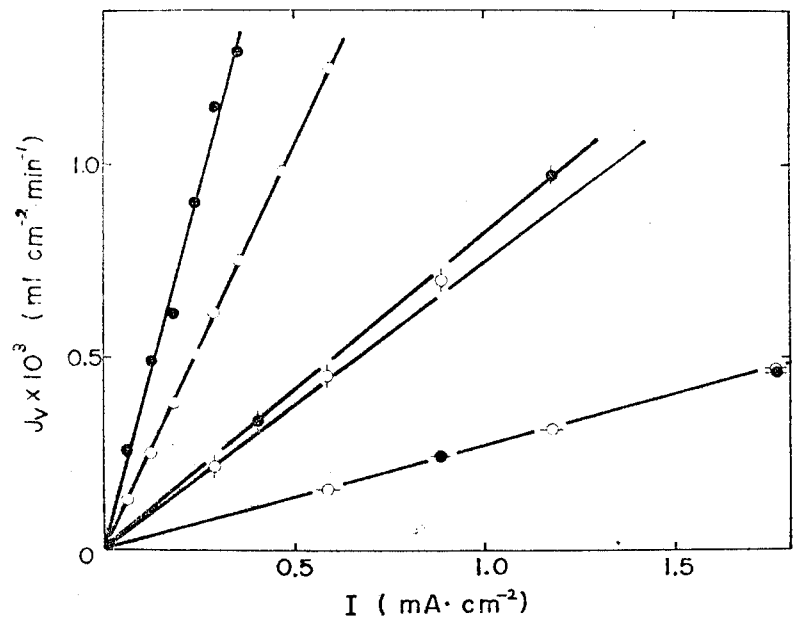

Fig. 8-2. The relation between J_v and I in various KCl concentration with and without stirring. Results with vigorous stirring, ○, 1/128 N; ◌, 1/16 N; -○-, 1/4 N. Results with no stirring, ●, 1/128 N; ◖, 1/16 N; -●-, 1/4 N.

last term in Eq.(8-12), becomes appreciable. Tracing back the derivation of Eq.(8-12), it is noticed that the last term is stemming from the osmotic pressure flow in the membrane, i.e. the term of dp/dx in Eq.(8-7). As illustrated in Fig.8-1, the direction of the osmotic pressure flow is the same as that of the electroosmotic flow. Therefore, J_v increases with insufficient stirring of the external solutions. Introducing the relevant characteristics of the membrane used into Eqs.(8-6) and (8-15) the equivalent thickness of the stagnant layer δ is evaluated to be 100mμ ($\nu = 0.094$) in the case of no stirring of the external solution.

In contrast with the case illustrated above, Fig.8-3 shows two examples in which J_v is not proportional to I when the bulk solutions are not agitated. The system is the same as that in Fig.8-2.except the concentration of KCl in the external solution is dilute. Even in this case, J_v increases linearly with I when the bulk solutions are stirred vigorously. Note that the non-linear relation decreases with increase of the current density, and that J_v /I with no agitation is always larger than that with vigorous stirring. Introducing the relevant characteristics of the membrane given in Table 8-1 into Eqs.(8-6) and (8-15), we obtain the difference of values of J_v /I for two cases with and without stirring, which is evaluated to give 0.037ν ($cm^3 min^{-1} mA^{-1}$) under the salt conditions shown in Fig.8-3. The observed value of this

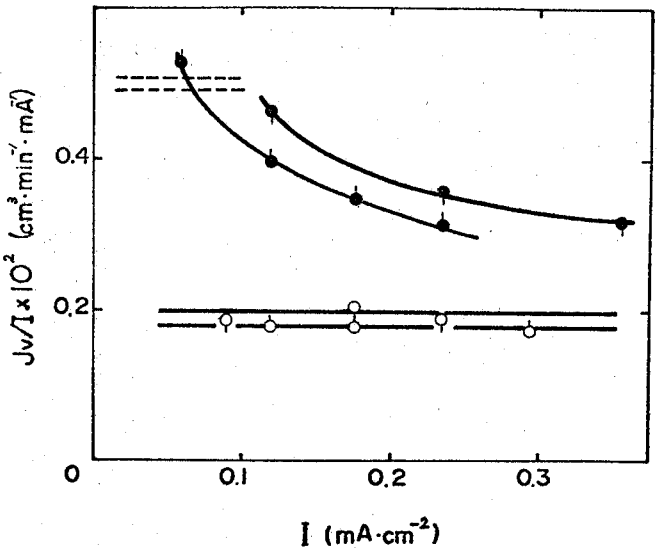

Fig. 8-3. The osbserved electroosmosis coefficient, J_v/I, as functions of current strength, I, in 1/1024 and 1/512 N of KCl solutions.

Results with vigorous stirring, ○ , 1/512 N; ♀ , 1/1024 N.

Results with no stirring, ● , 1/512 N; ♀ , 1/1024 N.

The dashed lines represent the value calculated from Eq.(8-15) assuming $\nu = 0.094$, which is obtained from the data of Fig. 8-2.

difference is approximately 0.003 ($cm^3 min^{-1} mA^{-1}$) for the same external condition at a small value of current density. The value of ν is then calculated to give 0.09. This value of ν agrees well with that obtained for the case of relatively concentrated solution (1/128 and 1/16 M KCl) given in Fig.8-2. This implies that the value of ν depends only on the stirring condition, and is independent of the concentration in the external solution. By use of the value of ν thus obtained, the second term in Eq.(8-1), i.e. $f(C)I$ can be evaluated to give 2.3×10^{-4} M even in dilute solution of 1/1024 M. Therefore, the linear expansion of Eq.(8-1) may be valid in the whole range of salt concentration encountered in the present study. As pointed out above, the non-linear relaion between J_v and I is attributed to the dependence of the thickness of the stagnant layer on the applied current density. When the current density is increased, the flux of species i in the stagnant layer must be increased correspondingly for retaining the steady flow of movable component in the system in problem. The steady state is attained by either an increase of C" (or decrease of C') at x = 0 (or x = L) in Fig.8-1, or a spontaneous decrease in the thickness of the stagnant layer δ. As seen in Eq.(8-6) the former does not lead to any non-linear relation between J_v and I. Therefore, the

non-linear character observed in J_V and I relation must be attributed to the thinning effect of δ. Since the thickness of the stagnant layer increases with decrease of the current density, the non-linear relation of J_V and I must be large in the low current density limit as seen experimentally in Fig. 8-3. Under the condition with vigorous agitation of the bulk solution, no such thinning effect of δ occurs at the membrane surface. Hence, the observed linear relation between J_V and I holds in the whole range of I studied.

References

1) G. Scatchard and F. Helfferich, Discussions Faraday Soc., 21, 70 (1956).

2) N. Lakshiminarayanaiah and V. Subrahmanyan, J. Polymer Sci., A2, 4491 (1964).

3) Y. Toyoshima, Y. Kobatake and H. Fujita, Trans. Faraday Soc., 63, 2814(1967).

Chapter 9. Membrane Potential of Oil Membrane

Membranes are commonly classified into two basic groups, "liquid" or "oil" membranes and "porous" membranes. The previous chapters deal with the electrochemical phenomena of porous membranes. In this chapter, the membrane potential of the oil membrane is considered, where highly ionic-selective character is observed. This type of membrane is investigated recently as a new device of electroanalytical sensor[1-8], which is called as ion-selective electrode. Oil membranes are constructed by dissolving ion-exchangers into organic solvents (preferably of minimal water solubility). Ion-exchangers are the substances that consist of an iongenic group which is attached to an organic molecule and are sparingly soluble in aqueous electrolyte solutions.

Theoretical

In the following discussion, ion-exchangers are positively charged and co-ions are assumed to be excluded completely. This assumption is not unreasonable since the membrane potential changes 59 mV by 10-fold change of the concentration in the aqueous phase. Let's consider the system where the liquid membrane are occupied between $0 < x < L$, and the membrane separates two electrolyte solutions. The solution located at $x < 0$ is referred to as solution I and concentration of i-anion in solution I is denoted by C_i^I. Similarly, the

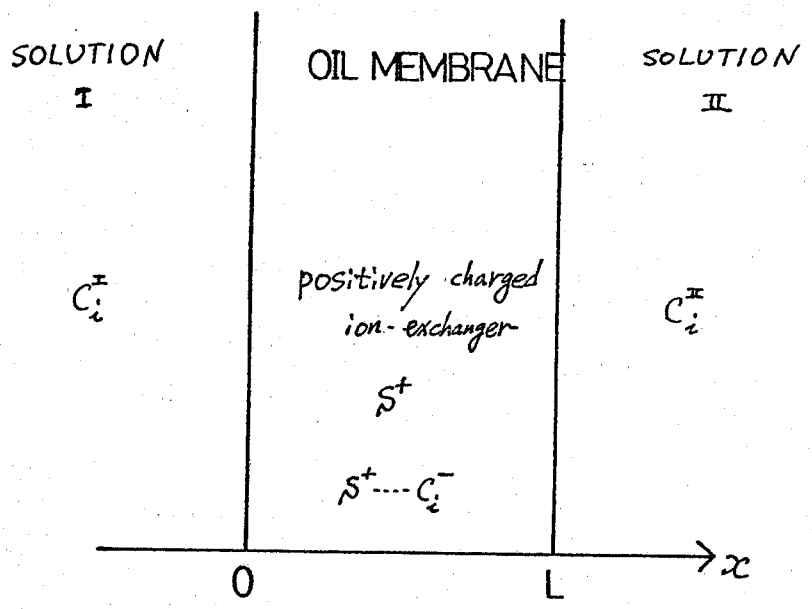

Fig. 9-1. Systems under consideration.

concentration of i-anion in the solution at $x < L$ is denoted by C_i^{II}. All anions are confined to be uni-valent. In the membrane phase, there exist following ionic species; s^+, 1, 2, ---- i, ----k anions, where s^+ stands for the positively charged ion-exchanger. Since s^+ is confined completely within the membrane phase, the flux of s^+ must be zero at the steady state. The Nernst-Planck flow equation is written as follows;

$$F J_i = -RT u_i C_i \frac{d \ln a_i}{dx} + F u_i C_i \frac{d\varphi}{dx} \qquad (9\text{-}1)$$

Here, the movement of mass is ignored. Introducing the electrochemical activities,

$$\lambda_i = a_i e^{-\frac{F\varphi}{RT}} \qquad (9\text{-}2)$$

Eq.(9-1) is recast to

$$\frac{d\lambda_i}{dx} = -\frac{F}{RT} \frac{1}{u_i \gamma_i} e^{-\frac{F\varphi}{RT}} J_i \qquad (9\text{-}3)$$

At the interfaces at x = 0, the electrochemical potential of i-ion is considered to be continuous, i.e. Eq.(5-17) holds. When the difference between activities and concentrations is neglected, Eqs. (5-17) and (9-2) are transformed to give

$$[\lambda_i]_{x=0} = b_i C_i^I e^{-\frac{F\varphi^I}{RT}} \qquad (9\text{-}4)$$

Here $$b_i = \exp\left[-\frac{\mu_i^{0}(m) - \mu_i^{0}}{RT}\right] \tag{9-5}$$

and φ^{I} stands for the electric potential in solution I. Similarly, Eq.(9-6) is derived at x = L.

$$[\lambda_i]_{x=L} = b_i C_i^{II} e^{-\frac{F\varphi^{II}}{RT}} \tag{9-6}$$

Integration of Eq.(9-3) under the condition that the system is steady state, i.e. J_i is constant, leads to

$$b_i C_i^{II} e^{-\frac{F\varphi^{II}}{RT}} - b_i C_i^{I} e^{-\frac{F\varphi^{I}}{RT}} = -\frac{F}{RT}\frac{J_i}{u_i}\int_0^L e^{-\frac{F\varphi}{RT}}\,dx \tag{9-7}$$

where Eqs.(9-4) and (9-6) have been introduced as the boundary conditions. The current I, passing through the membrane, is defined as $I = -F\sum_i J_i$

and introducion of Eq.(9-7) into the above equation yields

$$I = \frac{RT\, e^{-\frac{F\varphi^{I}}{RT}}}{\int_0^L e^{-\frac{F\varphi}{RT}}\,dx}\sum b_i u_i \left(C_i^{II} e^{-\frac{F\Delta\varphi}{RT}} - C_i^{I}\right) \tag{9-8}$$

where $\Delta\varphi = \varphi^{II} - \varphi^{I}$

Since the membrane potential is measured under the condition that I = 0, Eq.(9-8) leads to

$$\Delta\varphi = \frac{RT}{F}\ln\frac{\sum b_i u_i C_i^{II}}{\sum b_i u_i C_i^{I}} \tag{9-9}$$

This is the basic equation to proceed with the discussion in the present chapter.

Let's consider the system where solution II contains two ionic species denoted by 1-ion and j-ion, and solution I contains only 1-ion, whose concentration is kept constant throughout the experiments. Then, Eq.(9-9) is simplified to give

$$\Delta\varphi = \text{const.} + \frac{RT}{F} \ln (C_1 + K_j C_j) \qquad (9\text{-}10)$$

where $K_j = (b_j u_j)/(b_1 u_1)$

and is referred to as the selectivity coefficient. When the membrane potential observed with $C_j = 0$ is denoted by $\Delta\varphi'$, the above equation is transformed to

$$K_j C_j = C_1 \exp[F(\Delta\varphi - \Delta\varphi')/RT] - C_1 \qquad (9\text{-}11)$$

If the right hand side of Eq.(9-11) is plotted against C_j, the slope should give the value of the selectivity coefficient K_j.

For the sake of illustration, the analysis of membrane potential will be described when saccharin anion is chosenas 1-ion in this chapter. Fe(II)-bathophenantrolin chelate is s^+ - ion, which is dissolved into nitrobenzene to construct the liquid membrane.

Experimental

Preparation of the Liquid Membrane

The ion association which exists between iron(II)-bathophenantrolin chelate and saccharin ion was prepared as follows; Bathophenantrolin (6×10^{-5} mole) was dissolved in 100 ml nitrobenzene, into which 50 ml ferrous ammonium sulfate aqueous solution (8×10^{-4} M) was added and shaken. After a time, 200 ml aquous sodium saccharin (1×10^{-2} M) which was a large excess compared with the amount of iron chelate, was mixed and shaken vigorously for 10 min. The nitrobenzene solution of the ion-association separated from the aqueous phases was used as the liquid membrane. The stock solution thus prepared was diluted to a disired concentration with nitrobenzene, when necessary.

Measurements of the Membrane Potential

The emf across the liquid membrane was measured using following cell;

Hg, Hg_2Cl_2/ salt bridge/ Solution I (reference solution)/ Liquid membrane/ Solution II/ salt bridge/ Hg_2Cl_2, Hg.

The solution I and II were separated by the liquid membrane located in the bottom of a U-shaped glass tube. As the reference solution, an aqueous solution of 10^{-2} M sodium saccharin was used. The emf in the above cell was measured with a vibrating reed electrometer

(Takeda Riken Co., Tokyo, Japan, Type TR-84 B) and recorded with a pen-writing recorder (National Electric Co., Yokohama, Japan, Type VP-652 A) to confirm that the observed potential was steady. The experiments were performed in an air oven regulated at 20° C.

Results and Discussion

Membrane potentials were measured in the concentration range of sodium saccharin between 10^{-1} and 10^{-5} M with 3 liquid membranes containing different concentrations of ion-association between Fe(II)-bathophenantrolin chelate ion and saccharin. The concentrations of ion-association in liquid membrane examined were 5×10^{-5}, 2×10^{-4} and 10^{-3} M. A linear relation was obtained when the observed potential was plotted against the logarithm of the saccharin concentration ranging between 10^{-1} and 10^{-4} M, with a slope of 57 mV per ten-hold change of concentration(see Fig. 9-2). In this range, the potential observed was independent of the concentration of the ion-association in the membrane phase. This behavior of membrane potentials consists with Eq.(9-10). When the concentration of saccharin of the sample solution is as low as 10^{-5} M, the observed potential deviates slightly from the linear relation. The deviation increases with an increase in the concentraion of the ion-association in organic phase. This implies that the concentration of ion-association in membrane phase is more dilute, the electrode is able to respond to more dilute

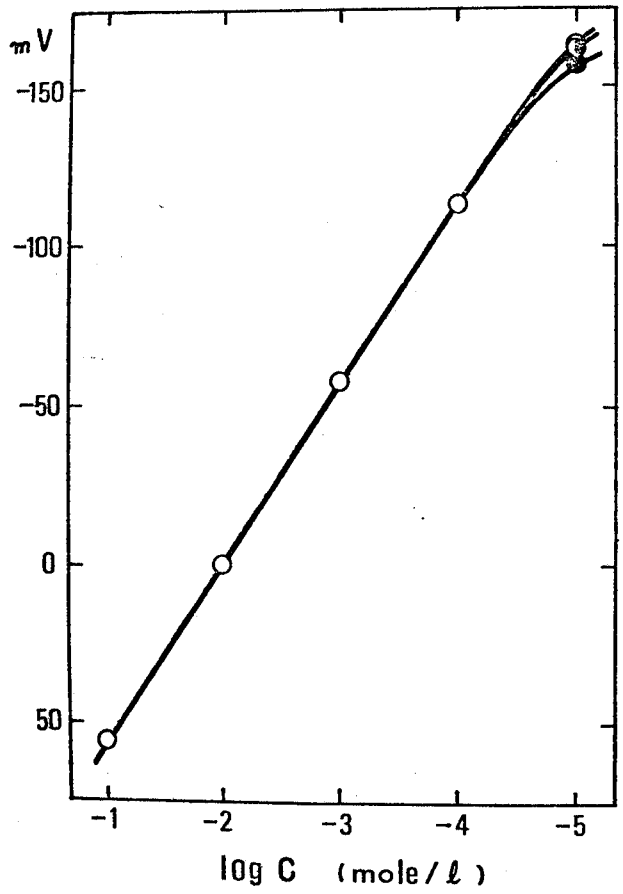

Fig. 9-2. Observed potential vs concentration of saccharin in logarithmic scale under the various concentration of ion-exchanger.

● , 10^{-3} N; ◐ , 2 x 10^{-4} N; ○ , 5 x 10^{-5} N.

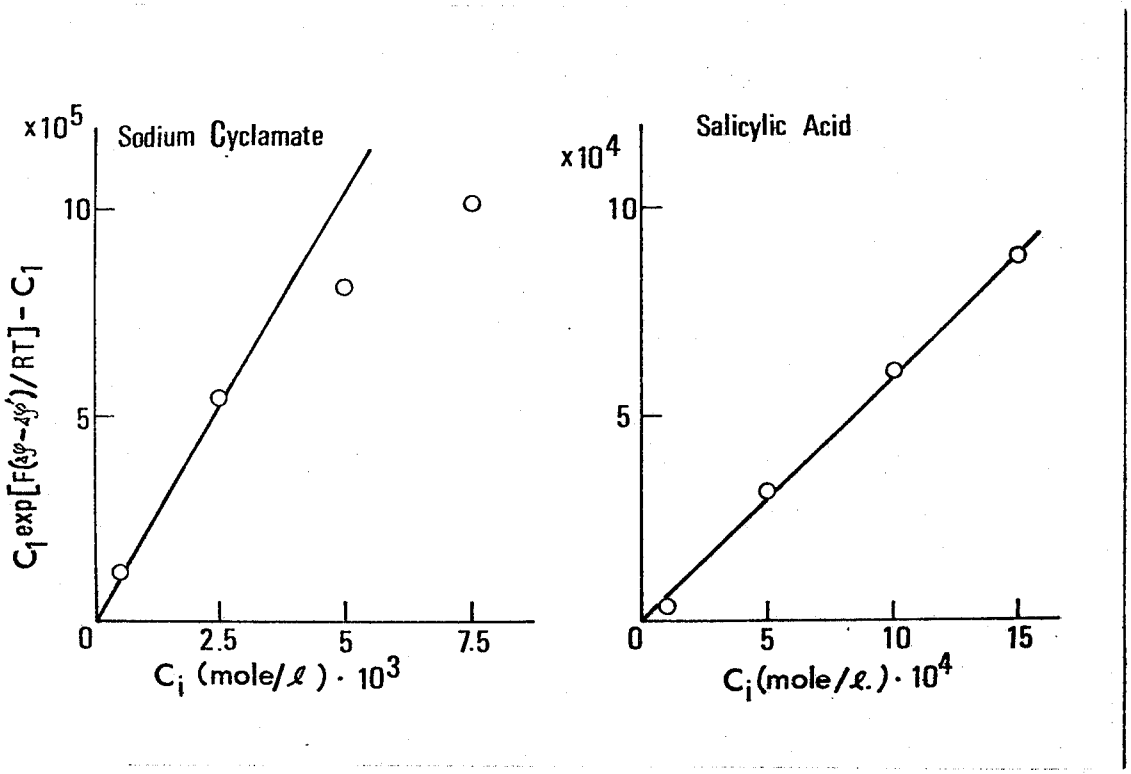

Fig. 9-3. Examples of determination of selectivity coefficients, K_j.

Table 9-1. Selectivity Coefficients, K_j.

Saccharose	10^{-4}	Lactose	10^{-4}
Glucose	10^{-4}	Fructose	10^{-4}
Sodium Cyclamate	2×10^{-2}	Citric Acid	9×10^{-4}
Sorbitol	10^{-4}	Sodium Chloride	4×10^{-4}
Benzoic Acid	5×10^{-3}	Sodium Phosphate	10^{-4}
Salicylic Acid	6×10^{-1}		

solution of saccharin. The membrane potential observed, however, is not stable when the concentration of ion-association is too dilute. Then, 2×10^{-4} M is employed for the concentration of ion-association in the liquid membrane in the subsequent experiments. The electrode potential was not affected appreciably by variation of the pH between 3 and 10.

According to Eq.(9-11), the data of membrane potential was analysed which were obtained when solution II contains saccharin anion (C_1) and other interfering ions (C_j). Some examples of the analysis are exhibited in Fig. 9-3 , where sodium cyclamate and salicylic acid are chosen as the interfering ion species. The reason why the linear relation cannot be obtained in the case of sodium cyclamate is not clear to us. Table 9-1 shows the values of K_j for several interfering anion, which are obtained from the slope of linear reltion in accordance with Eq.(9-11).

In this chapter, we have dealt the membrane potential of oil membrane only for the special case where co-ions are completely excluded, and it is found that the membrane potential is described adequately by the Nernst-Planck equation and by introducing the difference of the standard chemical potential between the aqueous and membrane phases.

References

1) E. Pungor, K. Toth, and J. Havas, Acta Chim. Acad. Sci. Hung. 48, 17 (1966).

2) J. W. Ross, Science, 156, 1378 (1967)

3) G. A. Rechnitz, M. R. Kresz, and S. B. Zamochnick, Anal. Chem. 38, 973 (1966).

4) J. Ruzicka, C. G. Lamm and J. Chr. Tjell, Anal. Chim. Acta, 62, 15 (1972).

5) G. Baum and F. B. Ward, Anal. Chem. 43 947(1971).

6) K. Kina, N. Maekawa and N. Ishibashi, Bull. Chem. Soc. Japan 46, 2772(1973).

7) C. J. Coetzee and H. Freiser, Anal. Chem. 40, 2071 (1968).

8) K. Srinivasan and G. A. Rechnitz, Anal. Chem., 41, 1203(1969).

Chapter 10. Membrane Potential of Compact Membranes

When two 1:1 type electrolyte solutions having the activities a_1 and a_2 are separated by a charged membrane at a constant temperature and hydrostatic pressure, the membrane potential, $\Delta\varphi$ is represented by Eq.(3-7), i.e.

$$\Delta\varphi = -\frac{RT}{F}\int_{a_1}^{a_2} \frac{u_+c_+ - u_-c_-}{u_+c_+ + u_-c_-}\, d\ln a \qquad (10\text{-}1)$$

Eq.(10-1) is valid even when the distribution of charges fixed in the membrane is not uniform in the direction of membrane thickness[1]. Therefore, this equation implies that the membrane potential should be zero when the membrane is placed between two identical solutions, i.e. $a_1 = a_2$, irrespective of the spacial distribution of the fixed charges. Besides Eq.(10-1), several basic equations of membrane potential are derived, which are applicable to general membrane systems on the bases of the thermodynamics of irreversible process or of pseudo-thermodynamics[2-4]. All of them predict that the membrane potential must be zero under the condition described above, i.e. $a_1 = a_2$.

Liquori and Botre[5], however, observed that a membrane potential was produced between two identical electrolyte solutions across an asymmetric membrane having a non-uniform distribution of fixed charges in the direction of membrane thickness. This potential is called the

asymmetric membrane potential. Fig.10-1 illustrates the theoretical model proposed by Liquori et al., where Si and So are two ion selective membranes having different charge densities. These two membranes are in contact with two electrolyte solutions i and o and an intermediate solution, m, containing the same electrolyte species. According to their analysis, the difference in the electric potential, $\delta\varphi$, between two solutions i and o is calculated to give

$$\delta\varphi = -(RT/F)(\alpha^{Si} - \alpha^{So}) \ln(a/a_m) \qquad (10-2)$$

where α^{si} and α^{so} are the constant related to the permselectivity of membranes and a and a_m are the mean activities of electrolyte component in the external solutions (i and o) and in the intermediate solution (m), respectively.

In this chapter, asymmetric potential data obtained with collodion membrane are presented. The asymmetric membrane is prepared by oxidizing the only one surface of the membrane. The condition is clarified for the appearance of the asymmetric potential. It is shown that Eq.(10-2) is inadequate to reproduce the concentration dependence of the observed asymmetric potential. A theoretical explanation for the asymmetric membrane potential is presented here on the basis of the surface potential, which accord with Ohki's theory explored for lipid bilayer membranes[6].

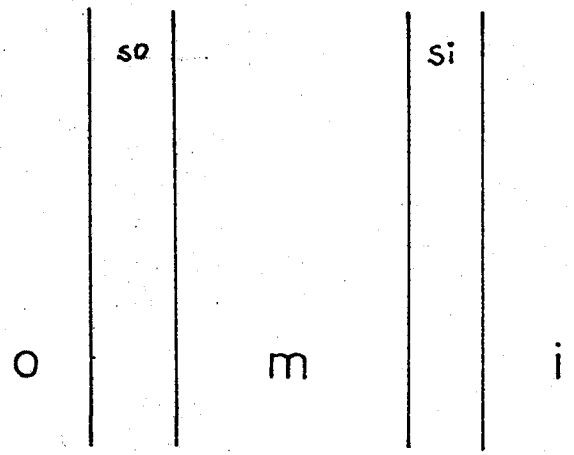

Fig. 10-1. The model for asymmetric membrane potential proposed by Liquori et al. The si and so are two ion selective membranes having different charge densities in contact with two 1:1 electrolyte i and o separated by a middle compartment containing a solution of the same 1: 1 electrolyte solution "m".

Experimental

Material Collodion solution was cast on a glass plate and 9 kinds of membranes were prepared by changing the period of air drying. Some characteristics of membranes used are listed in Table 10-1. In case of Memb.I, ethylene glycol (1 w/w %) was added in collodion solution for reducing the porosity of the membrane[7]. The water content of each membrane was determined by the same method as that used in chapter 3 and the results were also tabulated in Table 10-1. Various salts of analytical grade were used as delivered, and water was prepared by treating distilled water with both cation and anion exchangers.

Measurements of electric resistance of membranes For membrane of high water contents, e.g. Memb. A ~ F, the membrane resistance was measured by use of a pair of Ag - AgCl wire electrodes which were in contact with the membrane surfaces as described in chapter 5. For membrane with high electric resistance, the impedance of the membrane was measured by a dielectric loss bridge (Ando Elec. Co. Type TR-1B). A pair of pt-pt plate electrodes were placed as close to the membrane surface as possible so as to reduce the contribution of the resistance of the solution phases. In order to obtain the DC resistance, the electric resistance was measured in the frequency range between 30 and 500 Hz and was extrapolated to zero frequency[8]. By way of an example, Fig.10-2 illustrates the frequency dependence of conductance or electric

Table 10-1. Some characteristics of collodion membrane used

membrane	period of drying (hr)	thichness (mm)	water content (%)
A	3	0.75	79.7
B	6	0.65	76.8
C	8	0.57	75.9
D	10	0.53	68.6
E	12	0.22	51.6
F	18	0.11	12.3
G	28	0.11	8.7
H	48	0.11	6.3
I	200	0.11	5.8

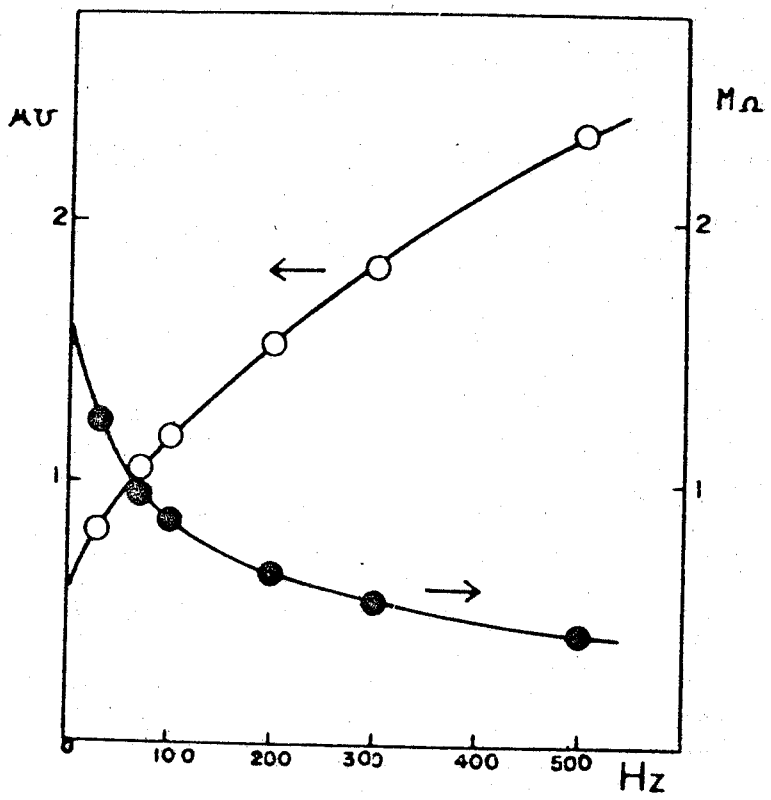

Fig. 10-2. The extrapolation of the observed membrane impedance measured by a dielectric loss bridge to zero frequency for combination of membrane G and 1/1024 N KCl. ○, the membrane conductance; ●, the membrane resistance. The dc resistance calculated from these two intercept was agreed within ± 3 %, and dc resistance was taken as the average of these two values.

resistance of a membrane.

Oxidation of collodion membrane and measurements of the emf.

The collodion membrane prepared above was mounted in a cell which was made of lucite. KOH solution of 0.1 N was filled in one compartment to oxidize one side of the collodion membrane and 0.1 N HCl solution was poured into the other compartment to prevent the oxidation in the other side of the membrane. The duration of oxidation was different for each membrane depending on the compactness of the membrane. For example, Memb.I was oxidized for about 1 hr. The asymmetrically oxidized membrane thus prepared had been linsed thoroughly with ion exchanged water for overnight, then the two compartments separated by the membrane were filled with identical salt solutions. The asymmetric membrane potential was measured with a vibrating reed electrometer (Takeda Riken Co. Type TR-64B) conducted from a pair of Ag - AgCl electrodes. The influence of stirring of the bulk solutions on the observed emf was negligibly small for the asymmetric potential, and hence the external electrolyte solutions were not agitated for the subsequent measurements. A pen writing recorder (National Elec. Co. Type VP-652A) was connected to the electrometer and the emf produced across the membrane was confirmed to stay constant for few hours.

All measurements were carried out in an air chamber regulated at 25°C.

Results

Fig.10-3 shows the specific resistance, K, of membranes as functions of concentration, C of the external KCl solution. Here K is defined by the equation;

$$K = r(A/L) \qquad (10-3)$$

where r, L and A stand for the observed membrane resistance, the geometrical thickness and area of the membrane, respectively. It is observed that the value of K varies inversely with KCl concentration C for membranes whose water contents are higher than 10 %, i.e. Membs. A ~ F. The broken line shown in Fig.10-3 represents the concentration dependence of the specific resistance of KCl solution. Note that the electric resistances of Membs. A ~ E are proportional to that of the bulk solution. The difference between the value of K for these membranes and the broken line is attributed to the tortousity factor of the membrane in problem. This factor means the ratio of the effective thickness of the membrane against that of geometrical[9]. From the results given in Fig.10-3, the tortousity factor of Membs.A ~ E is evaluated to be 0.33, which agrees well with the value reported in chapter 3 for systems of polystyrene sulfonic acid-collodion membranes in KCl solution. Contrary to the data for Membs.A ~ F, the values of K for membranes with low water content, i.e. Membs.G,

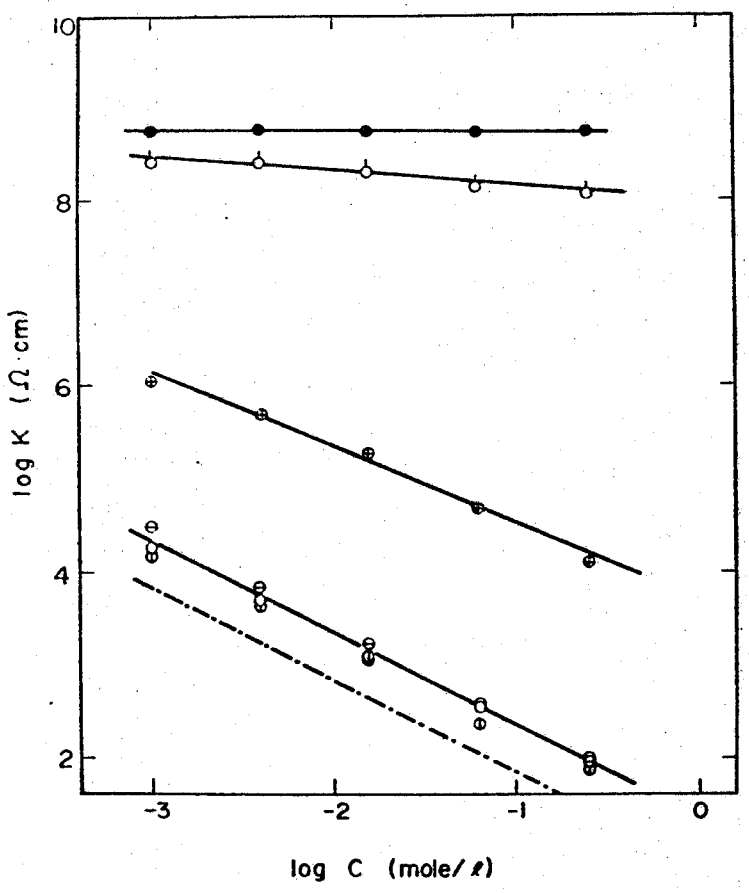

Fig. 10-3. The relation of specific resistance, K and the concentration of external solution, C for collodion membrane of various water contents. ○, Memb. B; ⊖, Memb. D; ⊖, Memb. E; ⊕, Memb. F; ◑, Memb. G; ●, Memb. H and I.

H and I scarcely depend on the salt concentration in the external solution. This fact implies that ions are hard to penetrate through the membrane phase with decrease of the water content.

Experiments showed that the asymmetric membrane potential was observed only for the case in which the membrane resistance was high and hardly depended on the salt concentration. In other words, it is possible to observe an asymmetric membrane potential only for Membs. G, H and I. For Memb. I the observed asymmetric potential varied less than 1 % within for 3 days in all salt concentrations of the external solution studied. For this membrane the electric resistance of the membrane did not change by oxidation, and hence the oxidation reaction was considered to occur only at the membrane surface. The asymmetric potential was also observed for the asymmetric membrane made of methylene blue or of polyacrylic acid with collodion, which was dried completely. This fact implies that the asymmetric potential is not caused by chemical products of oxidation reaction of collodion but is generated by the fixed charges on the membrane surface. If the fixed charges were distributed uniformly in the membrane phase, or densities of charges fixed on a membrane were the same each other on two surfaces of the membrane, the asymmetric membrane potential did not appear even when the electric resistance of the membrane was extremely high. Therefore, two conditions, i.e. non-uniform distribution of fixed charges and the

compactness of the membrane, seem to be the indispensable prequisite to appearance of the asymmetric potential of a membrane.

Fig.10-4 shows the dependence of the asymmetric membrane potential on the concentration of the external KCl solution for two kinds of membranes prepared from Memb. I (designated as Memb. 1 and 2). The potential in the solution which is contiguous to the more negatively charged surface of membrane is always positive with respect to the other. It is noted that the observed potential never becomes in the reverse direction. The asymmetric membrane potential becomes approximately a constant value with decrease of the external salt concentration, and approaches to zero with increase of concentration in the media.

Discussion

According to Eq.(10-2), the asymmetric membrane potential vanishes at $a = a_m$, and becomes negative with increase of the activity of salt in the external solution when a exceeds a_m. Then, if we try to interpret the concentration dependence of the observed asymmetric membrane potential by use of Eq.(10-2), we must assign a_m as high as 1 N. It is evident that this high value of a_m is quite unreasonable if we consider the condition of preparation of membranes and the high values of the electric resistance of the membrane in problem. Therefore, we have to consider some other mechanism of the generation of the asymmetric

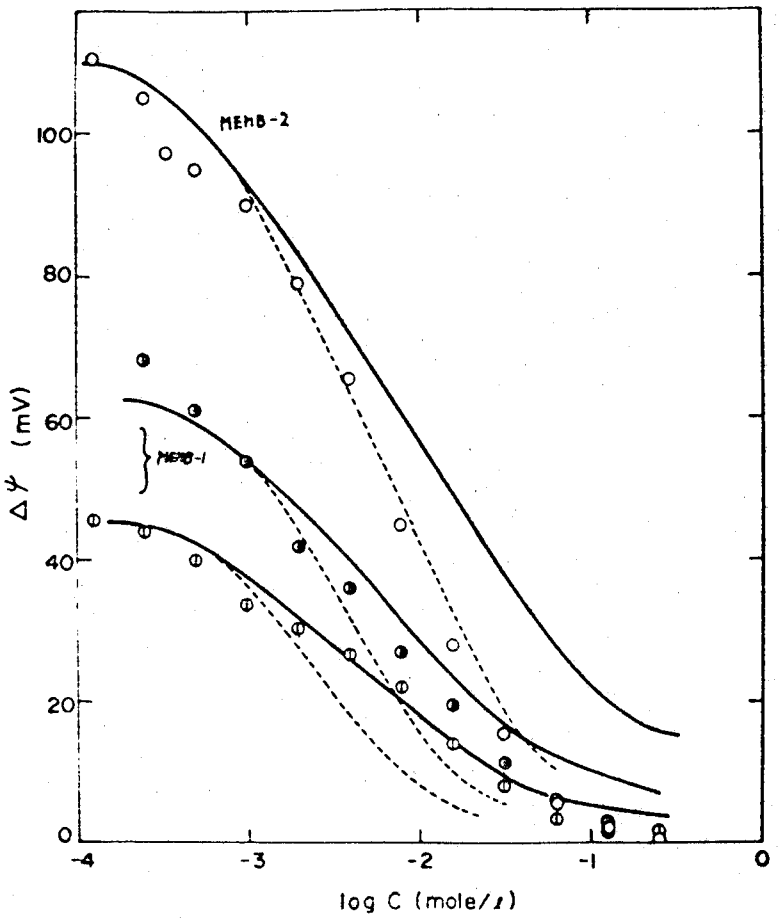

Fig. 10-4. The plot of asymmetric membrane potential $\Delta\psi$, against the concentration of external KCl solution, C. ⊕, for Memb-1; ◍, the observed potential difference when the oxidized surface is always faced to more dilute solution, keeping the concentration ratio of the two external solution at 2 for Memb-1. The value of C represents the concentration of more concentrated solution. ○, the asymmetric membrane potential produced between two identical solution for Memb-2.

membrane potential instead of Eq.(10-2) at least for the present membrane.

As pointed out above, the asymmetric membrane potential can be observed only when the charge densities fixed on two surfaces of membrane are different each other and when no ion penetrates across the membrane. From these experimental facts, it is reasonable to assume that the asymmetric membrane potential is mainly stemming from the difference of surface potentials at two membrane-solution interfaces, and that the diffusion potential in the membrane phase does not play a decisive role for the observed emf.

Recently, Ohki[6,10] proposed a theory of the membrane potential for a system in which the membrane is not permeable to ion species. In the derivation of the theoretical expression, he implicitly assumed that the membrane is an electrically (non-ionic) conductive medium. When a surface having charge density, σ (coulomb/cm^2), is contiguous with an aqueous solution of 1:1 type electrolyte of concentration, C, the difference in potentials between the membrane surface and the bulk electrolyte solution can be obtained by solving the Poisson-Boltzmann equation and is given by[6,11,12]

$$2(RT/F)\ln\{\kappa C^{-1/2} + (1+\kappa^2 C^{-1})^{1/2}\} \quad (= (2RT/F)\sinh^{-1}(\kappa C^{-1/2}))$$

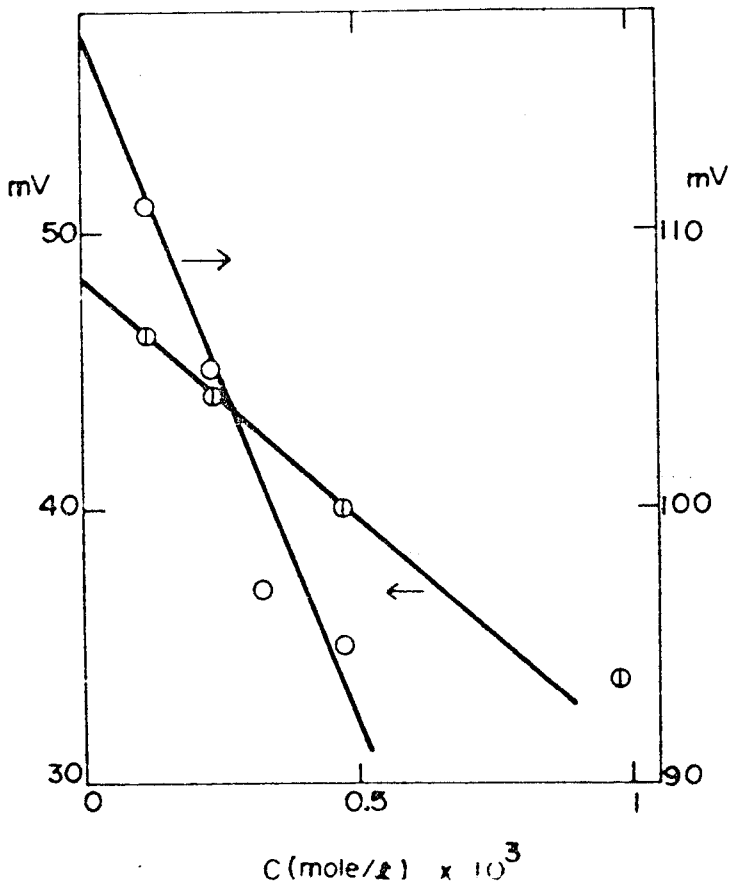

Fig. 10-5. The plot of $\Delta\psi$ against C according to Eq.(10-5). One can calculate the value of K_1 and K_2 from the ordinate intercept and the slope of the figure. Notations are the same as in Fig. 10-4.

where K stands for $(\mathcal{R}/2RT\varepsilon)|\sigma|$ with ε being the dielectric constant in solution phase. When two surfaces of the membrane have different charge densities σ_1 and σ_2, the difference in electric potential in two bulk solutions (asymmetric membrane potential, $\Delta\psi$) is calculated to give

$$\Delta\psi = \left(\frac{2RT}{F}\right) \ln \frac{K_2 + (K_2^2 + C)^{1/2}}{K_1 + (K_1^2 + C)^{1/2}} \qquad (10-4)$$

where the potential gradient within the membrane phase is assumed to be zero. This assumption is not unreasonable since the membrane is impermeable to ions, but it is still electrically conductive[6]. Expansion of Eq.(10-4) in powers of C leads to

$$\Delta\psi = \frac{2RT}{F} \ln\left(\frac{K_2}{K_1}\right) + \frac{RT}{2F}(K_2^{-2} - K_1^{-2})C + O(C^2) \qquad (10-5)$$

when both $K_2C^{-1/2}$ and $K_1C^{-1/2}$ are much larger than unity. Eq.(10-5) implies that $\Delta\psi$ depends linearly on C in the dilute region, and that the ordinate intercept and the slope of the straight line in $\Delta\psi$ vs C plot give the values of $2(RT/F)\ln(K_2/K_1)$ and of $(RT/2F)(K_2^{-2} - K_1^{-2})$, respectively. Then the values of K_1 and K_2 are allowed to be determined. Fig.10-5 shows the linear relation between $\Delta\psi$ and C of Eq.(10-5), and the values of K's calculated from this figure are tabulated in Table10-2. The values of K_1 & K_2 for Memb-2 mean that a unit electric charge distributes

Table 10-2. Values of parameter, K_1, K_2, θ_1 and θ_2 for the calculation of theoretical values depicted in Fig. 10-4 and 7.

membrane	K_1	K_2	θ_1	θ_2
Memb-1	0.0251	0.0643	0.00126	0.0076
Memb-2	0.0172	0.163	0.00072	0.0521
Liquori's	0.0912	0.410	0.0166	0.332

K_1, K_2 in unit of mole$^{1/2}$ liter$^{-1/2}$, θ_1, θ_2 in unit of mole liter^{-1}.

per 7.0×10^3 and 7.3×10^2 Å^2, respectively. Comparison between the experiments and Eq.(10-4) is made in Fig.10-4, where the solid lines are calculated values by using K_1 and K_2 given in Table 10-2, and points show the experimental data. In Fig.10-4 points marked —⊙— are referred to the case where the oxidized surface is always faced to more dilute solution, with keeping the concentration ratio of external solutions at twice for Memb-1. The agreement between the theory and experiments is good, although the observed potentials fall down with concentration more rapidly than that expected from Eq.(10-4).

Another approach for the surface potential is based on the Donnan potential difference at the membrane-solution interfaces. The electrolyte component in the membrane phase immediately inside of the membrane surface is assumed to be equilibrated with the external solution. Then, the potential difference (Donnan potential) is set up at the interface. When the charge density, θ(in moles / liter) fixed in the membrane phase is constant irrespective of the salt concentration, C, in the external solution, the Donnan equilibrium condition gives the following expression for potential difference at the interface;

$$(RT/F) \ln \{ [\theta + (\theta^2 + 4C^2)^{1/2}]/2C \} \qquad (10-6)$$

As postulated above the asymmetric membrane potential in problem, $\Delta\psi$, is considered to be the difference of the surface potentials.

Then, we obtain

$$\Delta\psi = (RT/F)\ln\frac{\theta_2 + (\theta_2^2 + 4c^2)^{1/2}}{\theta_1 + (\theta_1^2 + 4c^2)^{1/2}} \qquad (10-7)$$

In Fig.10-4, the dotted lines represent the values calculated from Eq.(10-7), where the values of θ used in the calculation are listed in Table 10-2 for each membrane. These values for θ's were chosen so that Eq.(10-7) fitted the experimental values of $\Delta\psi$ in the dilute region.

The values of $\Delta\psi$ calculated from Eq.(10-7) are always smaller than that of Eq.(10-4), and the observed values lie between these two theoretical curves except the data of Memb-2 in concentrated external solution. Neither Eq.(10-7) nor (10-4) can reproduce satisfactorily the concentration dependency of the asymmetric membrane potential, but both of them are able to predict the qualitative behaviour of the asymmetric membrane potential; e.g. the asymmetric potential lies at a constant value when the external solution is dilute enough, and approaches zero with increase of concentration of the external solution.
The structural details of membrane-solution interfaces must be taken into consideration to proceed further quantitative analysis.

Eqs.(10-4) and (10-7) can be extended so as to include the case where the concentrations of external solutions are different.
Both Eqs.(10-4) and (10-7) imply that the emf across the membrane in a

dilute salt solution ($C \ll K$ or θ) varies ideally with concentration, i.e. the emf varies 59 mV per ten-fold variation of the external salt concentration, when the external concentration in one side of the membrane fixed at a constant. This type of behaviour of the membrane potential is observed with various oil membranes and metal membranes. (see, chapter 9) Fig.10-6 shows the observed potential between two electrolyte solutions separated by a mercury layer. The concentration of solution in one compartment was kept constant (1/1024 N) and that of the other solution was varied successively. When external solution is KCl or NaCl, the potential difference between two solutions at zero current varies -59 mV per ten-fold variation of concentration of the solution. In other words, mercury layer acts as a negatively charged and ideally permselective membrane when it is immersed in KCl or NaCl solution in spite of no permeation of any ion species. It is well known that Cl^- ion adsorbs specifically on a mercury surface[13]. Since the potential gradient within a mercury is apparently zero, the observed potential difference shown in Fig.10-6 must be attributed to the difference of surface potentials at electrolyte solution-mercury interfaces. On the other hand, when a mercury is immersed in a tetrabutyl ammonium chloride solution (TBA-Cl), the cation (TBA ion) adsorbs preferentially on the mercury surface. Then we can observe a potential difference opposite to the case of NaCl or KCl solution. When the

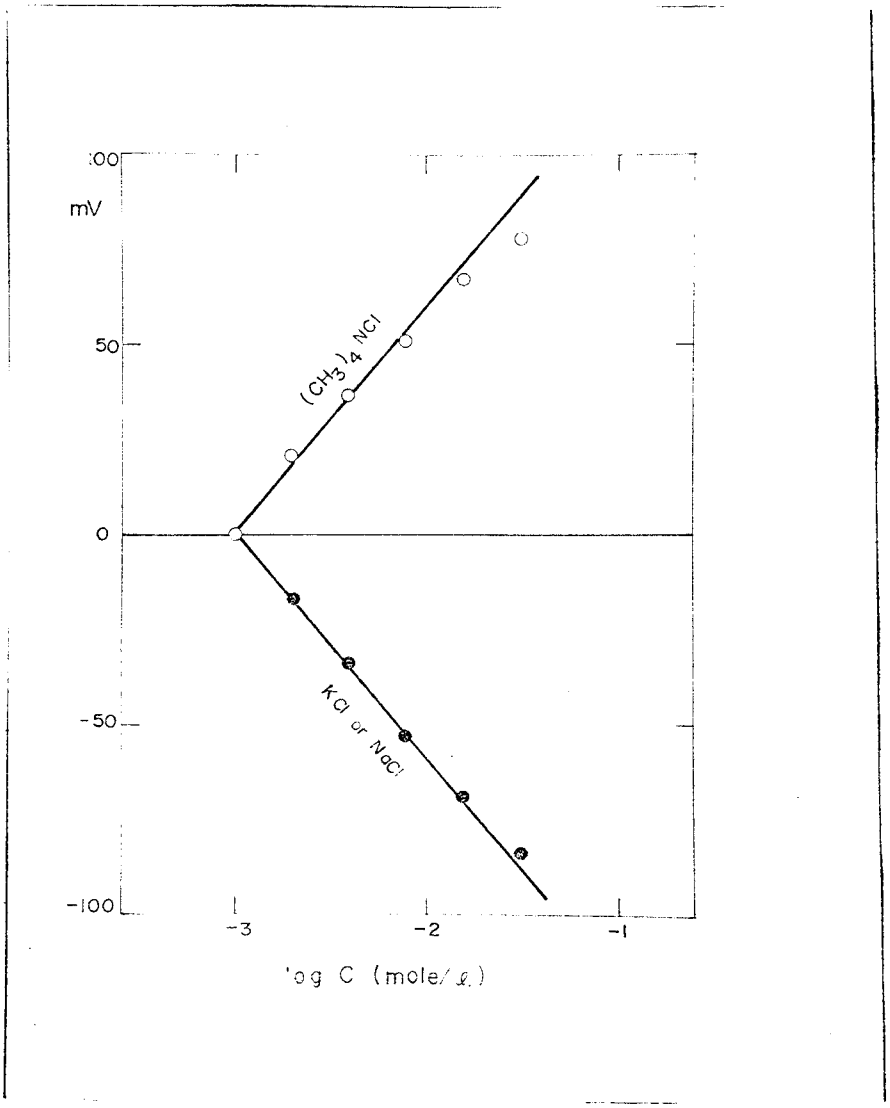

Fig. 10-6. The observed potential difference arisen between two electrolyte solutions separated by a mercury. The concentration of one compartment is kept constant at 1/1024 N and that of another compartment, C is varied. ○ , the potential difference arisen between two $(CH_3)_4NCl$ solution; ◉, the potential difference arisen between KCl or NaCl solution.

external solution is replaced by NaF solution in which either cation or anion does not adsorb specifically on the mercury surface, the observed potential difference is small and is not reproducible. These experiments show that the excess charges on the mercury surface due to the ion adsorption give rise to the surface potential and the difference of the surface potential at two interfaces is observed as a membrane potential. Definitely no permeation of ion across the membrane is accompanied with the membrane potential in the present system. Considering these facts, it is feasible that the surface charges on the membrane which is impermeable to ions, give rise to the surface potential at the interface, and the difference of two surface potentials is observed as the membrane potential.

Comparison between Liquori's data and the present theory

Fig.10-7 shows a comparison between Liquori's data of polystyrene sulfonic acid-collodion asymmetric membrane[5] and Eqs.(10-7) and (10-4). The solid line in the figure represents the calculated value of Eq.(10-4) and the dotted line is that calculated from Eq.(10-7). In these calculations, the values of parameters used are listed in Table 10-2. The value of K_1 of 0.41 $mole^{1/2}.l^{-1/2}$ corresponds to the charge density that one negative site is distributed per 300 $\mathring{A}^2$ on the average. $\Delta\psi'$ is measured under the condition that the membrane surface having

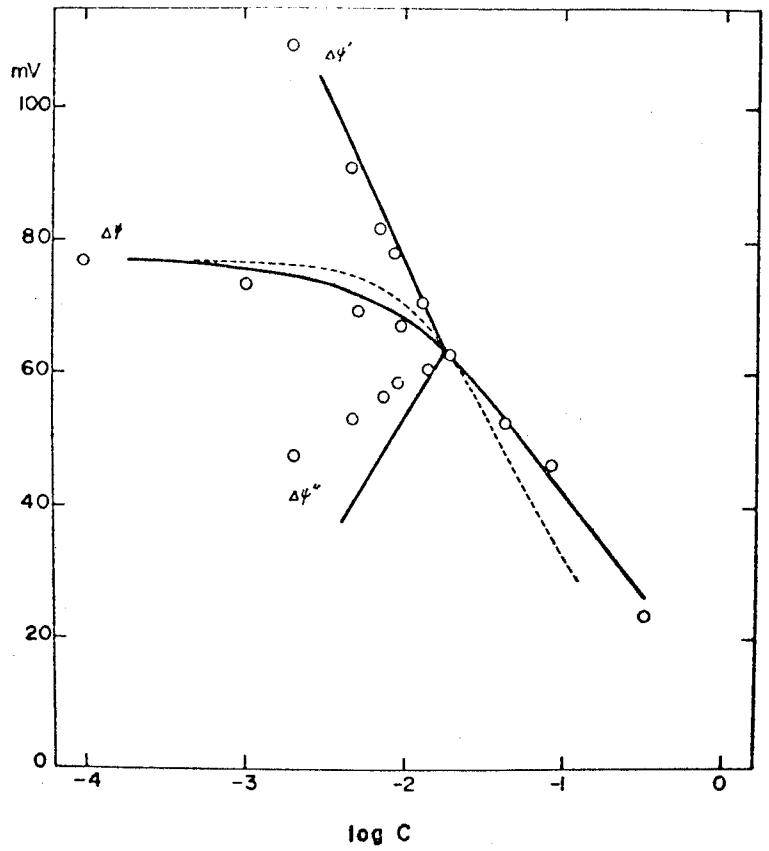

Fig. 10-7. Comparison between the Liquori's data and the theory, Eq.(10-4) or (10-7). The solid lines is the value calculated from Eq.(10-4) and the dotted lines is one from Eq.(10-7). The values of parameters for the calculation are listed in Tab. 10-2. $\Delta\psi$ is the asymmetric membrane potential arisen between two identical electrolyte solutions. The membrane potentials $\Delta\psi'$ and $\Delta\psi''$ are observed for two opposite orientations of the asymmetric membrane with respect to the two bathing electrolyte solutions of NaCl. The activity in one electrolyte solution is fixed at 1.7×10^{-2} whereas the mean activity of the other electrolyte solution is varied.

the charge density K_2 (or ϑ_2) is always faced to 0.017 N NaCl and the concentration of the other solution is varied successively, while $\Delta\psi''$ is measured under the reverse condition. The agreement between the experiments and the theory given by Eq.(10-4) is satisfactory except $\Delta\psi''$. Liquori et al. measured neither the electric resistance nor the water contents for their membranes. Therefore, it is hazadous to consider that the membrane potential is related uniquely to the permeability of ions across the membrane as they have assumed. We do not argue that the mechanism of the asymmetric membrane potential described here is the sole cause of the appearance of the potential of an asymmetric membrane, but the present analysis is consistent with the experimental results presented in this article and those in Liqori's paper.

In the present chapter, the asymmetric membrane potential which was arisen between two identical solutions across an asymmetric membrane was attributed to the surface potential at the membrane-solution interfaces. Simple calculation for the asymmetric membrane potential does not succeed to reproduce the observed potential quantitatively. However, it is evident experimentally that the necessary condition for the appearance of the steady asymmetric membrane potential is no permeation of ions across the membrane. If the ion species can penetrate freely through the membrane the difference between two surface potential

may be concealed by the diffusion potential set up within the membrane phase. In fact, the asymmetric membrane potential across an asymmetric membrane made of Memb. G or H varied with time and vanished eventually. This fact is stemming from the sluggish diffusion of ions in the membrane, and contradict to Liquori's theory of the asymmetric membrane potential. If the membrane is permeable to ions, the ions must diffuse through Si and So membrane given in Fig.10-1 until the condition that $a_i = a_m$ is attained. In an actual membrane, the capacity of the intermediate solution "m" is so small that the asymmetric membrane potential must be diminished rapidly.

References

1. Kobatake, Y., Toyoshima, Y., and Takeguchi, N., J. Phys. Chem., 70, 1187(1966).

2. Lorimer, J.W., Boterenbrood, E.I., and Hermans, J.J., Discussions Faraday Soc., 21, 141(1956).

3. Hills, G.J., Jacobs, P.W.M., and Lakshminarayanaiah, Proc. Roy. Soc., A262, 246(1961).

4. Scatchard, G., J. Am. Chem. Soc., 75, 2883(1953).

5. Liquori, A.M., and Borte, C., J. Phys. Chem., 71, 3765(1967).

6. Ohki, S., J. Colloid Interface Sci., 37, 318(1971).

7. Elford, W.J., Trans. Faraday Soc., 33, 1904(1937).

8. Toyoshima, Y., Yuasa, M., Kobatake, Y., and Fujita, H., Trans. Faraday Soc., 63, 2803(1967).

9. Mackay, D., and Mears, P., Trans. Faraday Soc., 55, 1221(1959).

10. Ohki, S., Biochim. Biophys. Acta, 282, 55(1972).

11. Verwey, E.J.W., and Overbeek, J.Th.G., in "Theory of the Stability of Lyophobic Colloids" p.32. Elevier Publishing Co., Amsterdam,1948.

12. Neumcke, B., Biophysik, 6, 231(1970).

13. Grahame, D.c., and Parsons, R., J. Am. Chem. Soc., 83, 1291(1961).

Chapter 11. Summary and Conclusion

In this thesis, various electrochemical phenomena observed with the membrane-electrolyte solution system have been investigated. The membrane used are (1) porous charged membrane, (2) oil membranes and (3) compact membranes which scarcely permeable to ions.

Much efforts are devoted to the membrane phenomena for porous charged membrane, through which ions and water diffuse from one bulk solution to another. The membrane phenomena observed with porous membranes can, then, be described by the appropriate rearrangement and/or the integration of the flux equation. According to the thermodynamics of irreversivle process, the flux equation or phenomenological equation can be written by Eq.(2-2). The molecular aspect for phenomenological coefficents l_{ki}, however, is not given. Considering this circumstance, the Nernst-Planck flow equation is used as a pertinent starting point and then, some consideration on the flow equation was perfomed in chapter 2.

In 1935, Teorell, Meyer and Sievers derived the expression for membrane potentials with use of the Nernst-Planck equation. However, several investigators have revealed that their theory is not in line with the experiments in quantitative manner. The failure is stemmed from the lack of precise information about the non-ideality of small ions in charged membranes. In chapter 3, the activity coeffi-

cients and mobilities of small ions within the membrane phase were determined for collodion membranes impregnated with poly-styrene sulfonic acid. The results are summarized as follows; (1) Activity coefficients of small ions is much smaller than unity when the membrane is equilibrated with dilute external solutions. (2) Mobilities of counter-ions are found to be depressed extremely, while those of co-ions are not appreciably affected by the presence of fixed charges. In polyelectrolyte solution study, many experimental investigations on the activities of small ions have been carried out. These studies show that the activity coefficient of small ions is the same as the results (1) mentioned above, and can be described by an empirical rule, Eq.(3-16), called as the "additivity rule". Since the depression of the activity coefficients comes from the strong electrostatic interaction between counterions and charges fixed in the polymer chain, it is not unreasonable to analyse the data obtained with charged membranes by invoking the additivity rule. Contrary to the case of polyelectrolyte solution, the value of ϕ exhibited the slight concentration dependence of added salt. Experimental investigations presented in this article showed that the concentration dependence of mobilities of counterions is the same as that of activity coefficients. Then, the expressions for activity coefficients and mobilities of

small ions in the membrane were obtained as

$$\gamma_+ = \gamma_+^\circ (c_- + \phi X)/(c_- + X), \qquad \gamma_- = \gamma_-^\circ \tag{3-16}$$

$$u_+ = u_+^\circ (c_- + \phi X)/(c_- + X), \qquad u_- = u_-^\circ \tag{3-18}$$

ϕX is referred to as the thermodynamically effective charge density. In chapter 4, theoretical consideration on the activity and mobility was performed.

Chapter 5 dealed with a simple method for characterization of membrane-electrolyte systems using Eqs.(3-16) and (3-18), where degree of permselectivity, P_s was introduced. The studies described in this chapter showed the wide applicability of Eqs.(3-16) and (3-18) for various membrane-electrolyte systems.

In chapter 6, the electrokinetic phenomena of membranes were discussed. From experimental data, it was concluded that the hydrodynamically effective fixed charge density, ψX, which governs the rate of mass movement in the membrane, was approximately 10 % of the value of ϕX. Using the value of ψX, the contribution of the mass movement on the membrane potential and salt flux was estimated, and it was shown that this contribution is negligibly small compared to the observed value.

In chapter 7, the transference number of small ions were measured so as to evaluate the effective concentration carried by the mass movement. Results were summarized as in Eq.(7-12), i.e.

$$\Gamma_+ = (c_- + \nu x)/(c_- + x) , \qquad \Gamma_- = 1 \tag{7-12}$$

This expressions are similar to those found in Eqs.(3-16) and (3-18). These results imply that all coins in the membrane are active both thermodynamically and hydrodynamically, while the counterions behave quite non-ideally in the membrane phase, i.e. only a part of the counterions dissociated from the polyelectrolyte skeletones are active for mobility and activity, and a much smaller part of the counterions are effective for the hydrodynamical properties.

In chapter 8, the effect of stagnant layer was considered. Taking the presence of the stagnant layer into consideration, the equations for transference numbers and electroosmosis have been derived. The implications of these equation accord with the experimental facts, and the effect of the layer is concluded to be eliminated when the solutions are vigorously agitated as usually employed.

Chapter 9 dealed with the oil membrane and showed that ionic selectivity can be expressed as the difference of standard chemical potential between aqueous and membrane phases.

In chapter 10, the membrane potential was investigated which arisen across the compact membrane. The membrane used were scarcely permeable to ions contrary to the membranes treated in the preceding chapters. For such membranes, it is concluded that the phase boundary

potential mainly contributes to the total membrane potential.

As a conclusion, for the membrane which permeate freely to ions, various membrane phenomena can be interpretated quantitatively only when the non-ideality of small ions and the difference of standard chemical potential are taken properly into consideration. As shown in chapter 5, the value of effective charge density, ϕX is determined for any combinations of membrane and electrolyte solution, and we can predict the value of other phenomena. But, the results given in chapter 10 show that careful consideration must be necessary in analysing the membrane potential data.